NEW DEPENDABLE ROLLING STOCK FOR A MORE SUSTAINABLE, INTELLIGENT AND COMFORTABLE RAIL TRANSPORT IN EUROPE

D3.4 Final Report

Due date of deliverable: 31/10/2016

Actual submission date: 23/11/2016

Leader/Responsible of this Deliverable: Eduardo de la Guerra Ochoa, Talgo

Reviewed: Yes

Document status		
Revision	Date	Description
1	10/10/16	First draft for internal review
2	17/10/16	Including the last version of the contributions and different corrections
3	21/10/16	Reviewed version
4	03/11/16	Update with the TMT comments received

Project funded from the European Union's Horizon 2020 research and innovation programme		
Dissemination Level		
PU	Public	X
CO	Confidential, restricted under conditions set out in Model Grant Agreement	
CI	Classified, information as referred to in Commission Decision 2001/844/EC	

Start date of project: 01/05/2015 Duration: 30 months

REPORT CONTRIBUTORS

Name	Company	Details of Contribution
Eduardo de la Guerra	Talgo	Task Leader
Erna Bao	Siemens	Fatigue load cases
Patrick Jumin	SNCF	Joining Technologies
Aurélie Goudé	SNCF	Joining Technologies
Jens König	DLR	Topology optimization for material assessment
Luis Lacarcel	SRV	Calculation of composite roof with rivet joint

EXECUTIVE SUMMARY

This deliverable (D3.4) corresponds to the Task 3.4 “Final Report” of the Work Package 3.

The purpose of this document is to describe all the open and closed points, aspects, conditions and conclusions to start with enough information the Shift2Rail Project.

The document is divided into three main sections dedicated to each deliverable of the Work Package 3: carbody specification, material assessment and joining technologies.

In the section dedicated to carbody specification, there are collected the load cases proposal, environmental conditions and the different studies made by topological optimization to evaluate the influence of slight modification in the basic geometry of the carbody (dimension of windows, doors, their positions, etc.).

In this study the percentage of weight improvement with respect to the base models defined in the beginning is calculated.

For the Urban model, different variables were analysed: widening door and window pillars, widening the window frame, division of the door by a door pillar, moving the doors to the ends walls, varying the number of windows (three smaller instead of two larger windows), etc. According to the study, the weight improvement can be between 6% and 20% in the most favourable case which is decreasing the width of the door 300mm (-15% in width).

For the High Speed model, different variables were analysed: position of the service door, with of door and window pillars, number of windows and window pillars according the force-flow-optimised. According to the study, the weight improvement can be between 3% and 16%.

In the second section, which covered the material assessment, the material alternatives for the different parts of the carbody (end wall, main frame, etc.) are presented.

The main material alternatives considered for the next generation of the carbody shell include: aluminium extruded profile, composite sandwich (with different combination FRP skin with foam, honeycomb or aluminium foam core), monolithic composite, high strength alloys… depending on their location and functional requirements. In addition, the mechanical properties needed for structural calculation for the main material alternatives are included.

A study for the preselected material is also done, showing the structural feasibility of composites, seeming only necessary to metalize specific zones with concentrated load like lifting points, connection to bogies and couplers.

In the third section, the evaluation of the main joining technologies is presented, taking into account advantages and disadvantages focused in the application of multimaterial joints and lightweight solutions. For joints where disassembly is required, bolting and screwing will be the best selection. To some extent also riveting and even bonding (secondary structures and elastic adhesives, e.g. windows and glazing, panelling, etc.) could be the choice.

If no disassembly is necessary a permanent joining technology should be used. The first choice will be welding, riveting and bonding or the combination of both might be used.

ABBREVIATIONS AND ACRONYMS

- *CFRP: Carbon Fibre Reinforced Plastic.*
- *EMC: Electromagnetic compatibility.*
- *FST: Fire Smoke and Toxicity.*
- *FSW: Friction Stir Welding*
- *FRP: Fibre reinforced plastic.*
- *GFRP: Glass fibre reinforced plastic.*
- *HAZ: Heat affected zone.*
- *HS: High Speed.*
- *HVAC: Heat Ventilation Air Conditioning.*
- *LCF: Low Cycle Fatigue.*
- *LOC: Locomotive.*
- *MIG: Metal Inert Gas*
- *MAG: Metal Active Gas*
- *RBE: Rigid Body Elements*
- *REFRESCO: Towards a REgulatory FRamework for the usE of Structural new materials in railway passenger and freight CarbOdyshells.*
- *S/N-Stress-Number of cycles.*
- *TBD: To be defined.*
- *TGV: Train à Grande Vitesse.*
- *TOR: Top of Rail.*
- *TS: Technical Specification.*
- *TSI: Train Specification for Interoperatibility.*
- *WP: Work Package.*

TABLE OF CONTENTS

LIST OF FIGURES

LIST OF TABLES

1. INTRODUCTION

The Roll2Rail project aims at developing key technologies required for the next generation of innovative rolling stock in Europe. The project is part of the Horizon 2020 program of the European Commission and has received funding under grant agreement No. 636032. Roll2Rail is a lighthouse project to Shift2Rail which will continue the development and implement the results of Roll2Rail in full scale technical demonstrators.

In Roll2Rail the work related with carbodies is carried out in Work Package 3 (WP3) which includes partners representing vehicle manufacturers (Bombardier Transportation, Hitachi Rail Italy, Siemens, Stadler Rail Valencia and Talgo), operators (SNCF) together with academia and research institutes (DLR, Fraunhofer and KTH).

This deliverable is summary of the different task of the WP3 and it is divided into three main sections dedicated to each deliverable of the WP3 (carbody specification, material assessment and joining technologies) and final section for the main conclusions with the closed/open points for Shift2Rail.

In the section dedicated to carbody specification, it is collected the load cases proposal for the fatigue assessment, environmental conditions and the different studies made by topological optimization to evaluate the influence of slight modification in the basic geometry of the carbody (dimension of windows, doors, their positions, etc.). This section is a summary of the Deliverable 3.1 containing the main improvements and progress achieved.

In the second section, that covers the material assessment, the material alternatives for the different parts of the carbody (end wall, main frame, etc.) are presented. In addition, the mechanical properties needed for the static structural calculation of the main material alternatives are included.

In the third section, the main joining technologies evaluation is presented, taking into account advantages and disadvantages focused in the application of multimaterial joints and lightweight solutions.

Finally, the main open points to be addressed in Shift2Rail and main conclusions of this Work Package are summarised.

2. TECHNICAL SPECIFICATION

The purpose of this chapter is to collect the main features for the High Speed and Urban carbodies for Roll2Rail Project. In this final report it is included the main achievements included in the Deliverable D3.1 [A1], with the final version of the fatigue load case table for HS and Urban. In D3.1 [A1], Technical Specifications describes the main characteristics and the minimum conditions or requirements to be met for the new generation of light carbody shell to be developed during Shift2Rail Project.

In addition, it has been included the working condition and a study of the impact in the weight of the primary structure of the carbodies (Urban and High Speed) due to modifications in the basic external geometry using topology optimization.

For clarity purpose, this chapter is divided into two main sections for each demonstrator: HS and Urban.

2.1 TECHNICAL SPECIFICATION FOR HIGH SPEED CARBODY

For detailed and complementary information regarding the Technical Specification, see D3.1 [A1].

In the section 2.1.1 it is included the proposal for generalized fatigue load cases for HS regarding cumulative damage approach. The fatigue load cases can be divided into low cycle fatigue (LCF) and high cycle fatigue (HCF). These load cases can be applied for all materials including composite or polymeric materials.

This fatigue load cases are intended to serve for the structural assessment of the carbody as an alternative of the current framework standard (EN 12663-1 [A2]), because of this standard is only prepared for the validation with metal, as showed during REFRESCO Project.

The inclusion of the low-cycle fatigue loads is justified due to the low slope of the S/N-curve of some polymeric materials in dependence of stress ratio and temperature that can lead to low cycle fatigue dominated behaviour of the material under typical railway load spectrum. So some static loads of EN 12663-1 [A2] have to be considered as low cycle fatigue loads with reasonable number of cycles.

This table is prepared with the agreement between the different contributors and this is a revised/corrected version of the tables presented in D3.1 [A1] and D3.3 [A3]. The table includes the numbering and naming of the different load cases in order to be prepared for the future assessment of the carbody and to be used for example, by working groups of the standardization bodies.

2.1.1 Fatigue loads

For self-understanding, in the Table 2.1 is explained the nomenclature used in the definition of the load cases for the masses according EN 15663 [A4].

Table 2.1 Masses according EN 15663 [A4]

Design mass of the vehicle in working order	m_1
Design mass of one bogie or running gear	m_2
Normal design payload	m_3
Exceptional payload	m_4

For the category P-II (fixed units and coaches) the following (Table 2.2) fatigue load cases should be taken into account:

Table 2.2 Fatigue load cases for HS

Load Case Name	Main Load Direction(s)	Load Ampitude (max/min Load)	No of Cycles	Vertical Load Condition	Reference/Comment
LC01 Longitudinal forces at buffers and/or coupler attachment	x	+1500kN/-1000kN	1	$1.0g*m_1$	Ref.:EN 12663-1 Table 2,5
LC02 Longitudinal forces at buffers and/or coupler attachment	x	+400kN/-400kN	10^3	$1.0g*m_1$	Ref.: EN 12663-1 6.7.4; Specification SBB BeNe
LC03 Longitudinal forces at buffers and/or coupler attachment	x	+300kN/-300kN	10^5	$1.0g*m_1$	Ref.: EN 12663-1 6.7.4; Specification SBB BeNe
LC04 Longitudinal forces at buffers and/or coupler attachment	x	+200kN/-200kN	10^7	$1.0g*m_1$	Ref.: EN 12663-1 6.7.4; Specification SBB BeNe
LC05 Compressivel forces in end wall area	-	-	0	-	Origin: EN 12663-1 Table 6-8, covered by crash calculation acc. To EN 15227
LC06 Maximum operating Load	z	$1.3g(m_1+m_4) / (1-0.15)g*m_1$	1	-	Ref.:EN 12663-1 Table 9
LC07 Lifting and jacking at one end of the vehicle at specified positions.	z	$1.1g(m_1+m_2) /(1-0.15)g*m_1$	1	-	Ref.:EN 12663-1 Table 10
LC08 Lifting and jacking the whole vehicle at specified positions	z	$1.1g(m_1+2m_2) /(1-0.15)g*m_1$	100	-	Ref.:EN 12663-1 Table 11
LC09 Lifting and jacking with a displacement in the support	z	+ 10 mm/-10mm	3	$1.1g*(m_1+2m_2)$	Ref.:EN 12663-1 6.3.3
LC10 Superposition of static load cases for the vehicle body	x;z	+1500kN/-1000kN	1	$1.0g(m_1+m_4)$	Ref.:EN 12663-1 Table 12
LC11 Track induced loading, acceleration in y-direction	y	$+0.15g*m_1/-0.15g*m_1$	10^7	$1.0g*m_1$	Ref.:EN 12663-1 Table 16
LC12 Track induced loading, acceleration in z-direction	z	$+0.15g*m_1/-0.15g*m_1$	10^7	$1.0g*m_1$	Ref.:EN 12663-1 Table 17
LC13 Aerodynamic loading, exceptional tunnel pressure	Hydrostatic Pressure	+6500Pa/-8000Pa	1	$1.0g*m_1$	Ref.:EN 12663-1 6.1, hydtrostatic pressure defined as outer Pressure(+) - inner Pressure(-)
LC14 Aerodynamic loading, fatigue tunnel pressure	Hydrostatic Pressure	+3500Pa/-3500Pa	10^6	$1.0g*m_1$	Ref.:EN 12663-1 6.6.5, hydtrostatic pressure defined as outer Pressure - inner Pressure
LC15 Traction and braking, acceleration in x-direction	x	$+0.15g*m_1/-0.15g*m_1$	10^7	$1.0g*m_1$	Ref.:EN 12663-1 Table 18
LC16 Proof load cases for body to bogie connection in x-direction	x	+3.0g*m2/-3.0g*m2	1	$1.0g*m_1$	Ref.:EN 12663-1 6.5.1 a)
LC17 Proof load cases for body to bogie connection in y-direction	y	$2*10^4N+1/6g*(m_1+m_4)$ $-2*104N-1/6g*(m_1+m_4)$	1	$1.0g*m_1$	Ref.:EN 12663-1 6.5.1 b), EN 13749 C.2.1
LC18 Static proof loads at interfaces, local load cases for equipment attachments	x	$+3.0g*m_c/-3.0g*m_c$	1	$1.0g*m_c$	Ref.:EN 12663-1 Table 13
LC19 Static proof loads at interfaces, local load cases for equipment attachments	y	$+1.0g*m_c/-1.0g*m_c$	1	$1.0g*m_c$	Ref.:EN 12663-1 Table 14
LC20 Static proof loads at interfaces, local load cases for equipment attachments	z	$+2.0g*m_c/-2.0g*m_c$	1	$1.0g*m_c$	Ref.:EN 12663-1 Table 15
LC21 Fatigue loads at interfaces			-		Ref.:EN 12663-1 6.7; Fatigue loads at interfaces are considered by attaching the equipments (with their masses and stiffnesses) to the carbody while calculating the load cases LC01 .. LC15
LC22 Combination of fatigue load cases			-		Ref.:EN 12663-1 6.8; combination is covered by taking into account the single axis load cases LC11, LC12 and LC14, LC15into the damage accumulation
LC23 Temperature loads		Maximum stress / strain due to thermal expansion (+10°C-+40°C)/(-10°C - -30°C)	Daily 10000 cycles, Seasonal 30 cycles, Tunnel 10-100/day	$1.0g*m_1$	Temperature changes in service conditions play an important role because of different thermal expansion of components, which yields mechanical loading of joints.
LC24 Manufacturing loads	to be defined in dependence of manufacturing process			$1.0g*m_1$	the special treatment the carbody or ist parts is exposed during manufacturing process shall be taken into account as additional load cases

*m_c is the design mass of the attached equipment

In some cases, it is important to note that the loads are defined according equivalent loads defined for metal due to no information for polymers or composite is available, e.g. track induced loads or the traction-compression.

In the case of combination of fatigue load cases (like track induced loads EN 12663-1 [A1], section 6.8), cumulative damage approach should be applied.

2.1.2 Working condition

Speed

According to TSI INF [A5] section 4.2.1, the design speed will be greater than 250km/h (69.44m/s).

Axle loads

According to TSI INF [A5] section 4.2.1, the axle load will be less or equal than 17t (17000kg).

Environmental conditions

In addition, theoretical environmental conditions are defined to cover as much as possible all the climatic conditions of Europe in order to have a design framework for material and joint.

The environmental conditions are defined in accordance to D3.2 Material Assessment [A6] and D3.3 Joining Technologies [A3].

- Environment temperature: from -40°C to +50°C.
- Inside the carbody temperature: up to 70°C.
- Relative humidity: from 5% to 100%.
- Surface temperature: up to 85°C.
- Solar irradiance: 1120W/m^2.

2.1.3 Geometry

The geometry defined in the D3.1 Technical Specification [A1] and collected here should be taken as a reference for the different studies made in Roll2Rail (mainly topology optimization, structural calculation and material alternatives) and can be used for similar purpose in the collaborative part of the Shift2Rail Project.

The configuration is based on a conventional high speed carbody which is in use in several European countries. This allows an international application of the demonstrator and furthermore of the projects results. Besides the definition of a “conventional” car body, like shown below, enables a wide range of operators and rail vehicle manufacturers to use and test the demonstrator. As a result, the project provides from the European Union´s perspective a maximum variety of possible application possibilities. The demonstrator has a length of ca. 25000 mm and is supported in 2 bogies with 2 axles (each).

Below a choice of possible configurations is illustrated how the “Demonstrator Car” could be tested (Figure 2.1 to Figure 2.3):

1. TGV + Demonstrator Car

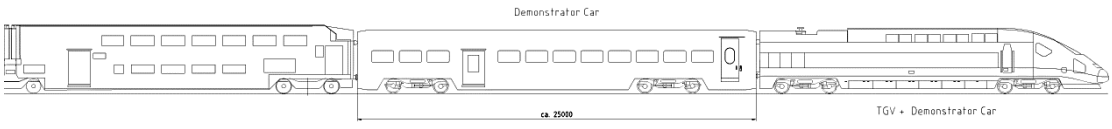

Figure 2.1 Demonstrator+TGV

2. LOC + Demonstrator Car

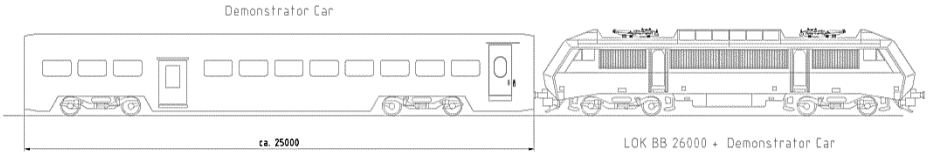

Figure 2.2 Demonstrator+Locomotive

3. Talgo + Demonstrator Car

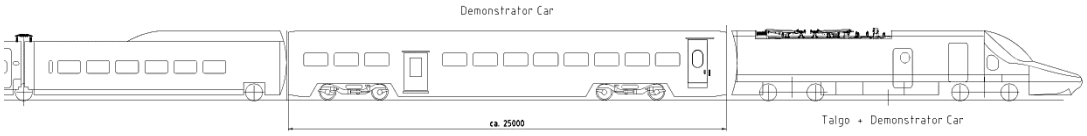

Figure 2.3 Demonstrator+Talgo

The purpose to include the geometry in the final report is to clarify and to provide a context for the studies covered in this report.

General dimensions

- Length: ca. 25000mm.
- Width: ca. 2940mm.
- Height: ca. 4150mm.
- Wheelbase: ca. 17500mm.

Loading gauge

According to EN 15273-2 Annex B, gauge GC [A7].

Exterior shell (master geometry)

The geometry of the car is as shown in Figure 2.4 and it is in accordance with the general dimensions and the gauge GC defined above.

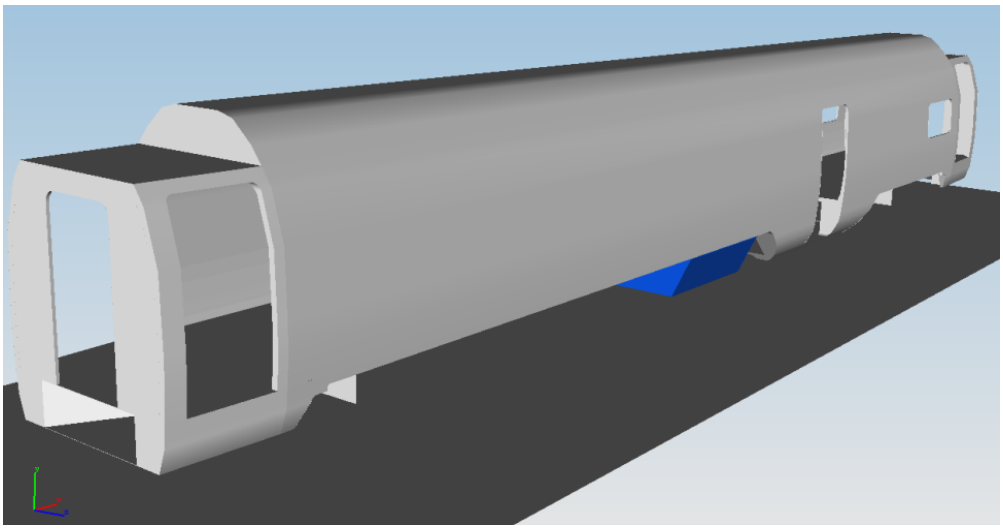

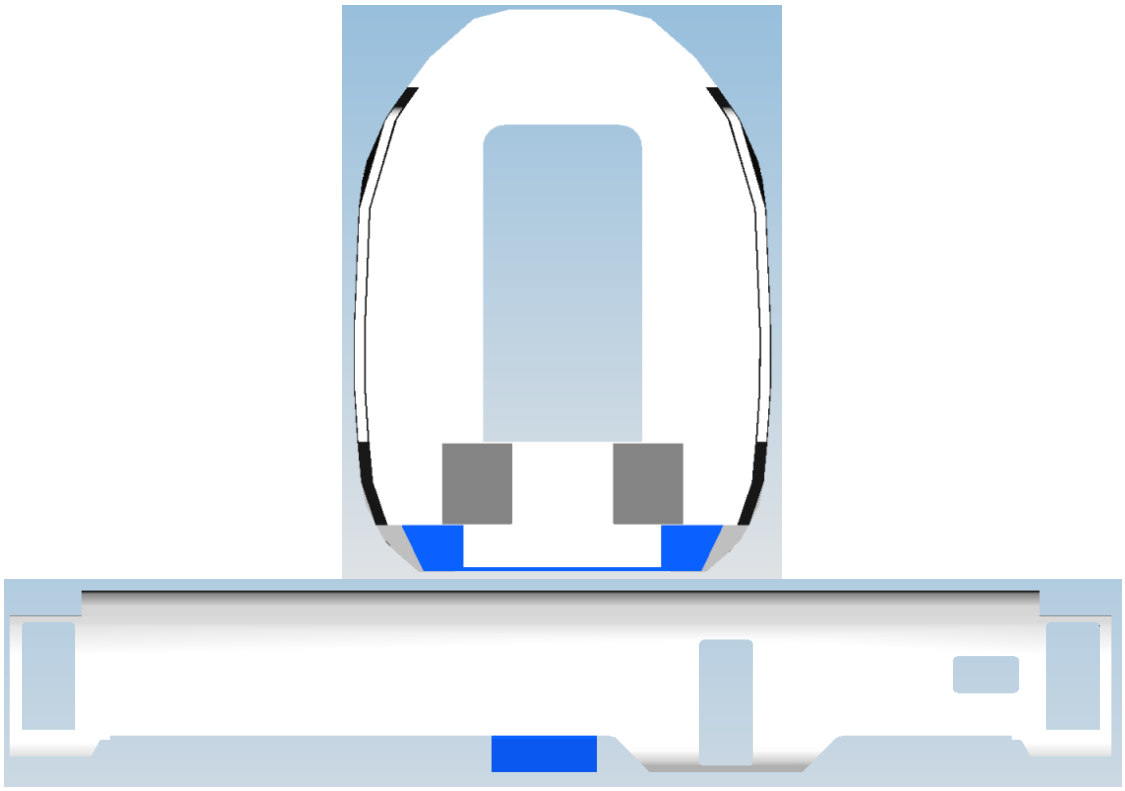

Figure 2.4 Exterior shell geometry for the basic HS demonstrator

In addition to the general dimension, the size of the elements with major impact in the structural calculation is defined:

- The dimension of the windows is 790x1462mm, 10 windows per side.
- The dimension of the service door is 2710x1170mm, one per side.
- The dimension of the entrance door is 2325x1168mm, two per side.
- The structural hole for the gangway corridor is 2200x1110mm.
- The dimension between the end walls and pivot point of the bogies 3362mm.

The research described in the section 2.3 consists on a topological optimization where have been analysed both location and geometry of cuts out for doors and windows and their impact on weight. The results of the topology optimisation can be seen in section 2.3.

2.1.4 Other requirements

Apart from the requirements developed in the previous chapter, other requirements (noise, vibration, thermal requirements, fire requirements, electromagnetic compatibility and maintenance) are developed in detail in the deliverable D3.1 “Car bodyshell specification”, Part 1 [A1].

2.2.1 Fatigue Loads

For the Urban, the fatigue load cases are presented in Table 2.3. As in the HS case, the version published here is the corrected/revised version of the load cases published in D3.1 [A1] and D3.3 [A3].

Table 2.3 Fatigue load cases for Urban

Load Case Name	Main Load Direction(s)	Load Ampitude (max/min Load)	No of Cycles	Vertical Load Condition (z-Direction)	Reference/Comment
LC01 Longitudinal forces at buffers and/or coupler attachment	x	+800kN/-600kN	1	$1.0g*m_1$	Ref.:EN 12663-1 Table 2,5
LC02 Longitudinal forces at buffers and/or coupler attachment	x	+120kN/-120kN	10^3	$1.0g*m_1$	Ref.: EN 12663-1 6.7.4; adopted acc. to TGL 33 398/08
LC03 Longitudinal forces at buffers and/or coupler attachment	x	+90kN/-90kN	10^5	$1.0g*m_1$	Ref.: EN 12663-1 6.7.4; adopted acc. to TGL 33 398/08
LC04 Longitudinal forces at buffers and/or coupler attachment	x	+60kN/-60kN	10^7	$1.0g*m_1$	Ref.: EN 12663-1 6.7.4; adopted acc. toTGL 33 398/08
LC05 Compressivel forces in end wall area	-	-	0	-	Origin: EN 12663-1 Table 6-8, covered by crash calculation acc. To EN 15227
LC06 Maximum operating Load	z	$1.3g(m_1+m_4) / (1-0.15)g*m_1$	1	-	Ref.:EN 12663-1 Table 9
LC07 Lifting and jacking at one end of the vehicle at specified positions.	z	$1.1g(m_1+m_2) /(1-0.15)g*m_1$	1	-	Ref.:EN 12663-1 Table 10
LC08 Lifting and jacking the whole vehicle at specified positions	z	$1.1g(m_1+2m_2) /(1-0.15)g*m_1$	100	-	Ref.:EN 12663-1 Table 11
LC09 Lifting and jacking with a displacement in the support	z	+ 10 mm/-10mm	3	$1.1g*(m_1+2m_2)$	Ref.:EN 12663-1 6.3.3
LC10 Superposition of static load cases for the vehicle body	x;z	+800kN/-600kN	1	$1.0g(m_1+m_4)$	Ref.:EN 12663-1 Table 12
LC11 Track induced loading, acceleration in y-direction	y	$+0.15g*m_1/-0.15g*m_1$	10^7	$1.0g*m_1$	Ref.:EN 12663-1 Table 16
LC12 Track induced loading, acceleration in z-direction	z	$+0.15g*m_1/-0.15g*m_1$	10^7	$1.0g*m_1$	Ref.:EN 12663-1 Table 17
LC13 Aerodynamic loading, exceptional tunnel pressure	Hydrostatic Pressure	-	0	-	Ref.:EN 12663-1 6.1, no high hydrostatic loads due to no pressure tight vehicle body
LC14 Aerodynamic loading, fatigue tunnel pressure	Hydrostatic Pressure	-	0	-	Ref.:EN 12663-1 6.6.5, no high hydrostatic loads due to no pressure tight vehicle body
LC15 Traction and braking, acceleration in x-direction	x	$+0.15g*m_1/-0.15g*m_1$	10^7	$1.0g*m_1$	Ref.:EN 12663-1 Table 18
LC16 Proof load cases for body to bogie connection in x-direction	x	+3.0g*m2/-3.0g*m2	1	$1.0g*m_1$	Ref.:EN 12663-1 6.5.1 a)
LC17 Proof load cases for body to bogie connection in y-direction	y	+3.3*(m1+m4) -3.3*(m1+m4)	1	$1.0g*m_1$	Ref.:EN 12663-1 6.5.1 b), EN 13749 C.5.3
LC18 Static proof loads at interfaces, local load cases for equipment attachments	x	$+3.0g*m_c/-3.0g*m_c$	1	$1.0g*m_c$	Ref.:EN 12663-1 Table 13
LC19 Static proof loads at interfaces, local load cases for equipment attachments	y	$+1.0g*m_c/-1.0g*m_c$	1	$1.0g*m_c$	Ref.:EN 12663-1 Table 14
LC20 Static proof loads at interfaces, local load cases for equipment attachments	z	$+2.0g*m_c/-2.0g*m_c$	1	$1.0g*m_c$	Ref.:EN 12663-1 Table 15
LC21 Fatigue loads at interfaces			-		Ref.:EN 12663-1 6.7; Fatigue loads at interfaces are considered by attaching the equipments (with their masses and stiffnesses) to the carbody while calculating the load cases LC01 .. LC15
LC22 Combination of fatigue load cases			-		Ref.:EN 12663-1 6.8; combination is covered by taking into account the single axis load cases LC11, LC12 and LC14, LC15into the damage accumulation
LC23 Temperature loads		Maximum stress / strain due to thermal expansion (+10°C-+40°C)/(-10°C - -30°C)	Daily 10000 cycles Seasonal 30 cycles Tunnel 10-100/day	$1.0g*m_1$	Temperature changes in service conditions play an important role because of different thermal expansion of components, which yields mechanical loading of joints.
LC24 Manufacturing loads	to be defined in dependence of manufacturing process			$1.0g*m_1$	the special treatment the carbody or ist parts is exposed during manufacturing process shall be taken into account as additional load cases

2.2.2 Working conditions

Speed

The maximum speed is 90 km/h.

Axle loads

Target axle load is 10t.

Environmental conditions

See section “Environmental conditions” of the High Speed Carbody.

2.2.3 Geometry

General dimensions

The following summarizes the main dimensions of the reference coach:

- Length: 15820mm.
- Width: 2530mm.
- Height: 3450mm.
- Wheelbase: 10850mm

Exterior shell (master geometry)

The geometry of the car is as shown in Figure 2.5.

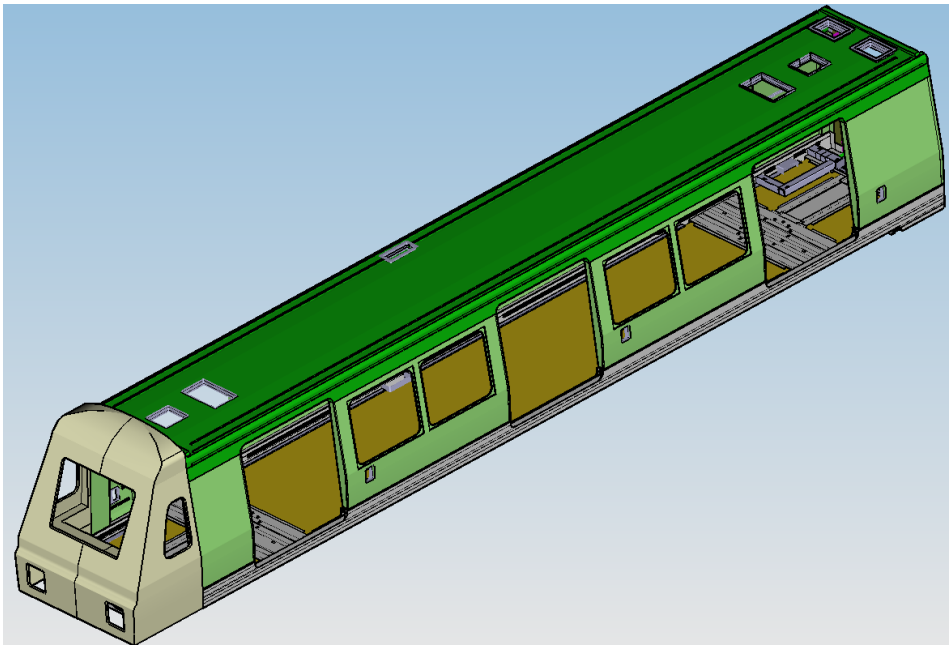

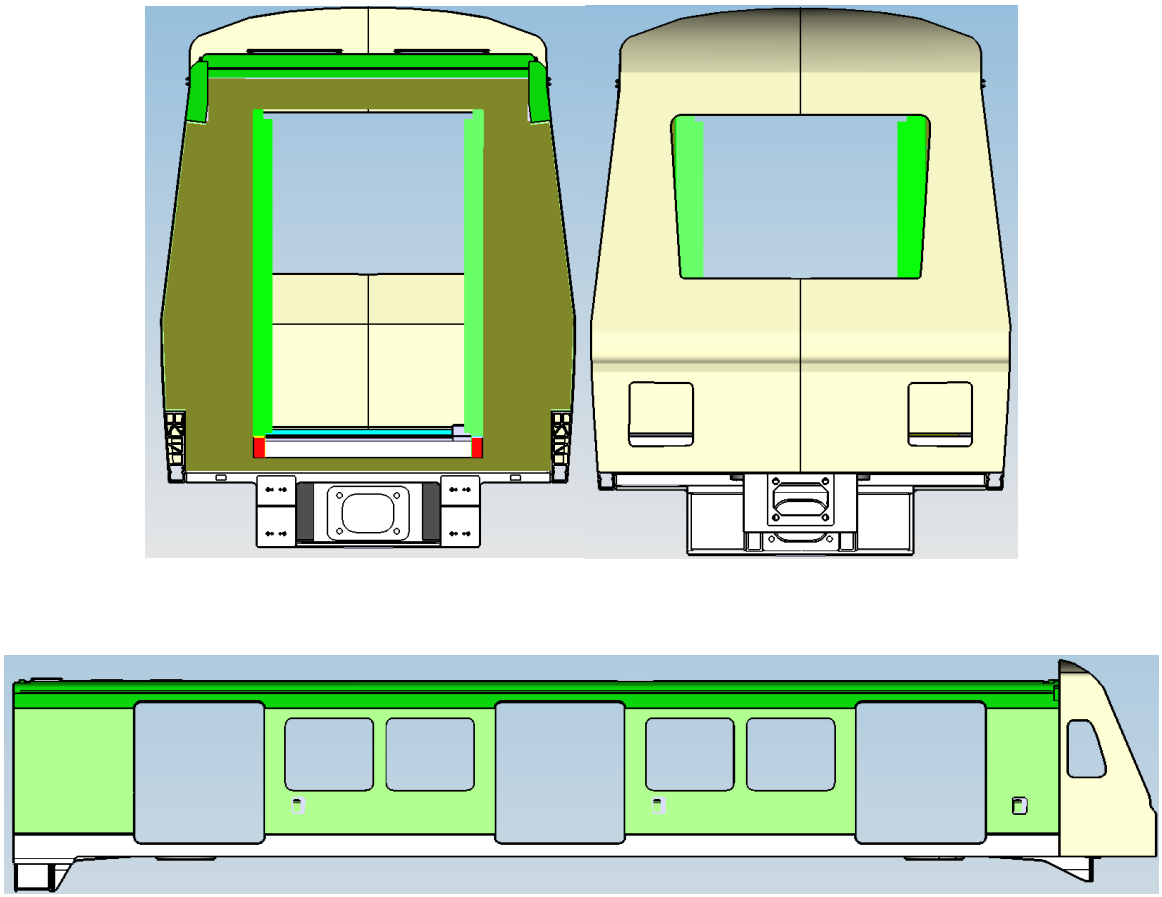

Figure 2.5 Exterior shell geometry for the Urban demonstrator

In addition to the general dimension, the size of the elements with major impact in the structural calculation will be defined:

- The dimension of the windows is 1070x1300mm, 4 windows per side.
- The dimension of the service door is 2040x1900mm, three per side.
- The structural hole for the gangway corridor is 2145x1410mm.
- The dimension between the end walls and pivot point of the bogies 1735mm.
- Floor height from TOR: 1000mm.

A topological optimization, like the one carried out for HS, has been performed in order to analyse the influence of both positioning and geometry of the cuts out in the weight of the carbody.

The analyses as well as the achievable lightweight impact under consideration of the frame conditions for the results of the topology optimization can be seen in the next section.

Train definition

As representative train rake of the “Urban Train” category, a four coaches conventional consist (not-articulated) has been identified.

Each coach rests on two bogies and they are linked together by means of semi-permanent couplers embodying not regenerative buffing devices.

To allow the expected acceleration 50% of the bogies are motor bogies.

2.2.4 Other requirements

Apart from the requirements developed in the previous chapter, other requirements (noise, vibration, thermal requirements, fire requirements, electromagnetic compatibility and maintenance) are developed in detail in the deliverable D3.1 “Car bodyshell specification”, Part 2 [A1].

2.3 TOPOLOGY OPTIMIZATION

2.3.1 Approach for lightweight adapted specification: High Speed

For an extensive weight reduction suitable basic carbody geometry is shown as necessary. The positions of the door and window cut outs have a significant impact on the achievable lightweight potential. For this reason the analysis focusses on the positioning of the door(s) and windows under consideration of the defined conditions. Different configurations and versions of the carbody featuring varying cut out positions are analysed regarding their weight in relation to each other, resulting in information regarding the weight-optimised positioning of cut outs for the doors and windows. For the creation of the configurations and derivatives, a methodical approach was developed to achieve meaningful solutions, see Figure 2.6.

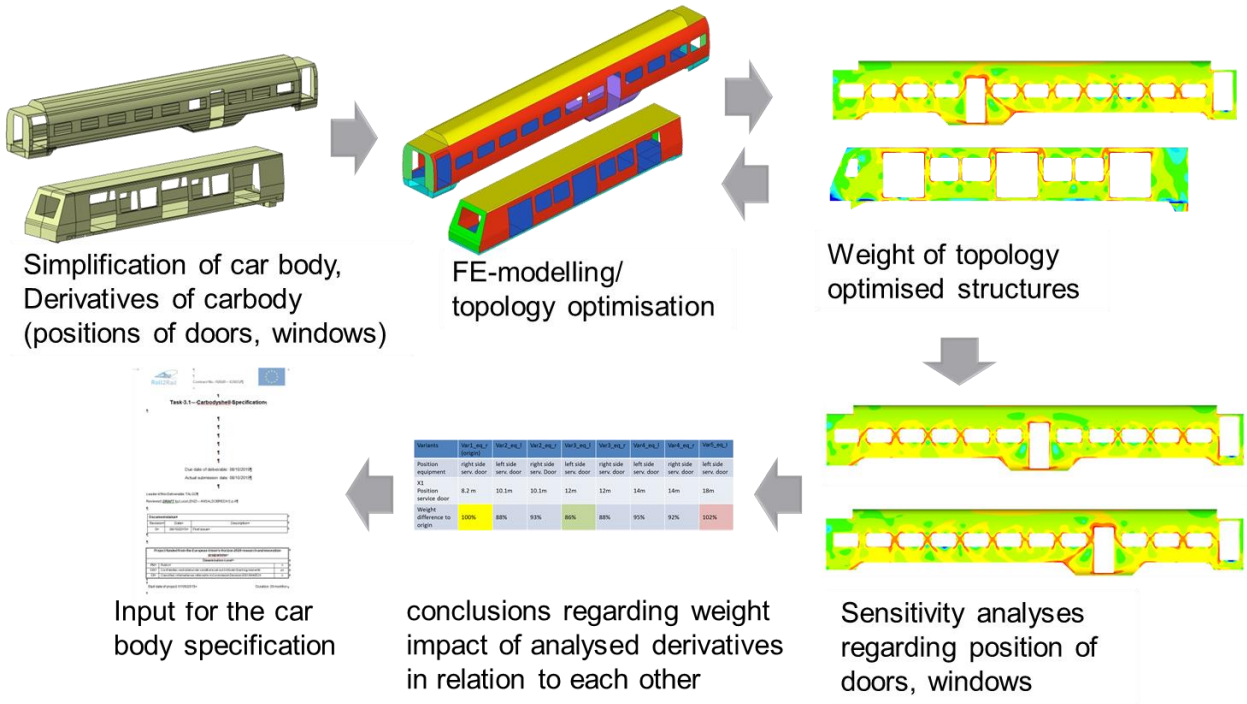

Figure 2.6 Methodical approach for lightweight-adapted cut out positioning

It is important to note that while the approach described here gives a statement in principle regarding the lightweight potential of the carbody derivatives, an exact definition of the achievable weight is not possible. The results of the topology optimisation also do not represent a finished mechanical design, but rather form the basis for lightweight design and sensitivity analyses. Significant simplifications and assumptions are necessary for the approach to function and deliver meaningful conclusions. The approach is useful to understand the impact of different configurations on the weight of the carbody in question. With these considerations taken into account, a comparison of the lightweight potential of the analysed variants is possible.

One of the most important simplifications concerns the material in question, because a topology optimisation is only possible for one material at a time. For this reason the properties of an aluminium alloy (AW6005) are used for the basic material. The use of fibre reinforced plastic (FRP) would require a different kind of optimisation with which weight estimation is not possible. The joining technology is also not considered. Another simplification is that the finite element (FE)-model of the carbody used in this analysis is based on shell modelling (2-D single shell elements with applied wall thickness). For the topology optimisation, a further limitation is that only static loads are possible. For this reason the longitudinal and vertical loads, and their combination according to EN 12663-1 [A2], are used. For the topology optimisation only the exceptional static loads of EN 12663-1 [A2] will be considered. The fatigue loads are overcompensated by the exceptional loads. For this reason, and because of the missing of joints in the optimisation model, the fatigue loads do not need to be considered.

The exceptional static longitudinal loads which were introduced in the High Speed carbody shell during the topology optimisation are shown in Table 2.4. The vertical loads of $m_1 \cdot g$ are considered in every load case.

Table 2.4 Longitudinal loads

Load description	Load
Compressive force at the buffers or coupler attachment (central introduction)	1500kN
Tensile force at coupler attachment	1000kN
Compressive force 150mm above the top of the structural floor at head stock	400kN
Compressive force at the height of the waistrail	300kN
Compressive force at the height of the cantrail	300kN

The vertical loads which are used for the topology optimisation are shown in Table 2.5.

Table 2.5 Vertical loads

Load description	Load
Maximum operating load	1.3g (m_1+m_4)
Standard operating load (SOL)	1g (m_1+m_4)
Load for lifting and jacking at one end of the vehicle	1.1g (m_1 + m_2)
Load for lifting and jacking the whole vehicle	1.1g (m_1 + 2m_2)

Simplification of the introduction of the vertical loads is necessary in order to keep the effort required for the modelling of variants at a manageable level. This also avoids significant manipulation of the load paths in the optimisation due to individual local load introductions. Undesirable effects on the load bearing structure of the topology optimisation are avoided by this.

The vertical loads used are based on the assumed weights of components of realised vehicles and available data. The weight of the windows is considered in relation to their area. The weight of the doors is the same for all the analyses. The vertical loads are divided corresponding to the area in which they are introduced:

- The dead weight of the carbody shell is distributed on the complete carbody shell. It consists of the weight of the optimised structure and the difference in weight between the optimised structure and a real carbody shell.

- The loads due to the equivalent mass on the carbody shell (panelling, insulation, weight of window glass, doors, etc.) are distributed over the areas in which the objects are located.
- The equivalent mass on the floor (seats, floor covering, and exceptional payload) is distributed over the entire floor.
- The weights of the underframe equipment and the roof equipment are located in the corresponding areas. The loads are introduced as concentrated masses.

The exceptional longitudinal and vertical loads are also superposed corresponding to EN 12663-1 [A2]. The superposition of the static load cases can be seen in Table 2.6.

Table 2.6 Superposition of static load cases

Load description	Load
Compressive Buffer force + Standard operating load	1500kN + 1g (m_1+m_4)
Tensile force + Standard operating load	1000kN + 1g (m_1+m_4)

While using the load cases described above, the goal for the topology optimisation is the minimisation of the mass under consideration of limits on displacement and stress. The stress limit corresponds to the basic material which is used in the topology optimisation. The simulation tool OptiStruct uses the Von Mises equivalent stress. The limitation of the displacement depends on the position on the carbody shell and is based on the displacements of realised carbodies, Table 2.7.

Table 2.7 Displacement constraints HS

Constraint	Load steps	Value
Vertical under-floor displacement	Maximum operating load	1‰ of the distance between pivots
Vertical roof displacement	Maximum operating load	2‰ of the distance between pivots
Vertical lifting displacement	Lifting and jacking at one end of the vehicle/ of the whole vehicle	20mm
Longitudinal end wall area displacement	All load steps (except lifting and Maximum operating load)	3‰ of the car body length

Different variants were analysed under consideration of the described parameters and loads. The weight reduction is defined in relation to the reference carbody shell describe previously (Figure 2.7) which is defined as 100% of the weight. Note that the results are based on the explicitly defined conditions and parameters.

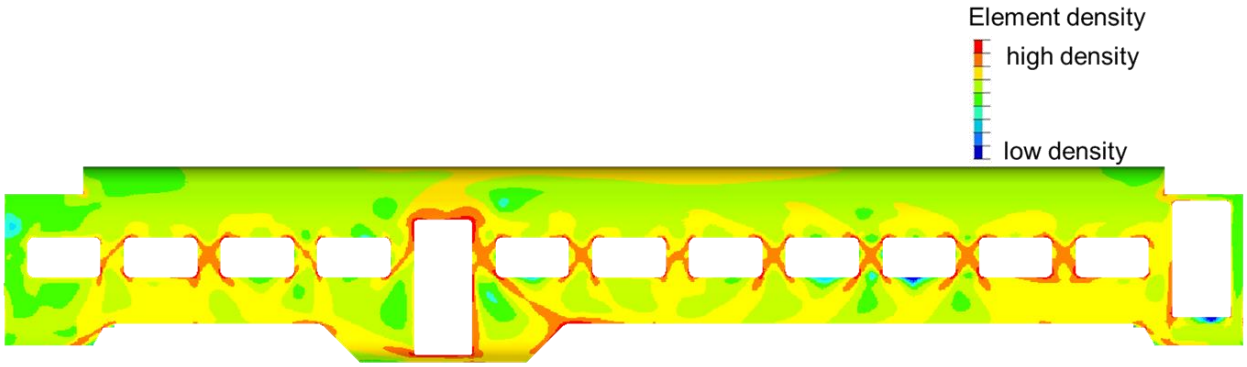

Figure 2.7 Reference carbody shell defined as 100% weight

The following figure (Figure 2.8) gives an impression of the force flow in the underframe resulting from the loading.

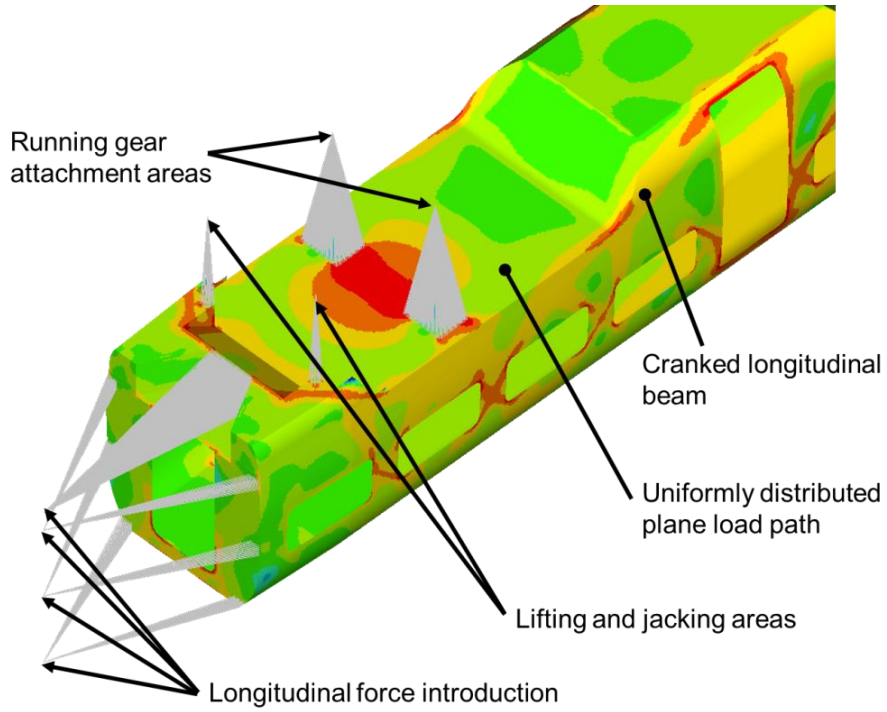

Figure 2.8 Description of the load introduction (HS)

Because of the fanned longitudinal loads in the structure, the structural elements are distributed. Every finite element has an increased element density. Hence the complete area behind the load introduction is a part of the bearing structure. For this reason no shaped load paths are obvious. This is a result of the frame conditions for the weight optimization which is in contrast to the topology optimisation regarding the discrete load path creation.

Different variants were analysed, taking as a reference the base model of the carbody shell shown in Figure 2.7. The results of the analyses are summarized in the Table 2.8.

Table 2.8 Impact of the modifications of the HS carbody shell regarding weight reduction

Derivatives	Maximum weight reduction (based on the frame conditions)
Variation of the service door position	-14%
Service door is omitted (reference: reference carbody)	-5%
Elongating of the pan (reference: optimal service position)	-16%
Enlarging of the window pillars (reference: reference carbody)	-3%
10 instead of 11 windows (reference: optimal service position)	-5%
12 instead of 11 windows (reference: optimal service position)	+5%
Trapezoidal window shapes (reference: reference carbody)	-3%

In the following the analyses of the derivatives are described and discussed.

Variation of the position of the service door

The first variants were generated by moving the service door and underframe equipment without intruding into the space dedicated for the bogies as outlined in Figure 2.9. The windows were moved accordingly.

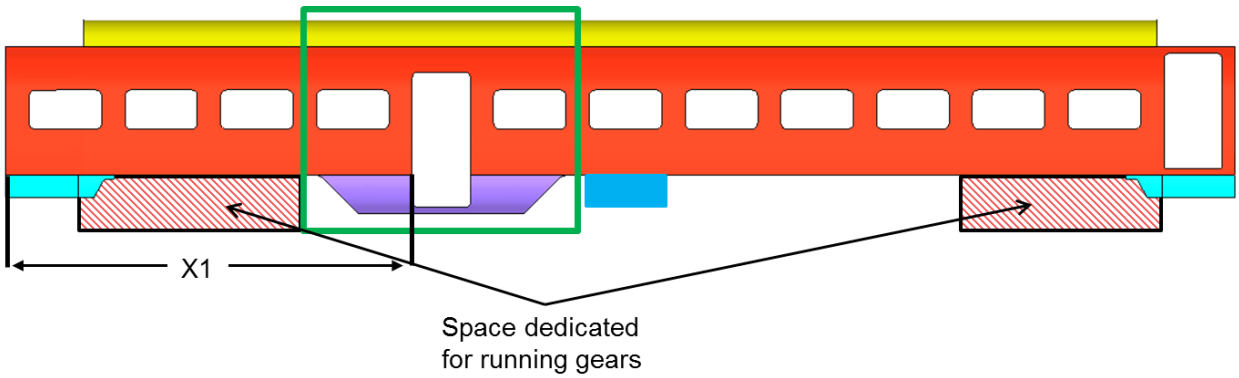

Figure 2.9 Topology optimisation case study for carbody shell

In Table 2.9 the weight differences for the variants can be found in comparison to the reference model. In this case the best behaviour was obtained by locating the service door in the middle of the coach and the equipment on the left side. The reason is that the section of the service door has more inertia than the rest of the coach, so it is achieved more inertia in the most critical section. In addition, taking into account that compression load at coupler level has been also considered, if the change of section is away from the end walls a smoother load path transition is attained.

Table 2.9 Weight improvement according to the variants in the study

Variants	Var1_eq_r (origin)	Var2_eq_l	Var2_eq_r	Var3_eq_l	Var3_eq_r	Var4_eq_l	Var4_eq_r	Var5_eq_l
Position equipment	right side serv. door	left side serv. door	right side serv. Door	left side serv. door	right side serv. door	left side serv. door	right side serv. door	left side serv. door
X1 Position service door	8.2 m	10.1m	10.1m	12m	12m	14m	14m	18m
Weight difference to origin	100%	88%	93%	86%	88%	95%	92%	102%

Service door omitted

For this case, the service door was omitted and the weight impact was analysed. The percentage of weight in comparison to the reference carbody shell is 95% here. The reason for this is the avoidance of the disturbance caused by the service door cut out. Note that a convenient positioning of the service door including the pan and heavy underframe equipment has a higher positive weight impact than the omission of the service door. The pan leads to an increase of the geometrical moment of inertia.

The cut outs of the service doors and the geometry of the pan have an effect on the load bearing structure. For this reason the carbody shells without service doors and pan were also analysed with regard to the effect of widened window pillars. The percentage of weight here is 96% compared to the carbody shell without service doors and 91% compared to the reference carbody shell.

Widened window pillars

The window pillars of this variant have been widened by 100mm, reducing the space available for the glazing. For this case, the percentage of weight compared to the reference carbody shell is 97%

Variation in the number of windows

The number of windows has an effect on the load bearing structure. For this reason the influence of the number of windows on the structure was analysed. The basis for these analyses is the carbody shell with an optimal service door position (Var3_eq_l), with the goal again being to define the carbody variant with the highest lightweight potential. Also the window positioning is more advantageous with the service door in the middle.

In one case the carbody shell has 12 windows instead of 11. The widths of the window and door pillars are reduced (from 470mm to 330mm). The window width is not reduced. The percentage of weight here is 105% compared to the carbody shell with the optimised service door position. The reason for this is that less space is available for a force-flow-adapted load bearing structure in the area of the pillars. This leads to more material being necessary and thus a higher mass.

In the other case the carbody shell has 10 windows instead of 11. The window and door pillars are broadened to 630mm (the reference carbody shell has 470mm). The window width is not increased. The percentage of weight is 95% compared to the carbody shell with the optimised service door position. The percentage is similar to results of the analyses regarding the enlarging of the window pillars. The reason for the low weight benefit is that a nearly optimal force-flow-adapted structure between the windows is already possible for pillars with a width of 470mm. A larger pillar size does not contribute significantly to further mass savings.

Trapezoidal window shapes

The effect of the window shape was also analysed. The window pillars in this variant are diagonal, resulting in trapezoid-shaped windows. The area of the windows is the same as for the reference carbody shell, hence the diagonal pillars have a width of 350mm instead of 470mm.

The percentage weight here is 97% compared to the reference carbody shell. The reason for the limited benefit is that the width of the pillars is smaller than it is in the reference carbody shell. The diagonal pillars indeed offer the possibility of a load-adapted force flow with regard to the global load bearing structure, but not between the windows. A significant weight reduction could be achieved by optimising the position of every pillar, but this would have the effect that geometry of every window is different.

2.3.2 Approach for lightweight adapted specification: Urban

The methodical approach which is used and described for the HS carbody shell is adapted and also used for the urban carbody shell. The main frame conditions are the same for HS and Urban. For this reason only the differences are described here.

The material for the basic metro carbody is steel instead of aluminium. For this reason the properties of a steel (S355) are used for the basic material. For the topology optimisation also only the exceptional static loads of EN 12663-1 [A2] will be considered. The fatigue loads are overcompensated for by the exceptional loads.

The exceptional static longitudinal loads which were introduced in the Urban carbody shell during the topology optimisation are shown in Table 2.10. The vertical loads of $m_1 \cdot g$ are considered in every load case.

Table 2.10 Longitudinal loads

Load description	Load
Compressive force at the buffers or coupler attachment (central introduction)	800kN
Tensile force at coupler attachment	600kN
Compressive force at the height of the waistrail	300kN
Compressive force at the height of the cantrail	150kN

The vertical loads which are used for the topology optimisation are shown in Table 2.11.

Table 2.11 Vertical loads

Load description	Load
Maximum operating load	1.3g (m_1+m_4)
Standard operating load (SOL)	1g (m_1+m_4)
Load for lifting and jacking at one end of the vehicle	1.1g (m_1 + m_2)
Load for lifting and jacking the whole vehicle	1.1g (m_1 + 2m_2)
Load for lifting and jacking the whole vehicle, position under dragbox	1.1g (m_1 + 2m_2)

The simplification of the introduction of the vertical loads is the same like for the HS carbody shells.

The vertical loads used are based on the assumed weights of components of realised vehicles and available data. The weight of the windows is considered in relation to their area. The weight of the

doors is the same for all the analyses. The vertical loads are divided corresponding to the area in which they are introduced (see HS carbody shell).

The exceptional longitudinal and vertical loads are also superposed corresponding to EN 12663-1 [A2]. The superposition of the static load cases can be seen in Table 2.12.

Table 2.12 Superposition of static load cases

Load description	Load
Compressive Buffer force + Standard operating load	800kN + 1g(m_1+m_4)
Tensile force + Standard operating load	600kN + 1g(m_1+m_4)

While using the load cases described above, the goal for the topology optimisation is the minimisation of the mass under consideration of limits on displacement and stress. The stress limit corresponds to the basic material which is used in the topology optimisation. The simulation tool OptiStruct uses the Von Mises equivalent stress. The limitation of the displacement depends on the position on the carbody shell and is based on the displacements of realised carbodies, Table 2.13.

Table 2.13 Displacement constraints Urban

Constraint	Load steps	Value
Vertical under-floor displacement	Maximum operating load	1‰ of the distance between pivots
Vertical roof displacement	Maximum operating load	2‰ of the distance between pivots
Vertical lifting displacement	Lifting and jacking at one end of the vehicle/ of the whole vehicle	20mm
Longitudinal end wall area displacement	All load steps (except lifting and Maximum operating load)	3‰ of the car body length

Different variants were analysed under consideration of the described parameters and loads. The weight reduction is defined in relation to the reference carbody shell (Figure 2.10) which is defined as 100% of the weight. Note that the results are based on the explicitly defined conditions and parameters.

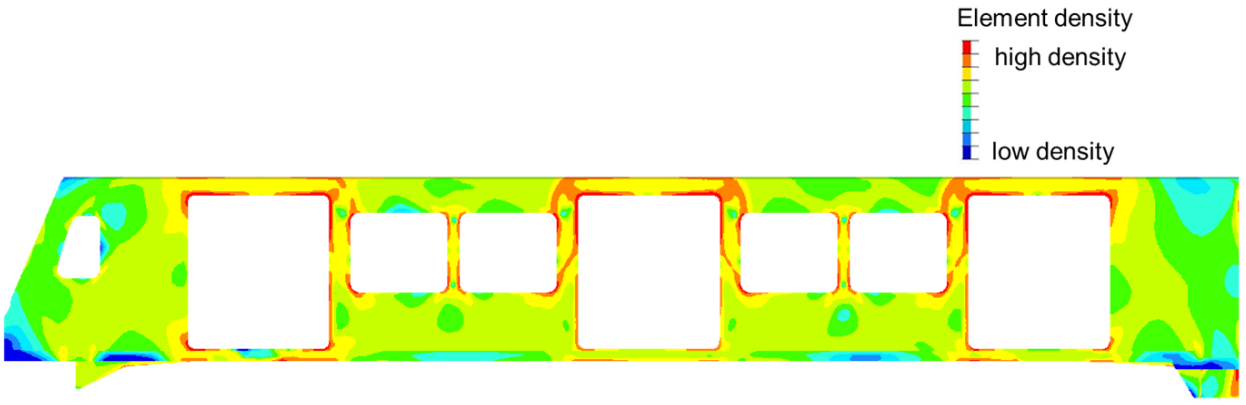

Figure 2.10 Reference carbody shell defined as 100% weight

The following figure (Figure 2.11) gives an impression of the force flow in the underframe resulting from the loading.

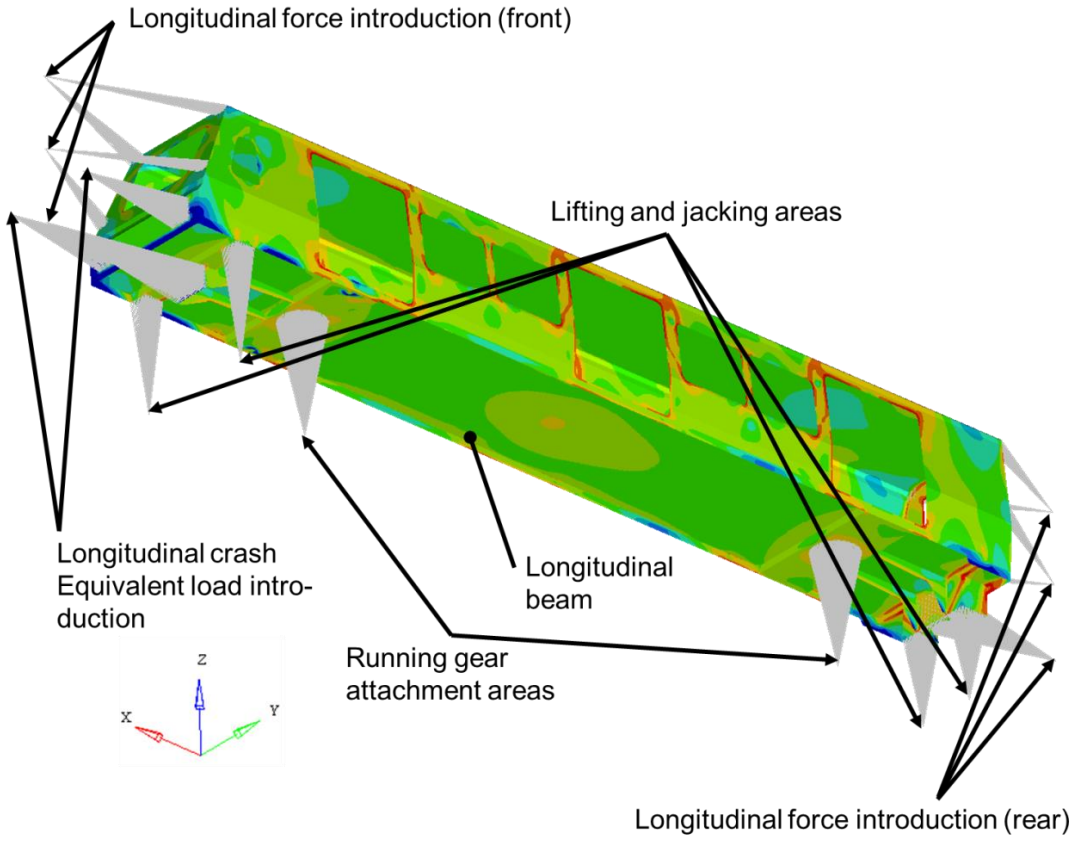

Figure 2.11 Description of the load introduction (Urban)

The reasons for the forming and shape of the load paths are comparable with the described for the high speed train (see above).

Different variants were analysed, taking as a reference the base model of the carbody shell shown in Figure 2.10. The results of the analyses are summarized in Table 2.14.

Table 2.14 Impact of the modifications of the urban carbody shell regarding weight reduction

Derivatives	Maximum weight reduction (based on the frame conditions)
Widened door and window pillars.	-6%
Widening the window frame.	-14%
Division of the door by a door pillar.	-10%
Reduction of the door width by increasing of the width of the window pillars.	-20%
Doors at the ends shifted in the directions of the end bulkheads.	-15%
Three smaller instead of two larger windows between the doors.	+2%
Force-flow-optimised window pillars.	-10.5%
Carbody shell without windows.	-22%

In the following the analyses of the derivatives are described and discussed.

Widened door and window pillars

The degree of optimisation of force-flow-adapted structures depends on the space available for the load path shapes in addition to other factors. For this reason the door and window pillars were widened to 305mm. The base was 282mm for door pillars and 162mm for window pillars. The percentage of weight here is 94% compared to the reference carbody shell

Widening the window frame

In a further step the width of the window frame was increased (+135mm) on all sides to achieve a further weight reduction. The result is a percentage weight of 86% against the reference carbody shell.

Division of the door by a door pillar

A door pillar is installed in the middle of every door to achieve a connection in the area of the large door cut outs. The effect is a weight reduction of 10% compared to the reference carbody shell.

The additional door pillars support the load bearing structure of the rest of the carbody in the areas which are weak because of the large cut outs. It is anticipated that door pillars with a greater width will have a higher impact on the lightweight potential.

Reduction of the door width by increasing of the width of the window pillars

The width of the doors was reduced from 1900mm to 1600mm to create a better basis for the dispersal of the force-flow-adapted load paths. The percentage weight of 80% was achieved compared to the base carbody shell.

Doors at the ends shifted in the directions of the end bulkheads

Analyses were done regarding an optimised door position. For this reason each of the end doors was shifted 500mm in the direction of the bulkhead nearest it. The widths of the door and window pillars were widened to 405mm. The result is a percentage weight of 85% compared to the reference carbody shell.

Three smaller instead of two larger windows between the doors

This case is based on the variant with the end doors shifted in the directions of the bulkheads. Instead of the two windows between the doors, this variant features three smaller windows.

The door and window pillars have a width of 205mm. The percentage weight against the base carbody shell is 102%. The reason for this is the larger disturbance caused by the larger cut out area.

Force-flow-optimised window pillars

In this case the angle of the window pillars is modified. There are two triangular windows on the sides and one trapezoidal window in the middle. All the other parameters are the same as in the base carbody shell. The pillars end at the corners of the windows. Thus a force-flow-adapted structure can be created in the window area. The percentage weight compared to the base is 89.5%.

Carbody shell without windows

For an optimally force-flow-adapted structure as much space as possible is necessary. Thus a carbody shell was created which does not have any windows in the side walls. All the other parameters are the same as the base carbody shell. The achievable weight reduction is here 22%. The percentage weight compared to the reference carbody is 78%. It is anticipated that further lightweight potential could be unlocked by also using optimised door positions.

Comparing both models (Urban and HS), additional conclusion seen in the simulation is that a cross-type structure appears in the lateral panels, in between doors and windows, in both cases. As seen in the results, the urban carbody is more sensitive to the modifications due to more standees allowed and the length of the carbody in combination with the layout of windows and door in the base model.

For more detail regarding the simulations done, see the annex of D3.1 Technical Specification [A1].

2.4 CARBODY TASK FINDINGS

Related with the task 3.1, the Technical Specification of the carbody a complete set of requirements is defined: structural requirements, compilation of thermal, noise and vibration requirements together with EMC and fire requirements. In addition, environmental conditions are defined to cover as much as possible, all the climatic conditions of Europe in order to be a design framework for the carbody, material and joints.

One of the main aspects of the Technical Specification carbody is the definition of the exterior geometry taking into account its impact in the structural calculation and final weight. It is laid emphasis on the weight reduction of the primary structure due to it is one of the expected impacts of Shift2Rail.

In order to evaluate the influence of the geometry of the carbody, a sensitivity study was performed to check the variation in the total weight of the structure owing to slight modifications in the basic geometry of two base models: High Speed and Urban carbodies.

Mainly, the considered modifications have been related with doors and windows: location, dimension of cut-outs in the structure… due to the models employed is based on existing coaches. For this purpose, topology optimization was used.

In this study is calculated the percentage of weight improvement with respect to the base models defined in the beginning. For urban model, different variants were analysed achieving a weight improvement up to 20% in the case of decreasing the width of the door 300mm (-15% in width). For High Speed model, different variants were analysed, being the most interesting alternative to move the service door to the centre of the coach achieving up to 14% in weight reduction.

After these results is necessary to objectify the results achieved with materials and manufacturing criteria and to continue being compatible with the accessibility, interior layout, attractiveness for the passenger and exterior design, being the results shown the master lines for the design phase of Shift2Rail.

The definition of the High Speed and Urban carbodies made in Roll2Rail are the baseline for future collaborative developments in Shift2Rail which has as one of the main goals a weight reduction between 15 and 30% in primary structure.

The experience gained with the use of this methodology shows its potential for an integral lightweight design approach in an early phase of the design process for the future demonstrators of the Shift2Rail Project in order to achieve a significant mass reduction.

3. MATERIALS ASSESSMENT

3.1 INTRODUCTION

This section provides the general overview regarding the material selection process applicable to a typical carbody structure for mass transit rolling stock. The information collected here consists on a summary of the main results of Task 3.2 and D3.2 Material Assessment [B1].

For the material selection the structural components must fulfil requirements covering, at least, the following aspects:

- Mechanical strength
- Thermo-acoustic insulation
- Structural strength in presence of high temperature or humidity
- Maintenance
- Aesthetic
- Lightweight
- Low smoke emissions in terms of optic density and toxicity in case of fire.
- Resistance to corrosion

In addition, materials and processes have to be chosen taking into account eco-design concept in order to reduce environmental impact.

3.2 MATERIALS DESCRIPTION

A brief definition of the different materials considered in this chapter is set out bellow:

- Aluminium extruded profile. Aluminium extrusion is a technique used to transform aluminium alloy into objects with a definitive cross-sectional profile for a wide range of uses. With this technique is possible to achieve very light sections with high area moment of inertia of the cross-section.

  Next it is showed different aluminium profiles in Figure 3.1.

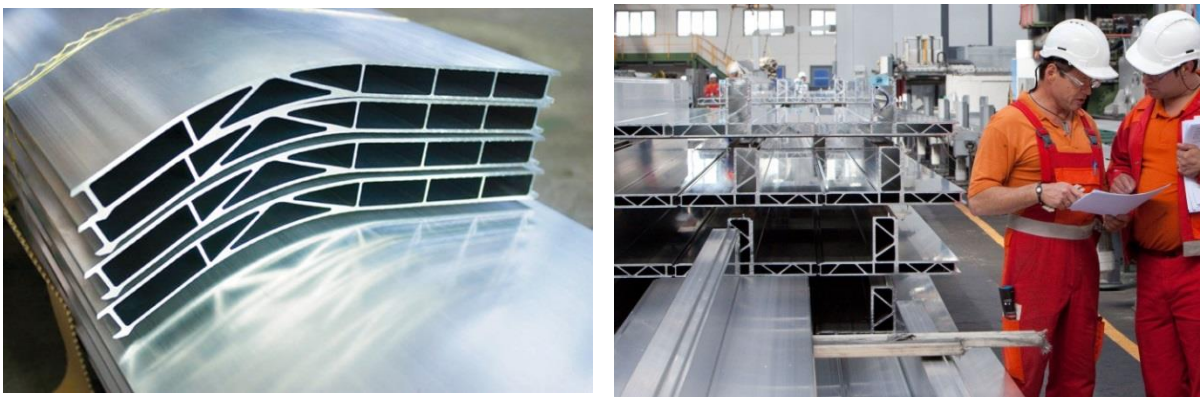

Figure 3.1. Aluminium extruded profiles (source: www.constellium.com)

- Aluminium foam sandwich (AFS) is a sandwich panel product which is made of two metallic dense face sheets and a metal foam core made of aluminium alloy. It is a structural material with a high stiffness-to-mass ratio

  Metal foam is a cellular structure consisting of a solid metal with gas-filled pores comprising a large portion of the volume. The pores can be sealed (closed-cell foam) or interconnected (open-cell foam). The defining characteristic of metal foams is a high porosity: typically only 5-25% of the volume is the base metal, making these ultralight materials.

  In the Figure 3.2 it is showed a section of an aluminium foam sandwich panel.

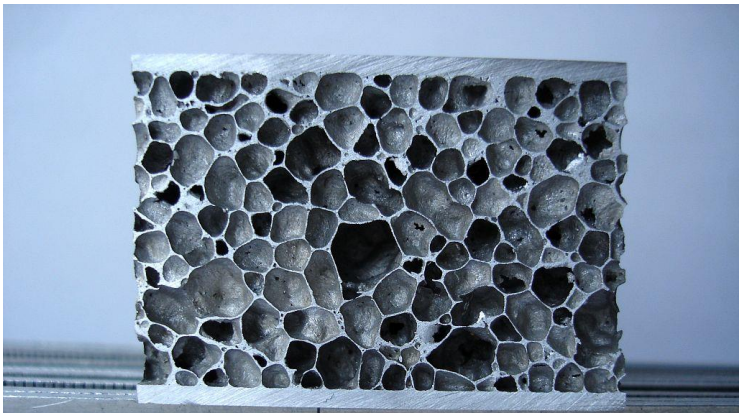

Figure 3.2 Aluminium foam sandwich

- Composite sandwich (FRP skin + foam core). Composite sandwich is a special class of composite material that is fabricated by attaching two thin but stiff skins to a lightweight but thick core (in this case foam core).

  FRP (fibre-reinforced plastic) is a composite material made of a polymer matrix reinforced with fibres. The fibres are usually glass, carbon, aramid or basalt. The polymer is usually an epoxy, vinyl-ester or polyester.

  Foam is a substance that is formed by trapping pockets of gas in a solid. In most foam, the volume of gas is large, with thin film of solid separating the region of gas.

  Next pictures show an example of sandwich with foam core and different foams, Figure 3.3.

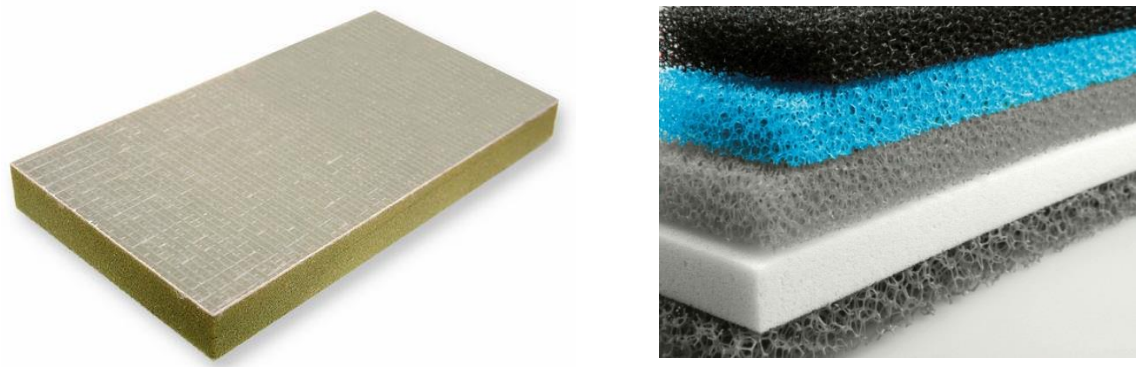

Figure 3.3 Foam core

- Composite sandwich (FRP skin + honeycomb core). In this composite sandwich the main characteristic is the use of a honeycomb as a core.

  Honeycomb core is a structure that have the geometry of a “honeycomb” to allow the minimization of the amount of used material to reach minimal weight and minimal material cost.

  Next it is showed in the Figure 3.4 the layout of a composite sandwich with honeycomb core.

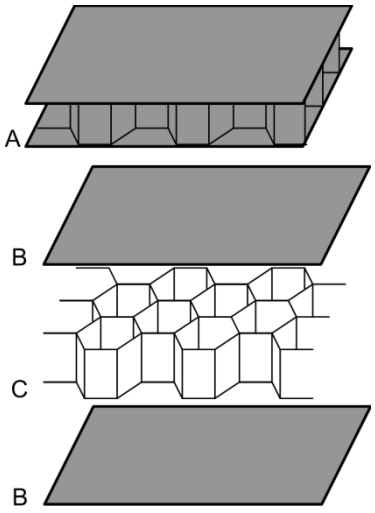

Figure 3.4 Lay out of a composite sandwich with honeycomb. (A) Honeycomb Sandwich, (B) skins and (C) honeycomb core.

- Monolithic composite (FRP) is a kind of composite, the main difference from sandwiches is the absence of a core.

  Next it is showed in Figure 3.5 different pieces of monolithic composite.

Figure 3.5 Monolithic composite

As can be seen, the technology approach has the same objective in the different options, achieving high bending stiffness with overall low density (a very light core with higher thickness and a thinner high strength skins).

3.3 MECHANICAL CHARACTERISTIC AND WEIGHT OF COMPOSITE MATERIALS

In this section is collected the values of the main mechanical properties of the main composite materials. These properties were used for the structural calculation made during the development

of the Work Package. In the section 5 of this document is included the structural calculation of the roof of an urban carbody.

In the laminae strength depends upon the fibres orientation. In particular it is determined by:

- Longitudinal traction strength → X_T (MPa)
- Transversal traction strength → Y_T (MPa)
- Shear strength → S_{XY} (MPa)
- Longitudinal compression strength → X_C (MPa)
- Transversal compression strength → Y_C (MPa)

Other mechanical characteristics are:

- Longitudinal Young's modulus → E_X (GPa)
- Transversal Young's modulus → E_Y (GPa)
- Poisson's ratio → v

In the following tables (Table 3.1 to Table 3.3) the mechanical characteristics of fibres, laminae and core are resumed:

Table 3.1 Fibres mechanical characteristic

Definition	E (GPa)	X_T (MPa)
Carbon fibre	130	4130
DuPont Kevlar® 49	130.98	3990
E-Glass fibre	72.4	3450
Honeywell Spectra®	111.4	3500

Table 3.2 Laminae mechanical characteristics

Definition	E_X (GPa)	E_Y (GPa)	v	X_T (MPa)	X_C (MPa)	Y_T (MPa)	Y_C (MPa)	S_{XY} (MPa)
Carbon/Epoxy Biaxial	66	66	0.3	545	655	545	655	50
Carbon/Epoxy Unidirectional	140	3	0.3	1455	938	24	132	50
Kevlar/Epoxy Biaxial	28	28	0.3	250	250	250	250	50
Kevlar/Epoxy Unidirectional	53	3	0.3	750	750	20	130	50
E-Glass/Epoxy Biaxial	20	20	0.21	492	492	492	492	50
PyroSic® 0/90 lay-up	60	60	-	275	300	275	300	-

Table 3.3 – Foam mechanical characteristics

Definition	$E_{compression}$ (GPa)	$E_{tensile}$ (GPa)	G (GPa)	X_C (MPa)	X_T (MPa)	S_{XY} (MPa)
DIAB Divinycell P60	65	-	13	0.7	1.2	0.45
DIAB Divinycell P100	100	-	28	1.5	1.8	0.85
DIAB Divinycell P150	152	-	40	2.3	2.45	1.25
DOW COMPAXX™ 900-X	55	65	22	0.9	1.35	0.85
3A Airex® T90.60	50	85	12	0.8	1.5	0.46
3A Airex® T90.100	85	120	20	1.4	2.2	0.8

Definition	$E_{compression}$ (GPa)	$E_{tensile}$ (GPa)	G (GPa)	X_C (MPa)	X_T (MPa)	S_{XY} (MPa)
3A Airex® T90.150	115	170	30	2.2	2.7	1.2
3A Airex® T90.210	170	225	50	3.5	3.0	1.85
3A Baltek® SB.50	1616	1682	136	5.5	3.9 (Polyester resin) 9 (Epoxy resin)	1.8
3A Baltek® SB.100	2526	2791	187	9.2	5.7 (Polyester resin) 12 (Epoxy resin)	2.6
3A Baltek® SB.150	4428	6604	362	22	12.2 (Polyester resin) 18.3 (Epoxy resin)	5.2
Duocel® Aluminium foam	103.1	101.8	199.95	2.53	1.24	1.31

Because of the main objective of this project is a mass reduction with respect to a classic aluminium/steel carbody structure from Table 3.4 to Table 3.7 is summarized the specific weight for skin and cores:

Table 3.4 – Typical core density

Core type	Core Density
Polyethylene-terephthalate (PET) foam	0.07-2.5 g/cm^3
Polyvinyl-chloride (PVC) foam	0.04-1.56 g/cm^3
Polyethersulfone (PES) foam	~1.37 g/cm^3
Polymethacrylimide (PMI) foam	0.032-0.191 g/cm^3
Polyurethane (PU) foam	0.025-1.39 g/cm^3
Polystyrene (PS) foam	0.013-1.18 g/cm^3

Table 3.5 – Commercial core density

Commercial core type	Core Density
AluFoam – reticulated foam	0.11 to 0.27 g/cm^3
AluFoam – regular stacked cell foam	0.41 g/cm^3
DOW COMPAXX 900-X structural foam	0.060 g/cm^3
DIAB Divinycell P60	0.065 g/cm^3
DIAB Divinycell P100	0.11 g/cm^3
DIAB Divinycell P150	0.150 g/cm^3
Airex® T90.60	0.065 g/cm^3
Airex® T90.100	0.1 g/cm^3
Airex® T90.150	0.145 g/cm^3
Airex® T90.210	021 g/cm^3

Table 3.6 – Typical fibre density

Fibre type	Fibre density
Carbon	1.76-1.78 g/cm^3
Glass	2.54-2.60 g/cm^3
Kevlar® 49	~1.44 g/cm^3
Spectra®	~0.97 g/cm^3

Table 3.7 – Typical resin density

Resin type	Resin density
Polyester	~ 1.65 g/cm^3
Epoxy	1.19-1.34 g/cm^3
Vinyl-ester	~ 1.03 g/cm^3
Phenolic	1.39-1.43 g/cm^3
Cyanate	1.19-1.25 g/cm^3

As a reference, the density of the steel is approximately between 7.75 and 8.05g/cm^3 and for aluminium 2.70g/cm^3.

3.4 CONCEPTUAL PROPOSAL FOR CARBODY STRUCTURE

A typical carbody structure can be divided into 5 main subassemblies which are:

- Underframe
- Side walls
- Roof
- Cabin
- End wall

Each one of such parts can be manufactured in various ways depending on materials architecture. A list of material alternatives will be presented per subassembly.

3.4.1 Underframe

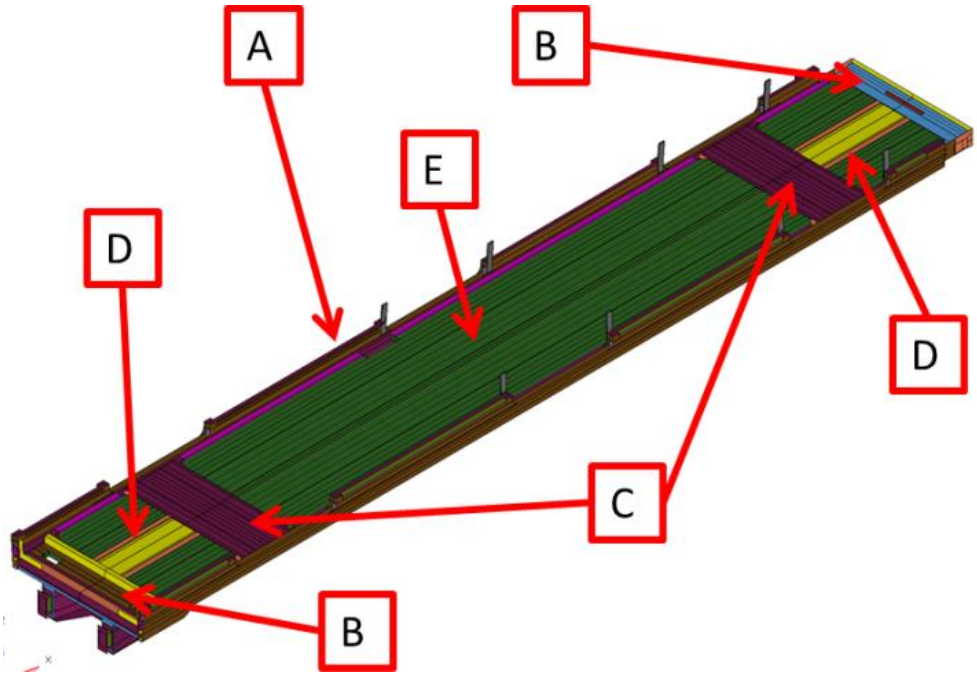

Figure 3.6 Typical metro underframe

The proposals regarding the realization of the underframe are the following according Figure 3.6:

A. Side sill:
    a. Aluminium extruded profile.
B. End beam:
    a. Aluminium extruded profile.
C. Bogie beam:
    a. Aluminium extruded profile.
D. Rafter beam:
    a. Aluminium extruded profile.
E. Floor:
    a. Aluminium extruded profile.
    b. Aluminium foam sandwich.
    c. Composite sandwich (FRP skin + foam core).

And every possible combination for any subcomponents.

3.4.2 Side walls

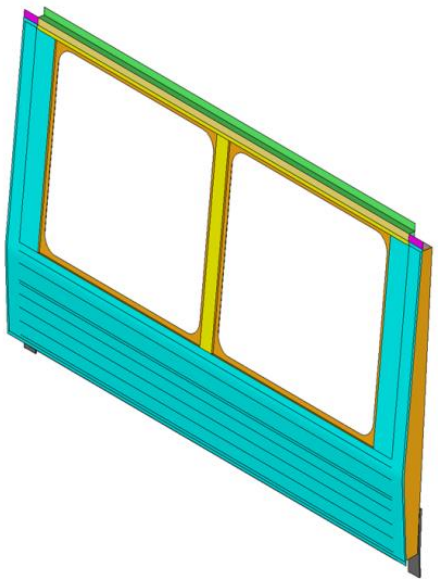

Figure 3.7 Typical metro side walls

The proposals regarding the realization of the side walls are:

A. Composite sandwich (FRP skin + foam core).
B. Composite sandwich (FRP skin + honeycomb core).
C. Aluminium foam sandwich.

And every possible combination for any subcomponents.

3.4.3 Roof

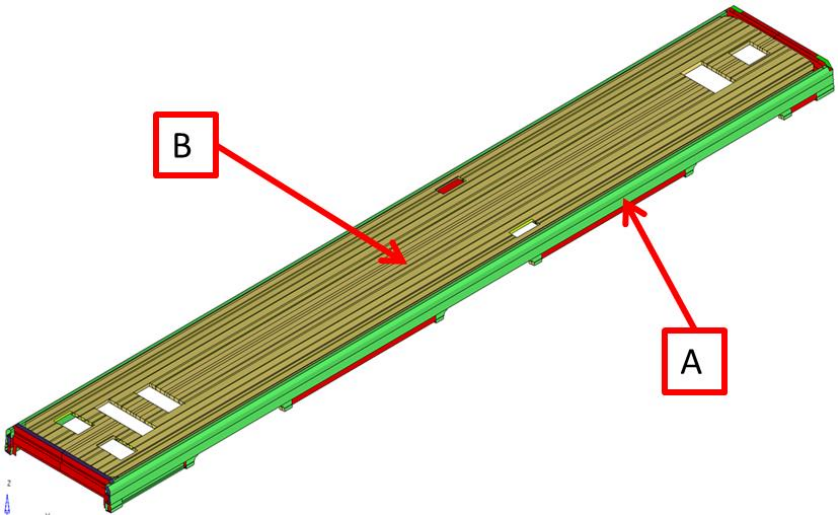

Figure 3.8 Typical metro roof

The proposals regarding the realization of the roof are the following according Figure 3.8:

A. Cantrail:
    a. Aluminium extruded profile.
    b. Composite sandwich (FRP skin + foam core).
B. Central roof
    a. Aluminium foam sandwich.
    b. Composite sandwich (FRP skin + foam core).
    c. Composite sandwich (FRP skin + honeycomb core).
    d. Monolithic composite (FRP).

And every possible combination for any subcomponents.

3.4.4 Cabin

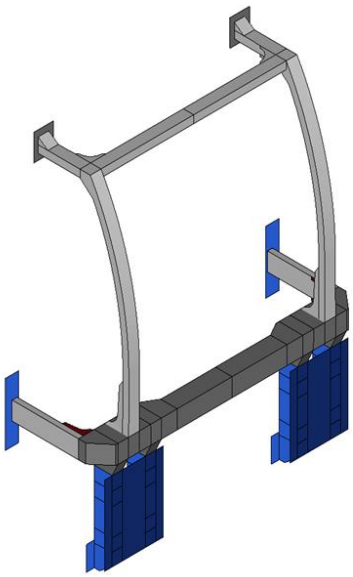

Figure 3.9 Typical metro cabin

The proposals regarding the realization of the cabin are:

A. Aluminium extruded profile.
B. Composite sandwich (FRP skin + foam core).
C. Steel tube.

And every possible combination for any subcomponents.

3.4.5 End wall

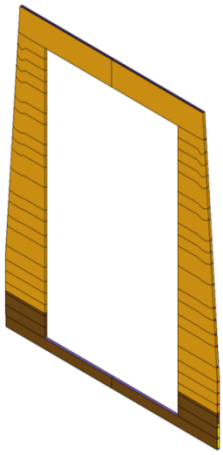

Figure 3.10 Typical end wall

The proposals regarding the realization of the cabin are:

A. Aluminium foam sandwich.
B. Composite sandwich (FRP skin + foam core).
C. Composite sandwich (FRP skin + honeycomb core).
D. Monolithic composite (FRP).

And every possible combination for any subcomponents.

3.5 REQUIREMENTS

3.5.1 Environmental Conditions

In addition to general requirement at train level, (see section Environmental conditions), in order to homologate the materials that will be chosen in the manufacturing of the carbody structure, tests in the climatic chambers have to be carried out. It is very important to set the proper parameters to obtain the most realistic and worst condition which the different components of the structure are subjected; such parameters are:

- Temperature → 70°C
- Humidity → 90%
- Exposition time → 1000h

3.6 CONCEPTUAL DESIGN FOR MATERIAL PRE-SELECTION

The force flow and the direction of forces in the carbody structure have a high relevance for the material assessment and the material choice in the corresponding areas (e.g. direction of the

fibres, pultruded profiles, use of sandwich elements, etc.). For this reason, knowledge of the load paths and the directions of the forces (unidirectional, multidirectional) is necessary to define the suitable local materials and the corresponding mechanical requirements of the local materials in the carbody structure. The target is the pre-selection of the most suitable material in the different areas of the carbody under consideration of the requirements and loads.

A pre-selection of the locally suitable material is accomplished by using a free-size optimisation in Optistruct. In this FE based optimisation tool the shell of the carbody (shell model) is built up with different ply orientations and ply thicknesses. Every ply has the properties of a unidirectional fibre reinforced plastic material with the same wall thicknesses at the beginning. The single plies are stacked and added together, with the fibre orientation different for every ply but constant within each ply. The orientation starts with 0° for the first ply and rises in +/-22.5° steps until 90° is reached. A foam core is located between the plies with negative orientations and the plies with positive orientations.

In the free-size optimisation the wall thickness of every ply is adapted to the local loads (only wall thickness reduction) for every finite element, under consideration of the imposed conditions (displacements). The loads which were introduced into the carbody and the displacement constraints are based on EN 12663 [B2]. These are the same which were used for the topology optimisation in D3.1 Carbody Specification [B3], see Table 2.4 to Table 2.7 for HS and Table 2.10 to Table 2.13 for Urban. The result of the free-size optimisation is the distribution of the wall thicknesses for every ply. The analyses of every ply show which local wall thickness are necessary in each area of the carbody shell to fulfil the requirements. For every single ply the fibres are oriented in only one direction. Under consideration of these it can be interpreted where load bearing elements are necessary with the corresponding orientation of the fibres.

The analyses and superposition of the results of the free-size optimisation of every ply provide information regarding the different orientation of the fibres for each area of the carbody shell. For example, if mainly one ply (one fibre direction) of all the plies is well developed then it is suitable to use fibre reinforced plastic reinforcements with a mainly unidirectional orientation. If several or even all plies are well developed in a load path area, then a (quasi-) isotropic FRP lay-up or a metallic load bearing element is suitable. Based on these results it can be estimated in which area which material is suitable.

This procedure is used for the Urban carbody as well as the HS. In the free-size optimisation the classical laminate theory is used. The optimisation strategy is the minimal volume. The material parameters are the same for the Urban and the HS. They are based on the typical parameters for CFRP which is used for example in the automotive industry (Table 3.8). For CFRP the orthotropic material law is used in the optimisation. The parameters of the foam core correspond with foam which is suitable for railway vehicles (Table 3.9).

Table 3.8 Material parameters for CFRP in the free-size optimisation

UD-CFRP (assumed orthotropic material law)	**Material parameters**
Young's Modulus longitudinal	140GPa
Young's Modulus transverse	8.5GPa
Poisson's Ratio:	0.35
Shear-Modulus	4.2GPa
Density	1.5g/cm^3

Table 3.9 Material parameters for the foam-core in the free-size optimization

Foam-core (assumed isotropic material law)	**Material parameters**
Young's Modulus longitudinal	75MPa
Shear-Modulus	25MPa
Density	0.52g/cm^3

For a compact overview of the results of the free-size optimisation, the wall thickness distributions of all plies are superimposed in the following figures. But for the interpretation of the main fibre directions and the suitable material behaviour it is necessary to compare the directions of the fibres ply by ply.

The interpretation of the results of the free-size optimisation for the Urban carbody and the HS carbody is realised here only qualitatively and in principle. It would be necessary to carry out detailed analyses under consideration of the details of the geometry and the load flow for the direct implementation of the mechanical design. Under consideration of the interpretation in principle, in areas showing quasi-isotropic orientation of the fibres, quasi-isotropic FRP or metallic elements are the most suitable materials. In the areas where the fibres are oriented in one main direction, it is suitable to use FRP with the corresponding main direction of the fibres. Note that the lightweight benefit of FRP use can nearly be cancelled out when using quasi-isotropic FRP elements with large wall-thicknesses and local force introductions, especially when compared to a suitable metallic implementation.

3.6.1 Interpretation of the results of the free-size optimisation (Urban)

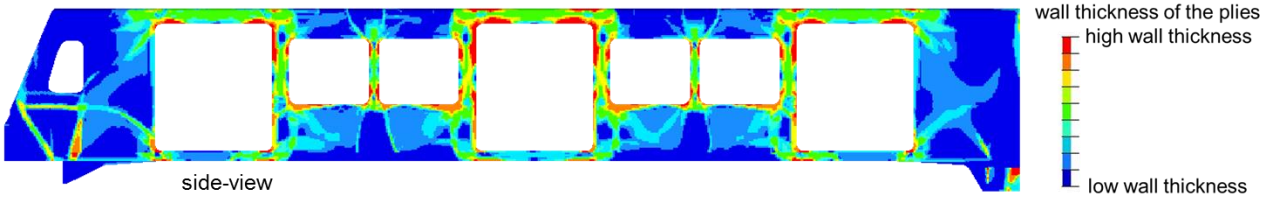

Figure 3.11 Superposition of ply thicknesses (Urban, side-view, fibre directions 0°, ±45° and 90°)

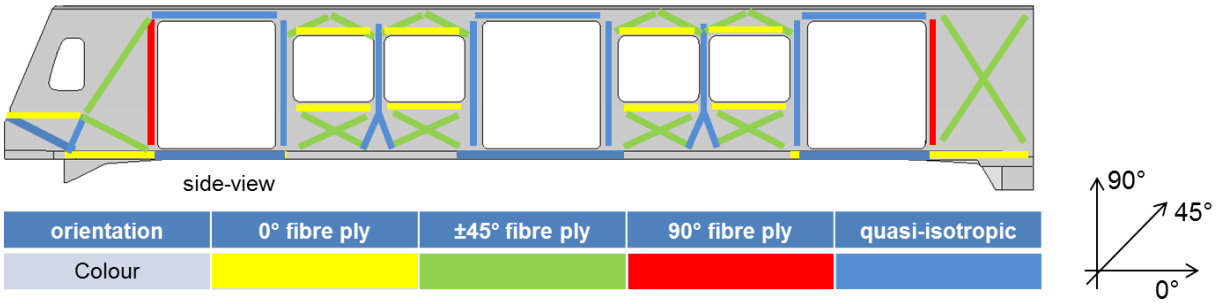

Figure 3.12 Qualitative interpretation of the main fibre directions (Urban, side view)

The qualitative illustration of the interpretation of the main fibre directions (Figure 3.12) of the side wall shows multiaxial loading around the doors and between the windows. For this reason a frame around the doors with a high stiffness and strength in all spatial directions is suitable. Stiffeners are also necessary between the windows. For these areas (quasi-)isotropic materials are most suitable, corresponding to Figure 3.12. Directly above and below the windows, longitudinal beams

with a primarily 0° orientation are necessary. Shear forces dominate in the carbody structure below and above the window beams. Thus 45° composite plies are suitable there. The rest of the sidewall structure needs local longitudinal and vertical beams and stiffeners as well as shear elements. In the transition from the sidewalls to the underfloor, longitudinal beams consisting of (quasi-)isotropic material and material with an orientation of 0° are necessary.

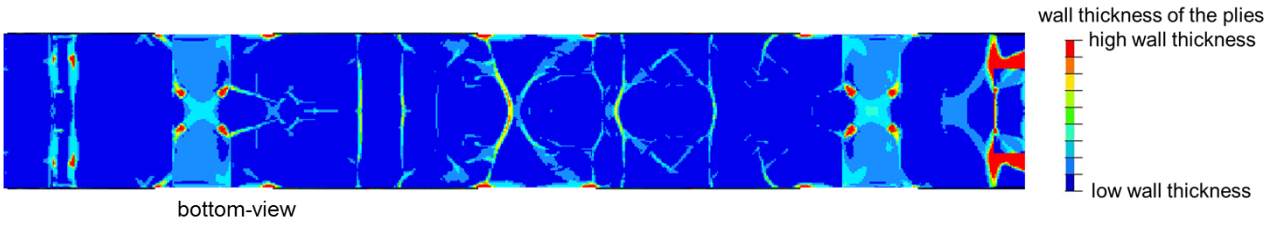

Figure 3.13 Superposition of ply thicknesses (Urban, bottom view, fibre directions 0°, ±45° and 90°)

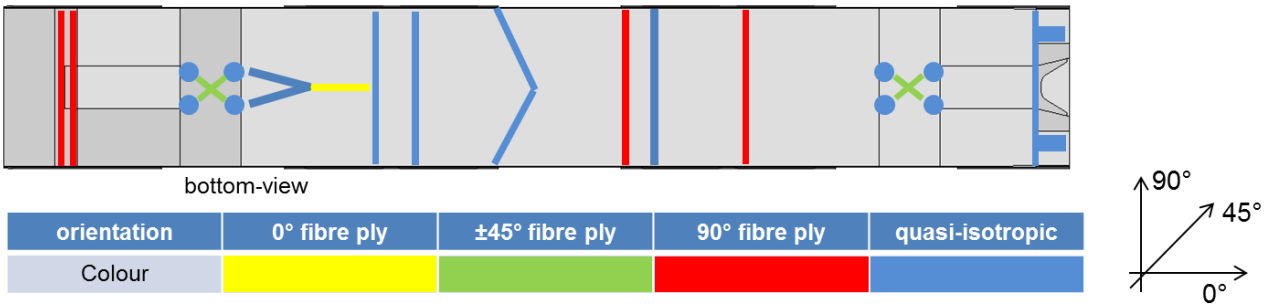

Figure 3.14 Qualitative interpretation of the main fibre directions (Urban, bottom view)

Different loads act in different directions in the underfloor. In the areas where the geometry of the carbody is complicated or uneven, or where high local loads with different force directions are introduced, (quasi-)isotropic material is suitable (Figure 3.13 and Figure 3.14). These areas are, for example, the points for lifting and jacking, connections to the bogies and the connection areas to heavy equipment.

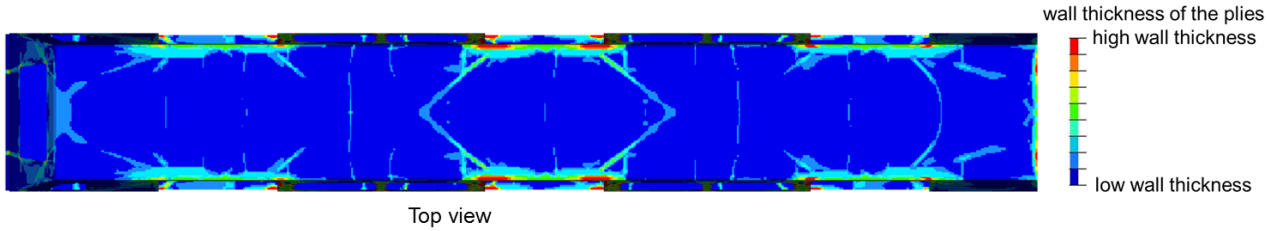

Figure 3.15 Superposition of ply thicknesses (Urban, top view, fibre directions 0°, ±45° and 90°)

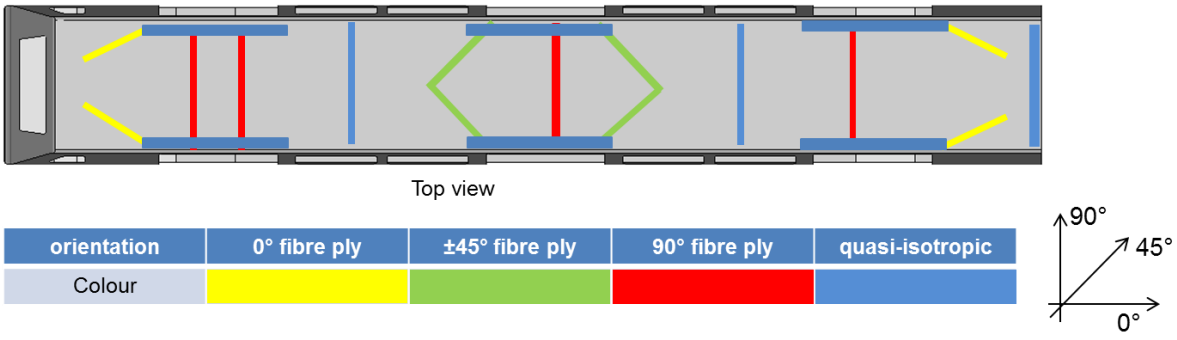

Figure 3.16 Qualitative interpretation of the main fibre directions (Urban, top view)

The interpretation of the thicknesses of the plies in the roof shows (quasi-)isotropic reinforcements (Figure 3.16) above the doors. The connection of these reinforcements to a longitudinal roof beam is suitable. Beside these beams, further lateral and diagonal beams with different fibre directions are necessary.

3.6.2 Interpretation of the results of the free-size optimisation (HS)

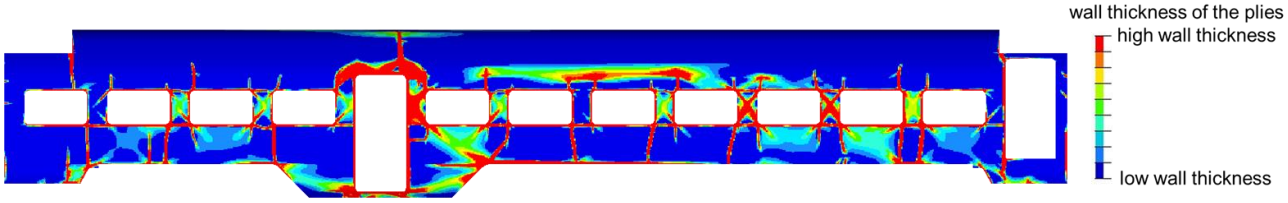

Figure 3.17 Superposition of ply thicknesses (HS, side-view, fibre directions 0°, ±45° and 90°)

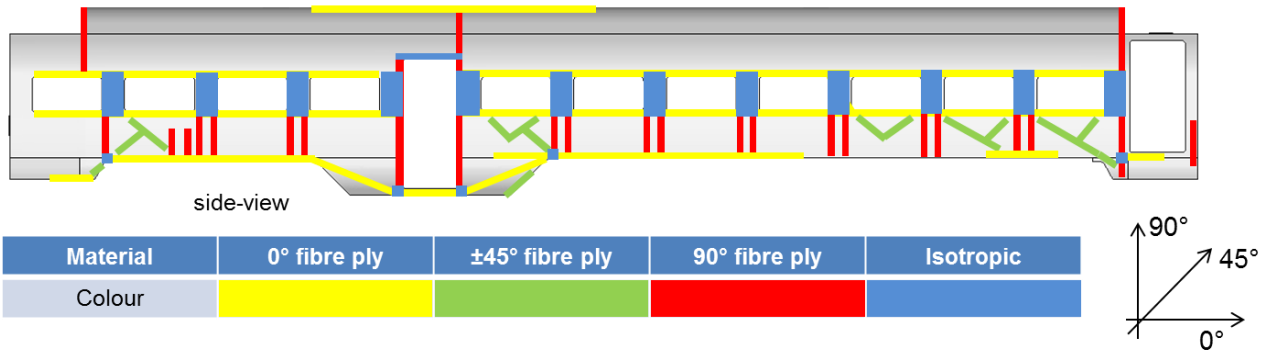

Figure 3.18 Qualitative interpretation of the main fibre directions (HS, side view)

The qualitative illustration of the interpretation of the main fibre directions (Figure 3.17 and Figure 3.18) of the side wall of the HS shows a multiaxial loading between the windows, which can be interpreted as ideal for isotropic material. This is due to high concentration of ±45°-load paths superimposed with highly concentrated 90° load paths vertical load paths at vertical edges of the window frames. Below and above the window pillars, a high concentration of 0° load paths can be interpreted as longitudinal beams. Further ±45° reinforcements at the ends of the car and in the area of the lower entrance provide additional stiffness.

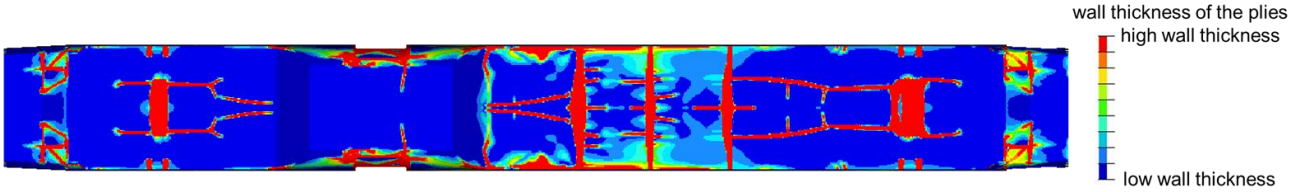

Figure 3.19 Superposition of ply thicknesses (HS, bottom view, fibre directions 0°, ±45° and 90°)

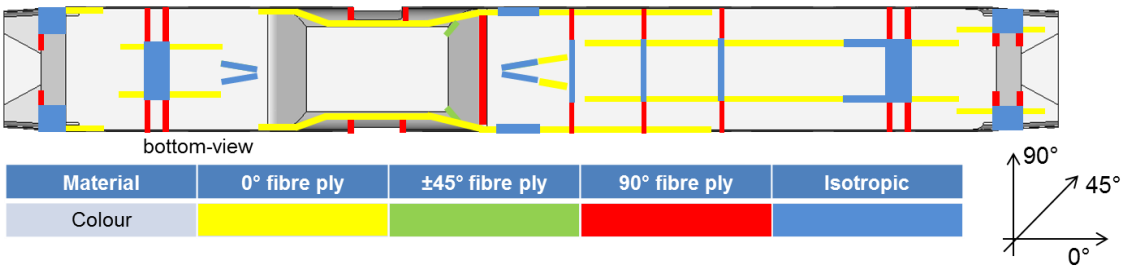

Figure 3.20 Qualitative interpretation of the main fibre directions (HS, bottom view)

The floor contains the highest concentration of 0° load paths (Figure 3.20). The results can be interpreted as a continuous frame of longitudinal beams, with longitudinal beams in the area of lower entrance following the narrowing of the outer skin (this is due to the restrictions of the railway loading gauge). As a result of the interpretation of the 90°-fibre direction results, this longitudinal frame is complemented by cross beams, where these beams are preferably in the area of the running gear attachment or the mounting area of the underfloor equipment. Load paths representing the ±45°-fibre orientation are not predominant. Areas where longitudinal, transverse and shear load paths are overlaid can be interpreted as suitable for isotropic material. These areas are for example the points for lifting and jacking, connections to the bogies and the connection areas to heavy equipment.

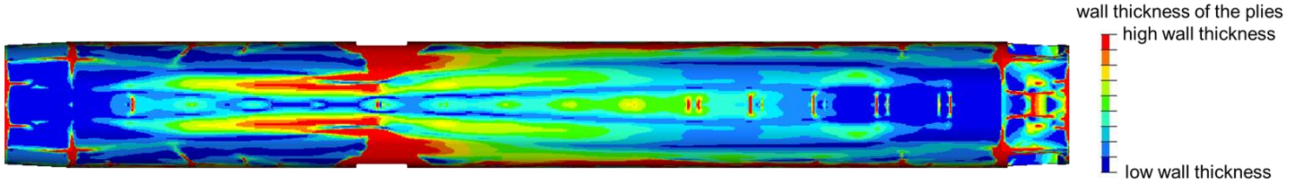

Figure 3.21 Superposition of ply thicknesses (HST, top view, fibre directions 0°, ±45°, and 90°)

Note: The colour scale has been modified for improved interpretation of the roof structure.

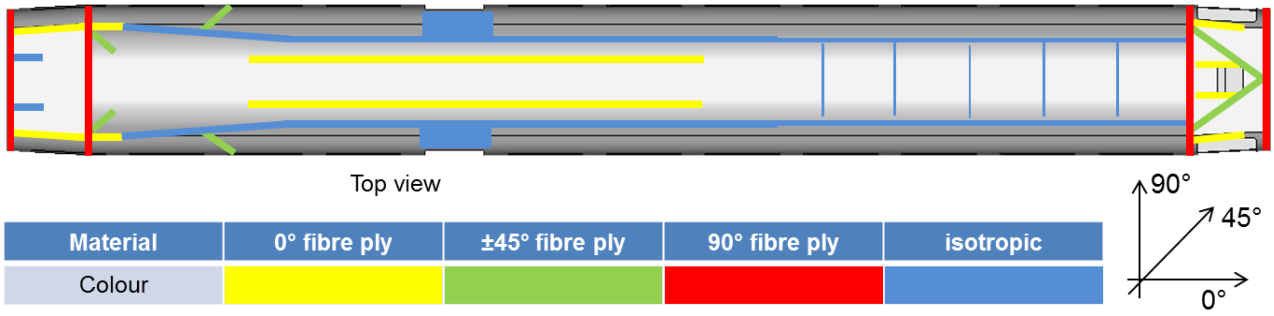

Figure 3.22 Qualitative interpretation of the main fibre directions (HST, top view)

The interpretation of the thicknesses of the plies in the roof shows (quasi-)isotropic reinforcements (Figure 3.21 and Figure 3.22) above the doors and an isotropic frame consisting of longitudinal and transverse beams. In comparison to other structural beams, they are more modestly dimensioned, as shown by thinner lines. Reinforcements in longitudinal direction mainly consisting of a 0°-fibre orientation are found at the outer ends and in the roof area in between the lower entrances. Discrete reinforcements with a preferred ±45°fibre orientation are shown in some areas, but the occurrence of ±45°- fibre reinforcement is mainly distributed over the roof-structure. Thus this can be interpreted as a large and thin skin panel.

3.7 MATERIAL TASK FINDINGS

Regarding materials, the most challenging part is the related with all the requirements associated with EMC, fire, thermal and acoustical properties because the use of composites seems structural feasible as shown in the studies, being only necessary to metalize specific zones with concentrated load like lifting points, connection to bogies and couplers.

The tool of carbody optimisation taking into account composite could give the first structural approach for the design phase (selection of the fibre orientation, where is most interesting part for local added reinforcements with specific insertions and orientations, etc.).

Related with the fire requirements, as shown also in REFRESCO Project, the resin has to be improved regarding fire. Usually epoxy resins are used for structural parts but they lack good fire properties. Conversely the used resins for interiors that have good fire properties, have limited structural strength.

The fibre itself, for example carbon fibres, has good fire properties.

For a correct characterization of the material, it is pending to characterize properly and according to the railway environment the new materials (fatigue, crash behaviour, aging…).

4. JOINING TECHNOLOGIES

4.1 INTRODUCTION

The new lightweight carbody will be designed with highly integrated structural components made out of different materials like steel and aluminium on one hand side and FRP on the other hand side. However, components in multi-material and FRP design have to be joined to each other. The main focus of this task is given to join fibre reinforced materials to other materials and themselves which cannot be welded as common steel or aluminium structures. Riveting, bolting and adhesive bonding or combination of adhesive bonding with riveting or other techniques will be able to join FRP as well as different materials to each other. The state of technology can be summarized as follows:

- **Mechanical fittings** (screws, rivets, clinching and hemming operations): Rivets and screws have been used in the manufacturing of the very first railway vehicles. They have been replaced by welded joints in the 1940 because of advances in manufacturing and weight gain. Replacing welding by ancient joining techniques is not considered here because of the low weight gain introduced by such fittings and the improvement in quality and reliability of existing welding technics.
- **Adhesive joining**: Although structural adhesives present better and better resistant properties, their use in railway vehicle manufacturing is still not considered for joining of structural metallic and polymeric components. This is due to the fact that, for the moment, that structural adhesive joints designed according to the implemented state of railroad technology cannot compete with welded joints as they are industrially designed and manufactured in terms of costs, mechanical resistance (traction, torsion, fatigue, etc.) and long-term behaviour (deterioration). Elastic adhesive joints for secondary structures, like front masks, roof components, panelling, windows etc. are state of technology in railway vehicle manufacturing, including verification and homologation processes.

The design and qualification requirements for joints in primary structures have to be developed with respect to existing standards and processes. One example is EN 12663-1 [C1], which describes the load cases and the procedure of verification. The standard is mainly focused on metallic materials. Neither EN 12663-1 [C1] nor other similar standards give any detailed description of the procedure which is required for joining of primary FRP and hybrid structures. Therefore, the development and verification of a method to approve appropriate joining technologies will be a critical point for introducing new carboy structures into the market. The standards regulate and simplify the processes of verification management and therefore speed up the acceptance process. For adhesive bonding with elastic adhesives, a framework exists but it needs to be further developed regarding to structural bonding (non elastic adhesives).

The final adaption of acceptance/assessment process to the requirements of new materials, new design approaches and joining technologies will only be possible for specific application cases, including possible manufacturing processes and all aspects which need to be considered to ensure safe and durable structures.

This document provides an overview about the state of technology for possible joining technologies, with the corresponding advantages and disadvantages.

4.2.1 MIG-Welding

Main description

The MIG welding is one of the most used technologies for carbody assembly. The main advantage can be found in the extensive experience and the detailed standardization existing for railway application.

The MIG Welding is a type of welding classified as a welding by electrical arc with gas protection (Figure 4.1). The arc takes place inside a protective atmosphere (shielding gas) through an inert gas, between an expendable electrode and the specimen to weld. It is also known as GMAW (Gas Metal Arc Welding). If the gas protection is active, i.e. the gas reacts with the weld pool, the process is called MAG (Metal Active Gas).

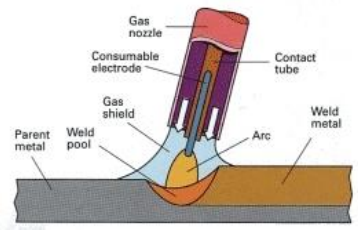

Figure 4.1 Schematic view of MIG welding process

Different types of material transfer can appear depending on voltage, intensity current, protective gas, wire length or current types of welding.

Advantages and disadvantages

The Table 4.1 shows advantages and disadvantages for this special welding technique:

Table 4.1 Advantages and disadvantages of MIG welding technique

Advantages	Disadvantages
Standard process.	Cannot weld different materials (*).
Standardized joint geometries and processes.	Heat introduction, deformation, shrinkage (thermomechanical treated materials).
Standardized and certified education of workers.	Loss in mechanical properties, especially Al-alloy.
Regulation is available for design and processes.	Shrinkage has to be considered during production in order to maintain the design tolerances.
Good and long experience in railway.	Process of welding is not robust (in many cases it is a manual process).
Car specification is prepared for welded structures.	
Design experience available.	
Possibility to automatize.	
Can be calculated.	
Quality inspection is good.	
Reparability is given.	
No ageing.	

Related with one of the disadvantages mention before (*), it is important to note that it is possible to weld dissimilar material, but taking special cares or using very specific techniques, as for example the described below.

This technique to weld steel and aluminium consists on using a transition element between steel and aluminium, Figure 4.2. The key element of the process is the construction of the transition element, which is made by explosive cladding process or other alternatives like rolling, friction welding, flash welding or hot pressure welding. The aim is to produce a full mechanical joint between the materials without voids or other elements and avoiding melting.

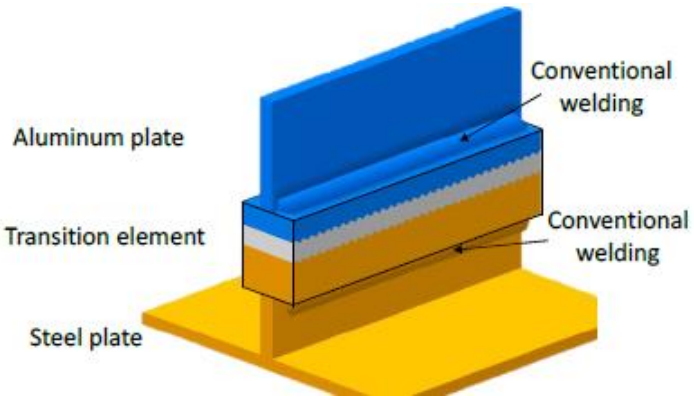

Figure 4.2 Dissimilar transition element for aluminium-steel welding

This method is used on existing train in France, with a particular attention to the thermal expansion on the weld between aluminium and steel.

Application

In the railway domain, welding, considered as “special process”, is well mastered with the use of specific standards and regulations, as the EN 15085 [C2] for the welding of railway vehicles and components. In the same way, this process is carried out by qualified workers with continuous monitoring and control of the parameters to ensure product compliance to specified requirements.

The static and fatigue structural strength parameters are well defined in different railway guidelines as the Eurocodes, ERRI B12 RP17/60 [C3], code of the IIW, FKM, British Standard, DVS,… for steel and aluminium materials. A special care must be taken for the aluminium and specific steels welding, where the structure strength decreasing is not negligible.

The definition of the safety categories of the structure (medium level generally used for the carbody) and the corresponding stress level in fatigue gives the performance class of the welds. This performance class corresponds generally to CPC2 for steel and aluminium railway carbody structures. It allows the evaluation of the weld inspection with the definition of the corresponding control class, Table 4.2.

Table 4.2 Maximum fatigue utilization regarding the stress and safety categories

		Safety categories		
Stress categories	Utilization	High	Medium	Low
High	$0.9 \leq U \leq 1.0$	CP A	CP B	CP C2
Medium	$0.75 \leq U < 0.9$	CP B	CP C2	CP C3
Low	$U < 0.75$	CP C1	CP C3	CP CD

Although the weakness of the railway carbody structure can correspond to the breakage of the welds, the crash structural strength of welding is well under control, Figure 4.3. This is particularly the case in France, where continuous welding is required for the structural parts of the carbody after the accident of “Gare de Lyon” in 1988.

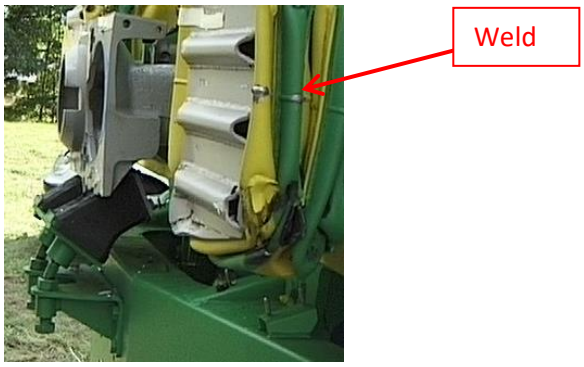

Figure 4.3 Crushed crashworthy steel devices without welds rupture

For maintenance, no specials watching are necessary during life of the welding. Only periodic maintenance inspection looking for cracks or corrosion is done using NDT (Non-Destructive Test) or visual inspection. Welding can also be used in the repair of vehicles if minimum conditions are complied, with a special care for repairing the aluminium carbody where new welds can have consequences on the structure strength.

4.2.2 Laser Welding

Main description

Laser welding is a line-of-sight, single-sided, non-contact joining process with deep penetration. It is characterised by its high focused energy density, which is capable of producing high aspect ratio welds (narrow weld width: large weld depth) in many metallic materials. It can be performed at atmospheric pressure, although inert gas shielding is required for more reactive materials. An outline of the process is shown in Figure 4.4.

Furthermore, laser welding can allow high productivity with its fast processing speeds that can be used in thinner materials (3 to 4 times faster than traditional process), or the fact that just a single pass is needed to make a deep penetration weld in thicker materials. These productivity advantages combined with the automated nature of laser welding, can be used in reliable, repeatable and autonomous welding operations.

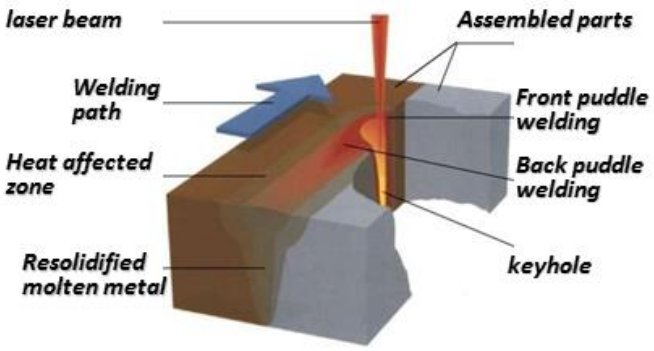

Figure 4.4 Schematic view of Laser welding process

Advantages and disadvantages

The Table 4.3 shows advantages and disadvantages for this special welding technique.

Table 4.3 Advantages and disadvantages of laser welding technique

Advantages	Disadvantages
Low energy input due to high energy density	Very expensive equipment
High ratio depth/width, up to 1/50; High penetration welding process	High precision for parts-positioning and focusing the laser beam
Possibility to weld high thickness plate with one pass without filler material	Very high quality of body edges and tight tolerances are necessary
Possibility to weld very thin plates as well	High surface finish of parts causing mirror effects of laser beam (i.e. complicated to weld).
High speed welding process	High rates of gas, water and electric consumption in the welding equipment
Automated process	Not possible for repair application
No electrical connection between specimens is necessary	Not foreseen for structural FRP materials; just thermoplastics with relatively low mechanical properties are weldable
Heat Affected Zone (HAZ) is very narrow	
Deflections due to thermal loads are very short	
Very refine grain due to high cooling rate	

Application

In the railway domain, this “special process” is applied nowadays in combination with the traditional process, benefiting from the very narrow heat-affected zone (HAZ) with deep penetration and high travel speeds. The Hybrid Laser welding combines the highly focused intensity of a laser with the joint filling capability of the traditional MIG process. By combining the two, hybrid laser welding provides a unique opportunity for thicker welds with less filler metal or higher travel speeds than typical welding, depending on the material thickness. An outline of the process is shown in Figure 4.5.

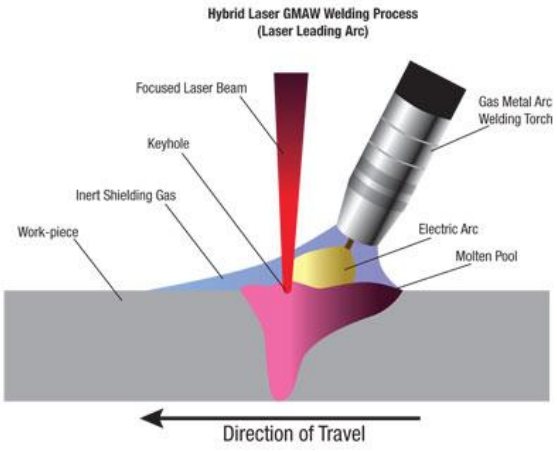

Figure 4.5 Schematic view of Hybrid Laser welding process

4.2.3 Friction Stir Welding

Main description

Friction Stir Welding (FSW) is a method of weld production with the friction heating and the mixing of material in the plastic state caused by a rotating tool that traverses along the weld. Two work pieces are rigidly clamped and a constantly rotating cylindrical tool with shoulder and welding pin

moves downward into the butt joint in longitudinal direction of the weld. In weld zone and the region affected by the tool shoulder, the material of both work pieces is plastic deformed by the moving welding pin and the friction heating. The deformed material builds the weld zone joining the two parent parts. At the end of the joint the welding tool moves upward and lets a hole exist. An outline of the process is shown in Figure 4.6.

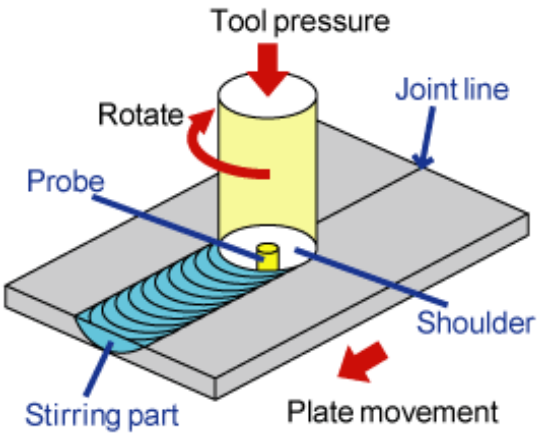

Figure 4.6 Schematic view of Friction Stir welding process

Advantages and disadvantages

The Table 4.4 shows advantages and disadvantages for this special welding technique:

Table 4.4 Advantages and disadvantages of Friction Stir welding technique

Advantages	Disadvantages
Excellent mechanical properties (less heat introduction) with high superior weld strength in static, fatigue and crash conditions	Exit keyhole left when tool is withdrawn
Low porosity, distortion, cracking and residual stress	Large down forces required with heavy-duty clamping necessary to hold the plates together
Possibility to join dissimilar metallic materials	Less flexible than manual and arc processes - difficulties with thickness variations, fillets and non-linear welds
No surface cleaning and no chemical pre-treatment	Requirement of higher tolerance accuracy of joints parts at the weld position
Generally good weld appearance and minimal thickness under/over matching, thus reducing the need for expensive machining after welding	Often slower traverse rate than some fusion welding techniques, although this may be offset if fewer welding passes are required
Improved safety due to the absence of toxic fumes, arc or the spatter of molten material	Repairing with conventional process have to be considered, reducing the benefit of the mechanical characteristics improvement
No consumables – a threaded pin made of conventional tool steel can weld over 1km of aluminium, and no filler or gas shield is required for aluminium	
Easily automated on simple milling machines – high robust and reproducible quality of the weld seam, lower setup costs and less training	
Can operate in all positions (horizontal, vertical, etc.),as there is no weld pool	
Low environment impact	

Application

Increasing in the railway domain, FSW is intended for aluminium alloys to improve the weld performance and gain more economic benefit. It can be used theoretically in any joint configuration as a conventional fusion welding.

Considering the major advantages of FSW in reducing distortion in larger joints, FSW was implemented by railway industry in joining panels in longitudinal direction of aluminium carbody, either single-wall or hollow double-skin extrusions, flat or curved, see Figure 4.7.

Figure 4.7 FSW welded Side walls of aluminium rolling stock by Bombardier

For the structural strength, the main requirements and criteria applied for the MIG welding can be extended to FSW. The permissible or limit strength values should be taken from the corresponding European, international or national standards, if available, or specific test results.

In the document D3.3 Joining Technologies [C4], the structural strength in both static and fatigue of two FSW welded joints are presented using DVS 1608 [C5] for the assessment.

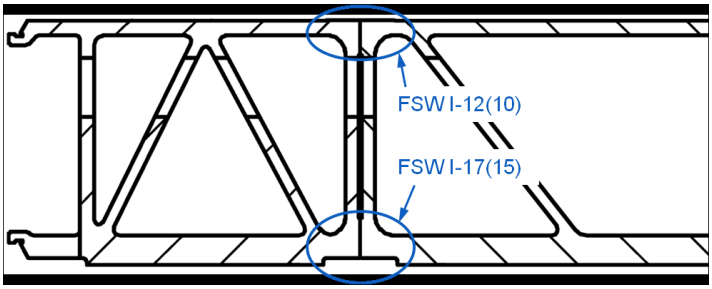

Figure 4.8 Aluminium hollow profiles welded by FSW and corresponding joints

The corresponding yield, ultimate and fatigue failure criterion are described in detail. By the static and fatigue tests, the FSW welded joints with their special geometrical notch situation have been demonstrated to have higher static and fatigue strength than the V butt welds made by arc welding.

For maintenance, as for the conventional processes, no specials watching are necessary during life of the welding. Nevertheless, a particular care must be considered for carbody repairing because friction stir welds are to be replaced by a conventional fusion weld, and then the improved mechanical characteristics obtained with FSW are cancelled.

The limitations of less standardized FSW design and processes including operation, repair and inspection will be improved by the further development of FSW technology.

For other domains, originally intended for aluminium alloys, the FSW technology is now extended to wide range of materials like other alloys including steels and polymers as shown in Table 4.5.

Table 4.5 Weldable materials of friction stir welded joints

FSW weldable materials	FSW weldable dissimilar materials
Aluminium and aluminium alloys	Dissimilar aluminium alloys
Copper and copper alloys	Al-Steel
Brass	Al-Cu
Magnesium	Al-Mg
Titanium and its alloys	Al-Ti
Steel and ferrous alloys	Cu-CuSn
Nickel	Cu-CuZn
Lead	St-CrNi
Hafnium and zirconium	
Inconel and super-alloys	
Thermoplastics	

4.2.4 Screwing and Bolting

Main description

Screwed and bolted joints are one of the most common elements in construction and machine design. A screwed or bolted assembly is an externally threaded fastener designed for insertion through holes in assembled parts, and is normally intended to be tightened or released by torquing a nut (see Figure 4.9). Generally, a bolted assembly includes the screw, the subset to join, the nut or the tapped hole, with the frequent use of washer under the screw head and/or the nut. The screwed assembly can be limited to one part tightening, the connected sub-structure, with the use of tapped holes in the main structures (with or without insert use). These elements are characterized by the quality class and not by the material class of the elements.

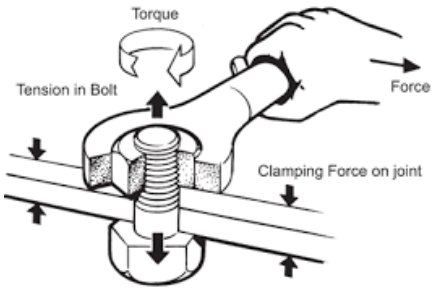

Figure 4.9 Schematic view of bolting process

A tension preload in the bolt or screw and resulting compression preload in the clamped components is essential to the joint integrity. The preload target can be achieved by applying a measured torque to the bolt or screw, close to the yield point.

Two types of bolted assembly can be clearly distinguished:

- the safety connections, the failure of the bolted assembly will lead to the train derailment or to a person injury (impact on the railway operation safety, with for example: the fall of an external equipment on the track), or with an important cost (e.g. operation or rolling stock stop);
- The other normal connections.

Advantages and disadvantages

The Table 4.6 shows advantages and disadvantages for this special joining technique:

Table 4.6 Advantages and disadvantages of bolting technique

Advantages	Disadvantages
Possible to disassemble; easy replacement of parts.	More weight due to overlap joints and joining elements.
Mixed materials joints possible.	Holes in the structure with bearing of holes and Local stress concentrations. In FRP-materials decreasing the advantages of the fibre laminate.
Modular approaches are possible.	Costs for joining elements.
Shorter time to assemble the carbody.	More space for accessibility necessary, with accessibility on both sides necessary.
The sizing process of screwed joints is well understood and described.	Corrosion protection of overlap joint and joining element.
Possible to disassemble; easy replacement of parts.	Orientation of loads has to be considered.
Qualification processes for operators and tools is limited	Screws might need special thread locks due to loosening risk during service life.
	Flat and parallel surfaces; tight tolerances.
	Laborious sizing process to proof the demanded load capability of high duty bolt joints.
	Expensive tightening methods in case of high duty bolt joints.
	Borehole drill can project dust and material fragments

Application

In the railway domain, these joining methods are used to fix equipment and all the subparts that have to be disassembled for maintenance purpose. For the existing and future hybrid and modular vehicles, these methods can mix different materials of the main structure. An important increase for structure application can happen (see Figure 4.10) with the composite development in railway industry.

The present state of standardization enables an industrial application without specific testing needs using DIN 25201-1 to 7 [C6] and VDI 2230-1 and 2 [C7] in Germany or NF E 25030-1 and 2 [C8] in France while awaiting a shared European standard.

Figure 4.10 Steel Driver cab bolted on the current aluminium carbody

The assessment of the bolts or screws strength can be demonstrated with calculations, under axial tension and transversal load. An initial tension (preload) must be applied to the screws to compensate their low intrinsic resistance. It avoids the loss of the fixings tighten and then the occurrence of dynamics effects in the screw, with the potential failure of the screw and the loss of equipment on track. With the friction coefficient and the characteristics of the screw (class and diameter), the torque and the initial tension can be determined.

For the maintenance, verification and inspection must be developed according to the function and safety aspect of the designed assembly. A simple visual inspection is enough, with the possible use of marker metal pen on the different parts forming the assembly. Other methods in case of safety risk can be used as the tightening at 70% or 80% of the maximum torque or the use of ultrasound for the elongation measurement in the bolt, Figure 4.11.

Figure 4.11 Application of the ultrasound method on trainset

Electro-chemical compatibility, with the associated risk of galvanic corrosion according to environmental influence, must be checked during the fasteners maintenance.

In the document D3.3 Joining Technologies [C4], a section is dedicated to the bolting application for the composite, with:

- the non-structural composites as the fairing, trapdoor and the covers;
- the structural composites for the main carbody structure for monolithic as well as sandwich materials.

For the first one, the return of experience is presented with the main origins of the failures and the measures implemented to improve the bolting assembly for these elements.

For the second, after the presentations of the failure type for the composite bolting (often within the composite elements and not the joining area) and of the different types of thread inserts resulting from aeronautic applications, rules and dimensioning criteria for bolted composite assemblies were addressed (including drilling process), with the verification method using specific tools.

An important part of the document is dedicated to the screwed connection between sandwich panels, with the presentation of the specific applications of the previous elements (with the specific inserts and their potting in the sandwich core, see Figure 4.12).

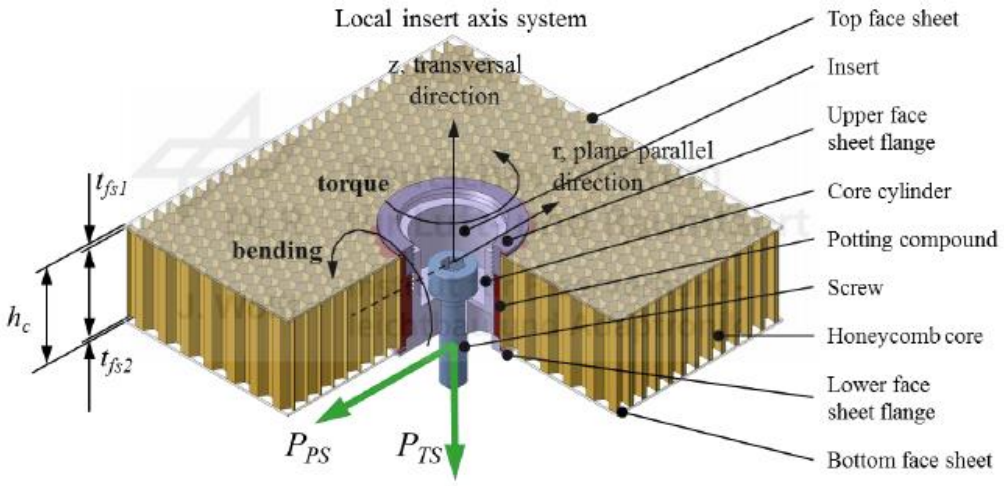

Figure 4.12 Load introduction with an insert element in a sandwich panel

A particular case of application for the basic structure of the Roll2Rail HS and Urban carbody concepts corresponds to the sandwich side wall insert connection. For this, the aluminium multi web side walls are replaced by side walls in sandwich design (FRP skins and foam core, an outline is in the Figure 4.13).

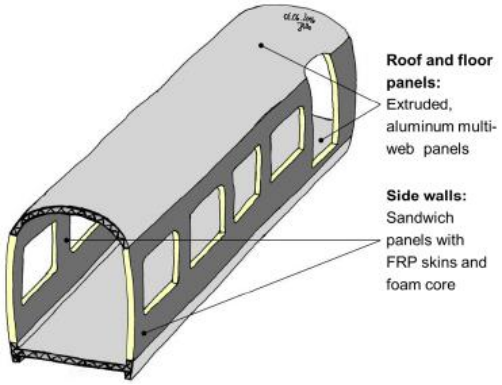

Figure 4.13 Case study approach: Application of the sandwich design to the side wall panels

This survey presents the DLR-FA's insert load introduction sizing approach for the hybrid joints technology, with the prospective applicable for the future Shift2Rail project. An optimization of the layouts is proposed according to the different waited properties of the panel, with the identifications of the loadings and the considered material characteristics.

The connection concepts (Figure 4.14) can lead as a discussion basis for the Shift2Rail concept, with screwed inserts for the sandwich side wall that is:

- inserted into the space between the protruding facings of the floor panel uprights;
- juxtaposed along the floor panel side faces

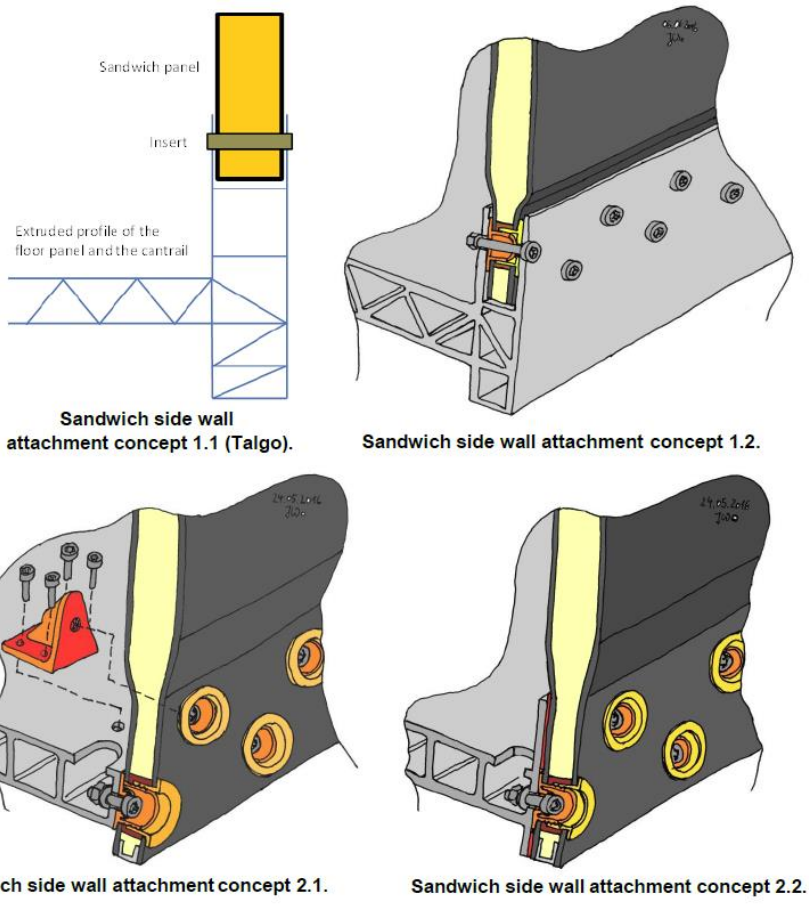

Figure 4.14 Case study concepts with side wall panel connections

The different advantages, disadvantages and drawbacks of the different concept types are assessed, with the identification of the corresponding maximal loads and moments, as the mechanical model.

4.2.5 Riveting

Main description

A rivet is a permanent mechanical fastener, used since a long time for joining primary aircraft components like fuselage shells and surrounding parts made of aluminium alloys. With the evolution of the practice, different types of rivet have been defined:

- The non-structural (“pop” rivet) or semi-structural solid rivets with low or medium strength level.
- The structural rivets with high strength level, length reduction and shaft expansion control (e.g. lockbolt with preload control or threaded fasteners).

For the first ones, called blind rivets, only one-side accessibility is necessary for their installation. The insertion of this type of rivet (one piece fastener) in the borehole takes place from only one side and the accessibility to squeeze the rivet must be given from the opposite side, Figure 4.15.

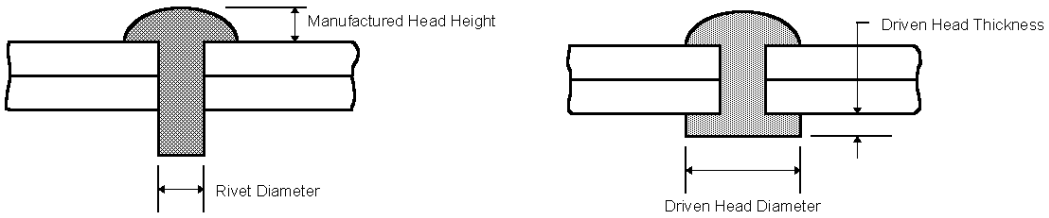

Figure 4.15 Schematic view of riveting process for solid rivet

The second one was developed by the aircraft manufacturers to use different materials, control the influence of the adherent damage and raise the joint preload during process. This two pieces fastener with collar developed a compressive loading onto the joints interfaces. For this type of fasteners, the diameter decreases during the installation process.

Threaded fasteners (e.g. Hi Loks, Hi Lites) work similar to screws or bolts tightened with a nut:

- maximum torque is reached;
- the friction within the thread guarantees a self-locking performance by a slightly oval collar;
- the joints preload in this case undefinable.

Lockbolts fasteners (Figure 4.16) present the following characteristics:

- used for joints where high clamping length and well defined high preload is need;
- locking mechanism is quite different to that of threaded fasteners (see Figure 4.16);
- special tooling grips apply an axial tension load onto the pintail during the squeezing process;
- the tension load is defined by the predefined reachable preload depending on the fastener diameter;
- the undesired part of the pin breaks at the predefined area;
- and, the installation of this kind of fastener takes place without torqueing and the friction influence can be neglected so that well defined preload values can be achieved.

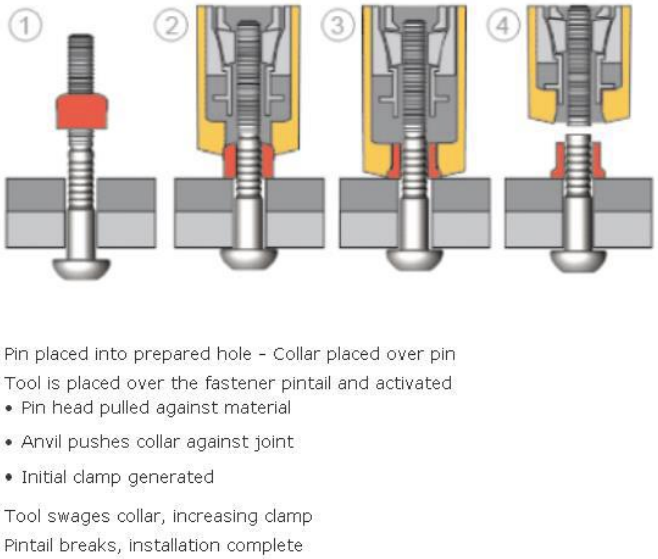

Figure 4.16 Schematic view of Riveting process for Lockbolt rivet

During the installation process, the metallic rivet is compressed in axial direction with specific tools. A special care must be taken for the borehole creation in order to limit the tolerance and damage problems.

Advantages and disadvantages

The table below shows advantages and disadvantages for this special joining technique:

Table 4.7 Advantages and disadvantages of riveting technique

Advantages	Disadvantages
Low temperature joining technology, no curing, solidification or post-processing is necessary	Very expensive equipment for highly automated installation processes (e.g. part-positioning)
Joining of different materials form very low thickness up to very thick multi material stacking is possible	Drilling boreholes weakens the partners to be joined, e.g. FRPs
Installation of fasteners is a highly automatable process	Accurate drilling of boreholes is necessary for a reliable installation process
Applicable for repair solutions	Drilling boreholes in FRPs cause strong wear of the drill bits
Combinable with other joining technologies (e.g. adhesive bonding)	When a damaged rivet is replaced it would be necessary to take again drilling and to pass to a higher diameter of rivet
Qualification processes for operators and tools is limited	The borehole drill can project dust and material fragments and the installation process can generate rising noise

Application

In the railway domain, the different types of rivet are used. The solid rivets fasteners are mainly used for joining sub-structures or interiors, meanwhile the lockbolt fasteners are mainly used for joining structural parts or fixation withstanding important loads.

Although there is no common standard for riveting in railway domain, manufacturers have defined specifications for the rivet fasteners configuration in terms of dimension (e.g. diameter, grip length and head shape angle), tolerances and mass, (ii) materials and coatings like finishes and lubrications, (iii) mechanical characteristics, and (iv) general characteristics like markings. Other test methods and qualification processes for rivet design result from the Aerospace Industry, with associated standards and guidelines.

D3.3 Joining Technologies [C4] presents general elements for the rivet design in terms of strength (rivet and assembled structures with load transfer, preloads and residual stress distribution), rows distribution and materials used for fasteners and installation processes for both solid rivets and lockbolts, for example Figure 4.17.

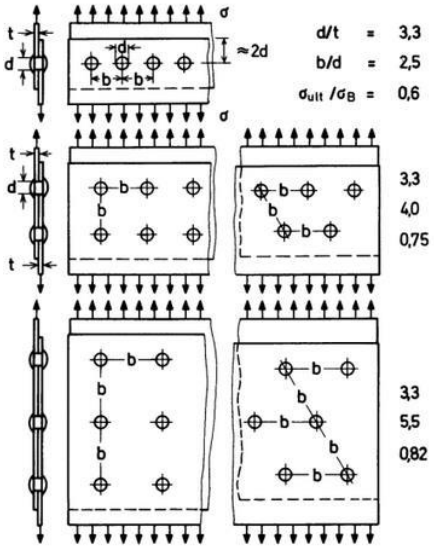

Figure 4.17 Geometry of a riveted joint with single and up to n=3 rivet rows

For the maintenance, verification and inspection must be developed according to the function and safety aspect of the designed assembly, mainly if the visual inspection is only possible on one-side according to accessibility. The implemented driven head of the rivet, with the strength, geometry and accessibility compliance, is the major element to check during the fastening in maintenance workshop.

4.2.6 Adhesive bonding

Main description

Adhesive bonding is used to fasten two surfaces together, usually producing a smooth adhesive interface. This joining technique involves various agents that bond by evaporation of a solvent or by curing a bonding agent with heat, pressure, or time. Adhesive bonding has the potential, not only to join secondary structural parts, but also to join primary structural parts yielding innovative technology development for carbodies, doors and other applications, as shown in Figure 4.18.

Structural bonding using adhesive with high performances (robustness, high cohesion, high mechanical strength, heat adaptation), can obtain a strength close to the one of the constitutive materials.

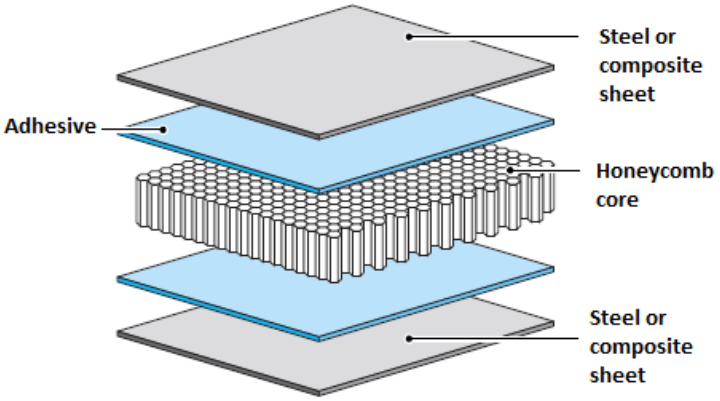

Figure 4.18 Sandwich panel with a bonding honeycomb core

Adhesives are by definition polymeric materials. For these types of materials some characteristics have to be considered during the design phase, which are different from the metallic materials:

- In a typical temperature range for rolling stock carbody structures of -50°C to 80°C the mechanical behaviour of adhesives can change dramatically. Therefore, all specific material data have to be considered at relevant temperatures.
- At temperatures below the glass transition, adhesives are energy elastic and behave as thermoset material. At temperatures higher than the glass transition temperature, adhesives are entropy elastic and behave as elastomer. In this case they are similar to rubber. The main characteristics of the adhesives are briefly summarized in the document D3.3 (section 3.7.3) [C4].
- For polymeric materials like adhesives, the physics of plastic deformation is different from metals. Plastic deformation is not carried out by dislocations, without (macroscopic) yield strength and with consideration of the volumetric parts of the stress.
- Adhesive joints are affected by humidity and water, with mostly reversible effect and high modification of the adhesives stiffness. Corrosion inhibitors should be added to a primer or to the adhesive to avoid or to reduce this effect.

Advantages and disadvantages

The Table 4.8 shows advantages and disadvantages for this special joining technique:

Table 4.8 Advantages and disadvantages of adhesive bonding technique

Advantages	Disadvantages
Can deal with tolerances (at least partly depending on the adhesive)	No catalogue of geometric solutions is available
Low temperature bonding technique, avoids deformation of thin materials due to heat in welding	No notch factor concept as available in welding
Many solutions available (elastic, structural adhesives)	Properties depending on temperature and humidity in the range service conditions with weathering dependence
Standardized processes (DIN 6701)	Low fire resistance might need special solutions
Joining of different materials possible	Special process in manufacturing is necessary
Distribution of the load is less concentrated	Creeping might have to be considered
Avoiding of contact corrosion is possible	Process time, time of curing process
Conductive and non-conductive adhesives can be made to fulfil special functions (as vibrations, airtight or waterproof, …)	Additional surface treatment and preparation is necessary
Lightening of the assembled structure (without, screw, rivet, bolt, …)	Needs dedicated area for manufacturing, maintenance and storage
Avoid the structure damage and weakening with the borehole drill	Education and training for persons involved in the process is necessary
Aesthetic aspect with smooth surfaces	Costs might be higher
	Ageing of adhesive joints is not well known, lack of experience for long term behaviour of structural adhesives
	Sensitive about the type of loading in term of strength

Application

In the railway domain, adhesive bonding can be considered as state of technology for joining secondary structural components and windows to railroad vehicles using hyper-elastic adhesives. Joining of primary structures has rarely been applied and the return of experience results from the bonding of windows, GFRP-panels, GFRP-roofs and other large components.

For this joining technology standardization and education system has been developed, mainly in Germany, in line with welding, including homologation. The standards DIN 6701-1 to -4 [C9] have been developed in Germany, driven by the industry and the German “Eisenbahnbundesamt”. These standards describe how to deal with adhesive bonding in railroad manufacturing. Other documents describe the state of technology of adhesive bonding in railroad applications as the EWF 515-01 [C10], EWF 516-01 [C11] and EWF 517-01 [C12].

An important task corresponds to the training and the supervising of the qualified personnel. The personnel should understand the bonding processes, should be able to instruct workers, to define the operating instructions and should be able to supervise the processes. Moreover, the requirements of the product handling have to be followed, because contact of all chemical ingredients (adhesive, primers activators and cleaners) with the skin represents a risk (good ventilation at the workplace has to be ensured).

In part three of DIN 6701 [C9] the bonded joints are classified in A1, A3, A3 and Z according to safety requirements:

- A1, high safety requirements: failure of the joint will yield an unavoidable danger for human body or human life or safe operation of railway vehicles
- A2, medium safety requirements: failure of adhesive joint might yield operational risk with damage to persons or impairment of the overall function of the railway vehicle
- A3, low safety requirements: failure of joint yields not more than reduction of comfort, the probability of damage to persons is low
- Z, no safety requirements: failure does not yield damage of persons or any impairment of overall functionality

According to the wide variety of possible adhesives and the relatively youthfulness of this technique, there is no checklist for certify adhesives and for test which have to be accomplished for a homologation process. Nevertheless, adhesion must be verified with the following criterion: only cohesive failure (failure in the adhesive and not in the interface between substrate and adhesive) is accepted as shown in Figure 4.19. Temperature and humidity might be additional parameters, contradictory to metals.

Figure 4.19 Bonding validation test of equipment fixing on rolling stock after detachment problems

The approval and homologation process can use the following ways:

1. Local stresses and strains are calculated and compared with allowable design values which are measured with coupon tests.
2. Components will be tested at conditions which are comparable to the structural load.
3. 1 and 2 can be combined.
4. From documented practice of similar applications and components.

With the documentation which contains:

- the list of requirements
- test reports for the qualification of the adhesive joints, surfaces, and adhesive systems
- approved drawings and design documents
- stress and strain analysis, assessment of stress and strain analysis
- report about verification process which approves that the load is smaller than the load resistance for all relevant service conditions

Detailed requirements are given in DIN 6701-4 [C9] about any documentation with regard to production processes, testing, quality management, personal and repair.

For fire and smoke behaviour, the adhesive bonding will usually be the “weakest link” in a load carrying structure during a fire. The only reliable way of verifying the capacity is to measure temperatures in the joint during a fire test, and/or to apply load during a realistic fire condition, with the knowledge of the thermo-mechanical properties of the adhesive. To obtain enough information and reduce the test cost, small-scale tests can be used with the same fire load as described for the full-scale tests. If “details” like panel and insulation joints behaves well, the correspondence between small and full-scale tests is usually good. Some insulation is necessary to reach high fire classes for bonded structures.

The smoke usually is no problem since only a small part of the adhesive layer is directly exposed to the fire.

General rules for methodical and geometrical design of adhesive joints can be defined. The design of an adhesive joint should be clear, simple and safe, with the following principles:

- A good design avoids strong changes of the load flux through the joint which appear at sharp corners or sharp changes of diameters of structural components
- Deformation of the adherents should correspond to the deformation of the adhesive in the joint. With additional features and symmetrical loading conditions, secondary loads and moments should be avoided or reduced.
- The geometry of the adhesive joint should be designed in a way that the joint is self-reinforcing, self-equalising and self-protecting. The design of the joint should yield a stable solution contrary to shown in Figure 4.20.

Figure 4.20 Unstable design of an adhesive joint due to local buckling in the overlap

The local stresses and strains in adhesive joints depend on the local stiffness of the surrounding structure and the stiffness of the adhesive. It is then recommended to design a joint in a way that peel forces should be minimized and shear forces should be preferred. This criterion sometimes is not easily to fulfil since real loads in structures are complicated and in most cases multi-axial.

The design process of adhesive joints has to take into account thermal expansion of structural components. As visco-elastic polymer materials, the mechanical behaviour of these adhesives depends strongly on the applied loading rate, with possible loading consequences at fatigue, impact and crash conditions (stiffening effect). The joint cannot fully be loaded until the curing is finished, with sometime the need of humidity, because of the non-uniform distribution of the joint cure.

The surface of the adherent is part of the adhesive joint. Surfaces must be prepared and pre-treated for adhesive bonding. Preparation and pre-treatment depends on the particular surface, the adhesive system and the manufacturing conditions and costs. For the case of bonding on a painted surface, the adhesive system should be selected in a way that the strength of the paint or lacquer is higher or equal to the strength of the adhesive.

Three types of damage mechanisms are known for adhesive joints:

- Change of physical properties like stiffness of the adhesive due to plastification by water.
- Corrosion and degradation of surfaces of metallic substrates.
- Chemical damage of the polymer due to water is also possible, but usually appears on a longer time scale.

Bonded joints should be avoided in areas with constant exposure to water and any solvents or cleaners to avoid these mechanisms.

During service life, no healthy/environmental/safety precautions are necessary since the adhesives are cured. Very acid or alkaline cleaners and graffiti removers should be avoided to not solve and destroy polymers. All cleaners and removers should already be considered in the design phase.

The structural strength of an adhesive joint is determined by the adherents (substrates, materials) which have to be bonded to each other and the adhesive. Different approach can be used for the strength calculation:

a) Static approach:

The aim is that the adhesion strength to the surface is larger than the bulk strength of the cured adhesive. This situation can be reached with many technical adhesives after certain pre-treatments of the surfaces to which the joint has to be bonded to (with adhesive or substrates strength).

Design parameters for adhesive joints are the thickness of the adhesive and the overlap area. Increasing the bonding area decreases the nominal stress (force/area). With structural high strength adhesives, adhesive joints with a reasonable short overlap length can be feasible between aluminium and steel sheets, which easily can sustain the strength of steel and aluminium. Failure will occur in the metal. Increasing the thickness of the adhesive joint will reduce the strain in the adhesive, yielding more deformation capacity which might be important for the joints between materials with different thermal expansion.

A very simple approach which does not consider any stress concentrations at the ends of the overlaps is obtained by the following two equations:

$$\tau = \frac{F}{w \cdot l} \qquad \sigma = \frac{F}{w \cdot t}$$

Where, *l* is the overlap length, *t* is the thickness of the adherents, *F* is the load applied to the joint, and *w* is the width in z-direction according Figure 4.21. Then, knowing the yield strength of the substrates and the lap shear strength of the structural adhesive, the overlap length and the thickness of the joint can be defined.

Figure 4.21 Sketch of a lap shear joint

In order to be able to design an adhesive joint:

- the moments need to be considered which appear from the applied force and the acting distance of the force to the midline of the joint,
- the stiffness of the adherents is some orders of magnitudes larger than the stiffness of the adherent.

The Figure 4.22 shows the stress distribution of a single lap bonded joint, for two steel and for two aluminium substrates of the same thickness. The stiffer the substrates are, the lower become the stress concentrations. The moment which appears for a given applied loading increases with increasing thickness of the adhesive and adherent.

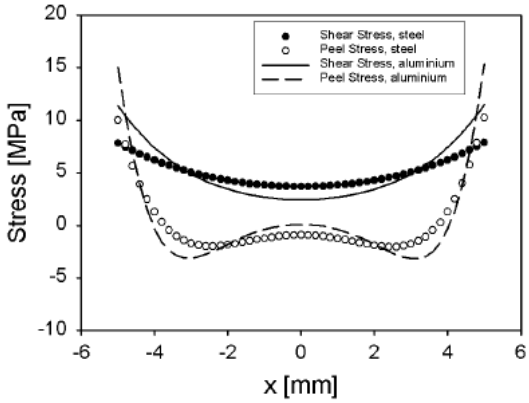

Figure 4.22 Shear stress and peel stress distribution in a single lap joint with 10 mm overlap length

The best adhesive joint between two plates in tension a symmetric joint with additional plates on each side with decreasing thickness according to the principle of corresponding deformation as shown in Figure 4.23.

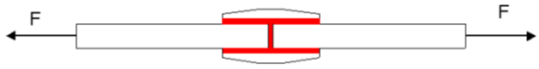

Figure 4.23 Adhesive joint between two plates loaded in tension

Nevertheless, single lap joint is more widely used, mainly in aircraft industry. Then, many theoretical approaches exist to describe this type of joint, as the easy-to-use design rules approaches described in the document D3.3 (as Volkersen and Goland-Reissner or Bigwood and Crocombe approach). These approaches are used to be seen as based on simple and reliable analytical formulas and equations, which can be used to design adhesive joints. In many cases certain assumptions are necessary to find analytical solutions. These assumptions have to be carefully considered before analytical solutions can be applied in a design process in order to avoid wrong results.

b) Fatigue approach:

The Figure 4.24 shows examples for S/N curves of adhesive joints with different ratio of shear to normal stress. The adhesive is a toughened structural adhesive. It can be seen that the slope of the S/N curve depends on the stress ratio.

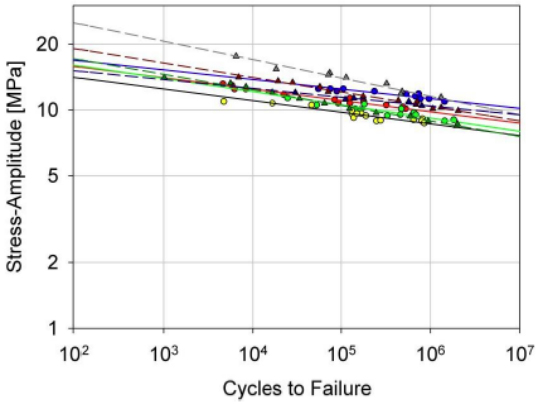

Figure 4.24 S/N-curves for a toughened structural adhesive joints at stress ratio R= 0.1 (minimum load / maximum load), room temperature, different ratios between shear and perpendicular loading

The Figure 4.25 shows an example for the temperature dependence of the S/N curves between -35°C and +80°C. The stress amplitude decreases with increasing temperature, below 50°C the slope of the S/N curve only slightly changes. But, at 80°C both slope and level of the S/N curve change drastically. At 80°C the temperature approaches the glass transition temperature of the adhesive. This is the reason for the drastic change of the fatigue behaviour. The influence of temperature has to be considered carefully: starting with a too conservative approach, which could mean to do all tests at highest possible temperature, certainly would yield an overloading of the joints. It also can be seen, that the slope parameter of adhesives and adhesive joints usually is larger than for metals. This means that low cycle fatigue events might have more influence on the cumulative damage of the joints compared to the high cycle fatigue than it is the case for metals. Therefore, equivalent load cases have to be derived from the applied loading differently than for metals. This is an open point for further investigation which requires a more specific understanding of the standardized load cases and their affect to polymeric materials.

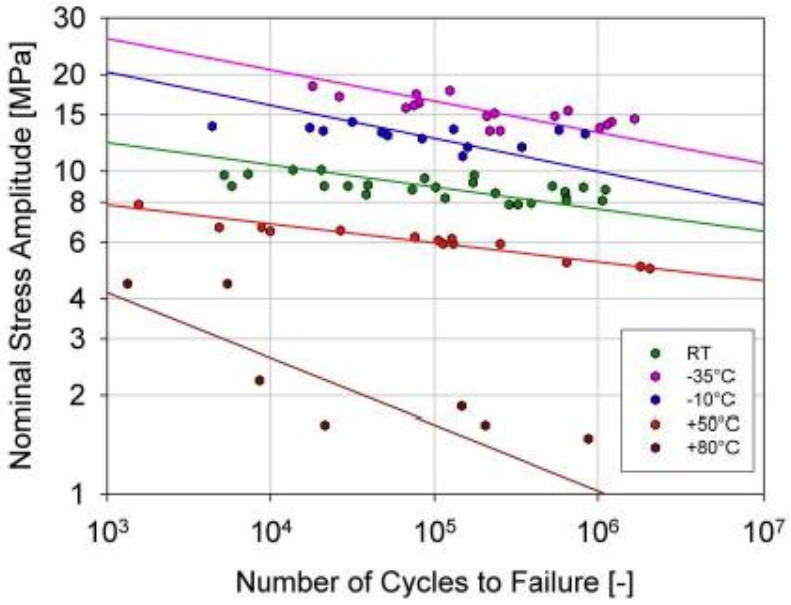

Figure 4.25 S/N-curves of a toughened adhesive at different temperatures (R=0.1)

Then, fatigue load cases might have to be considered differently as requested in the standards, because:

- no endurance limit exists for adhesives,
- the cumulative damage might have to be described with different equivalent load cases than applied for metals,
- the mid-load sensitivity of adhesives due to creep might need other approaches than for metals,
- low cycle load cases (LCF) might be more relevant for damage of adhesive joints than for metals, which might require to include some load cases into accumulation of damage which can be treated as static for metals.
- The slope of the S/N
- N curve for adhesives is significantly lower than for metals. For the parameter *k* a value can be found, typically between 10 and 30, depending on the adhesive, the loading conditions and the temperature.

$$\tau = \tau_{a,0} N^{-1/k}$$

Where τ is the shear stress amplitude, N is the number of cycles to fail, $\tau_{a,0}$ is a free parameter.

c) Crash approach:

Adhesives are visco-elastic like other polymers. With increasing loading rate, the strength and stiffness of adhesive joints increases. Toughened, hot-curing adhesives are used to improve the crash behaviour of cars. The main effect is that adhesive joints improve the folding of the crash absorber structures in order to dissipate more energy in plastic deformation of surrounding metallic structures. At strain-rates from $0.01s^{-1}$ and $10000s^{-1}$ the lap shear strength of joints, with an example for a toughened epoxy adhesives, increases from 30 to 60MPa.

In D3.3 Joining Technologies [C4], a paragraph is dedicated to the adhesive bonding application for the high speed train and the urban vehicles. For the studied cases to design a joint (with adhesive and with insert), the joints between lateral panels and main frame/roof were selected in order to calculate the force and moment under specified load cases with FEM analysis. After the deduction of the nodal forces and the moment, the reduced force and moment of the different sheets of the extrusion panel in the middle joint lines are calculated (upper left and right and down left and right) to obtain distributed force and moment along the length of the carbody, as outlined in Figure 4.26 an Figure 4.27.

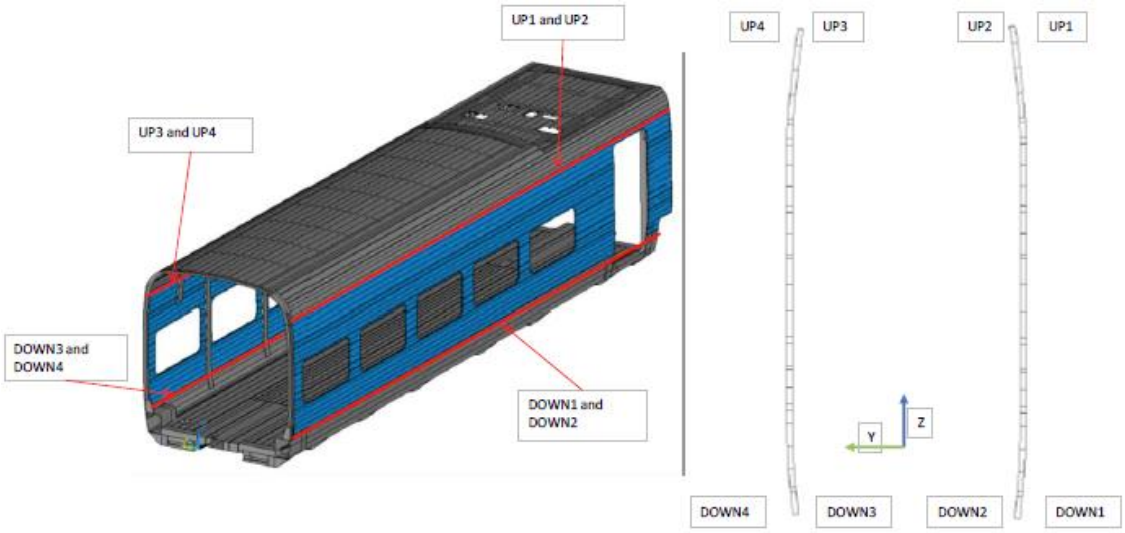

Figure 4.26 Joints between lateral panel and main frame studied for HST vehicle

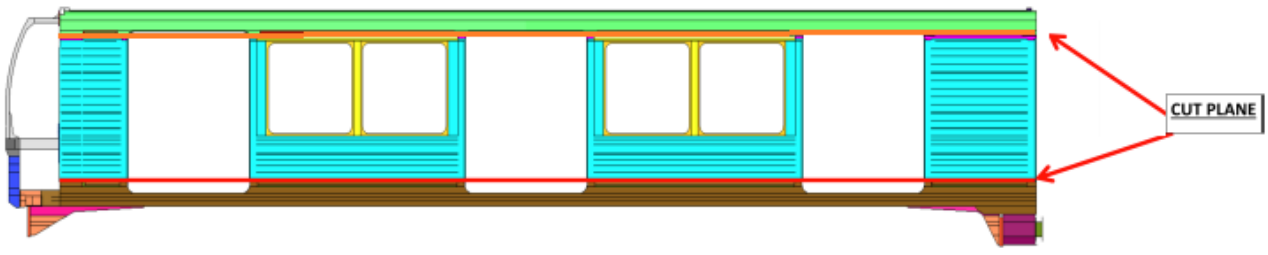

Figure 4.27 Joints between lateral panel and main frame studied for urban metro vehicle

For the HS vehicle, the critical load cases for the joint selected are the cases related with the pressure LC2: Over-pressure (+6000Pa) and LC3: Under-pressure (-6000Pa). For these cases, the more stressed zone is located between the door and the adjacent window, Figure 4.28. The

most stresses joints for the other joining sections are the joints located below ("down" joint for LC2-LC3) and over the door (LC1: Exceptional vertical load).

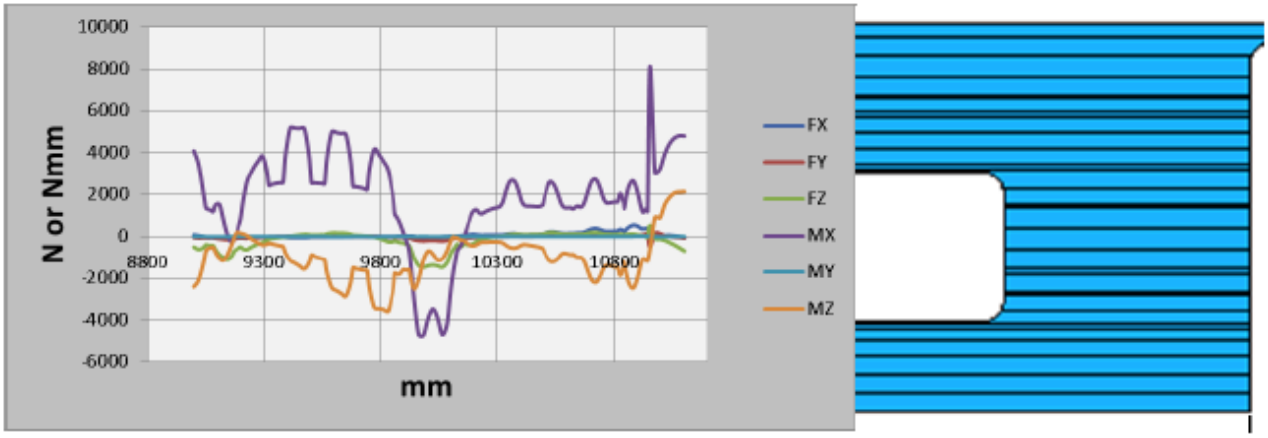

Figure 4.28 Distribution of forces and moments Up Right for LC2: Over-pressure (+6000Pa) on the left side of the door

For the Urban vehicle, the critical load cases for the joint selected are the cases related with the longitudinal force at sill level around the first door LC1: Compression at coupler (800kN) – LC2: Tension at coupler (600kN) and Compression at waistrail (400kN), see Figure 4.29.

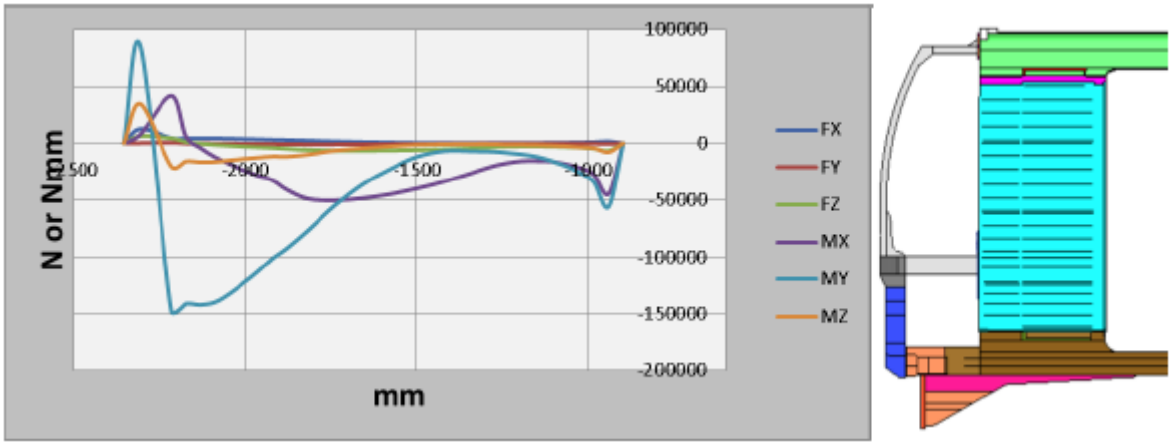

Figure 4.29 Distribution of forces and moments Sill for LC1: Compression at coupler (800kN) between cabin and door

For the studied vehicles, the loading of potential adhesive layers is studied on the basis of these section loads for two principal types of adhesive joints with prospective layer dimensions.

In both cases the aluminium sheet has a thickness of 4mm and the overlap length (perpendicular to the car length) of the joint is 30mm. The adhesive layer thickness is 0.3mm. The Young's modulus of aluminium is 70GPa and the Poisson's ratio is 0.3. The Young's modulus of the adhesive is 1.6GPa and the Poisson's ratio is 0.4. The mechanical data of the adhesive belong to the structural adhesive DOW Betamate 1496V. The lateral extensions (length direction of the car) of the joints depend on the considered load case. Predominantly highly loaded sections of the section line are studied. High loads could result from single components of forces and moments or from a resultant of those.

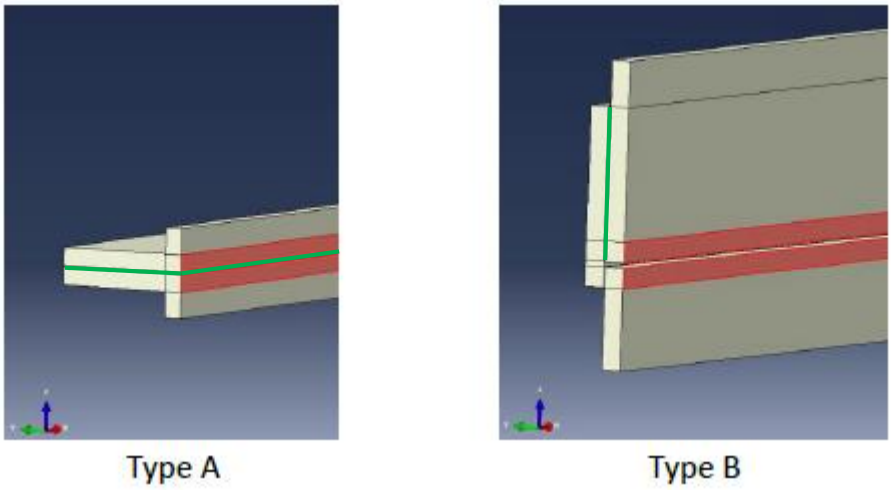

Figure 4.30 Two principle types of adhesive joints: A) "L" shaped butt joint and B) lap joint. The adhesive is coloured green (A: horizontal, B: vertical). Forces and moments are distributed over the surfaces coloured in red.

In joint geometry A of the Figure 4.30 the adherents are "L" shaped. Thus each adherent represents a small part of the vertical panel structure. In the shown case the panel part has a height of about 20mm. The bonding area is horizontal. In bonding geometry B of the Figure 4.30 one of the adherents has more or less the shape of a hand written "4" and the other adherent is plane. Due to the vertical orientation of the bond-line a more extended part of the panel structure is represented with this type. In the shown case it has a height of about 60mm. As a matter of fact, the stiffness of the considered joint types is different in length and in width direction and a dissimilar loading of the adhesive bond-line is to be expected if the same section loads are applied to the adherents.

In the FEM model of the joint types the critical forces and moments are distributed on the front faces of the adherents in close vicinity to the adhesive layer to avoid artificial levers. The signs of the loads are opposite on each adherent front face. To prevent the joint from translation and/or rotation the joint was fixed in space with engineering springs. Large bending of the joint results in stress concentrations in the areas where the joints are fixed with springs. Stress concentrations in these areas are artificial and are not analysed. The FEM results are shown as von Mises stress distribution of the complete joint and as distribution of the maximum principal stress in the middle of the adhesive layer.

Remark : It is to be mentioned that independently of the joint type the size of the vertical panel structure considered in the models influences the results of the calculations. For a coarse estimation of the loading of an adhesive layer the chosen models are a compromise between the quality of the results and the time needed for the calculations.

The analysis of the FEM results shows that the butt and lap joints are subjected to a noticeable bending under the applied loads, different for the two types of joints according to the different stiffness (see Figure 4.31). In most cases the highest stresses occur close to the overlap ends (normal to length direction of the car) of the adhesive layer. The stress maxima of all calculations are listed in the following tables (Table 4.9 and Table 4.10) for the two vehicles:

Table 4.9 Maximum stress in the middle of the adhesive layer of the calculated joints for HST

	LC1	UR	LC2	UR	LC2	DR	LC3	DR
	dominant component	maximum principal	dominant component	maximum principal	dominant component	maximum principal	dominant component	maximum principal
Butt Joint	62.2	63.8	14.1	16.7	23.9	24.8	98.4	104
Lap Joint	55.8	66.7	15.3	17.1	25.6	26.7	95.8	103

Table 4.10 Maximum stress in the middle of the adhesive layer of the calculated joint for UM

	LC1	Sill	LC2	Sill	LC3 left	Sill	LC3 right	Sill
	dominant component	maximum principal	dominant component	maximum principal	dominant component	maximum principal	dominant component	maximum principal
Butt Joint	66.6	108	24.0	25.4	32.5	35.5	37.5	37.6
Lap Joint	64.6	90.5	23.2	26.6	28.2	32.7	35.1	36.4

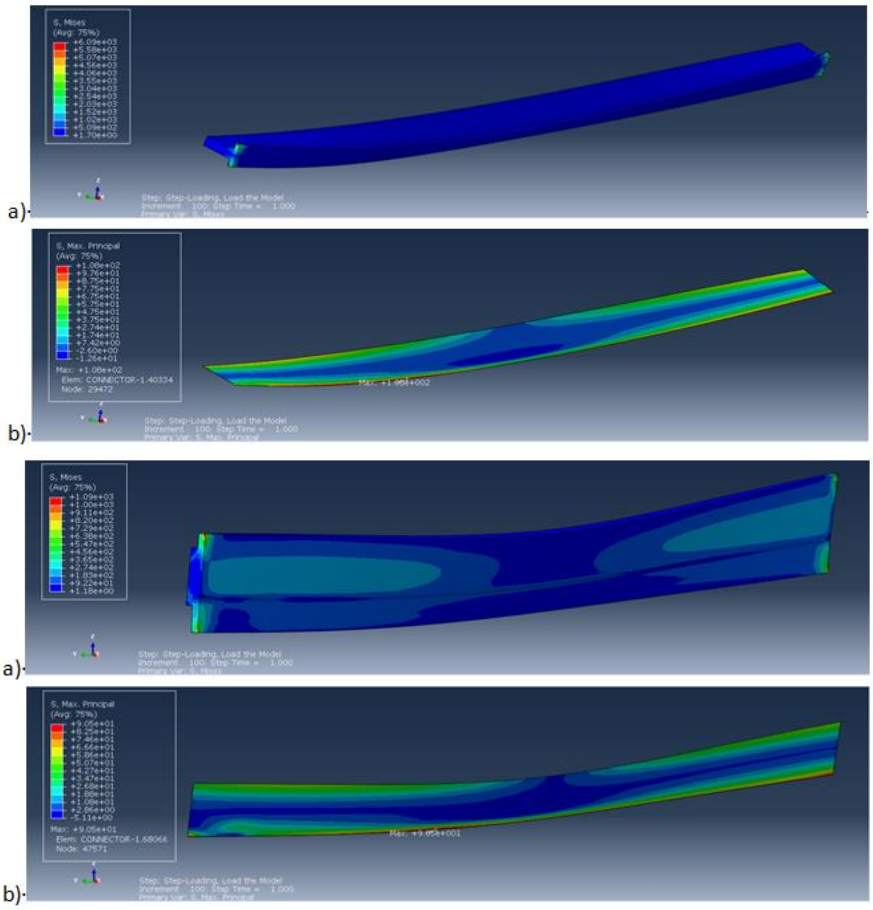

Figure 4.31 Butt Joint - FEM results Sill for LC1 between cabin and door of the Urban Metro vehicle a) complete joint, von Mises equivalent stress b) middle of adhesive layer; max. principal stress.

Without sound experimental background there is no failure criterion available. In order to assess the calculated stress maxima, the information of the technical data sheet of the sample adhesive is used. The stress maximum of the lap shear sample described in the data sheet is calculated and compared with the derived stress maxima of the considered joint types. Element sizes and mesh

refinement of the lap joint are about the same as in the case study of joint types. A load up to 7500N was applied (i.e. 30MPa nominal shear stress) to obtain the force at break. Then, the related maximum of the principal stress is 86MPa, Figure 4.32 and Figure 4.33.

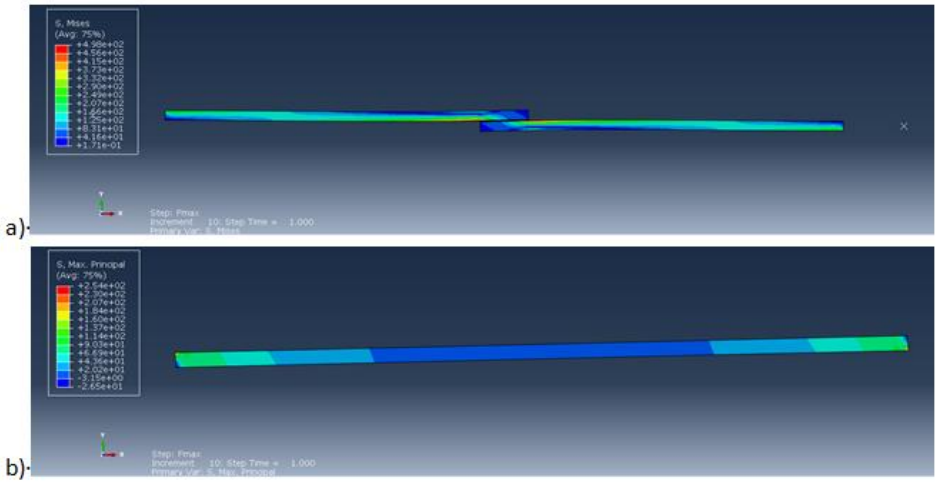

Figure 4.32 FEM results of a lap joint, according to technical data sheet of Dow Betamate 1496v a) complete joint, von Mises equivalent stress b) middle of adhesive layer; max. principal stress.

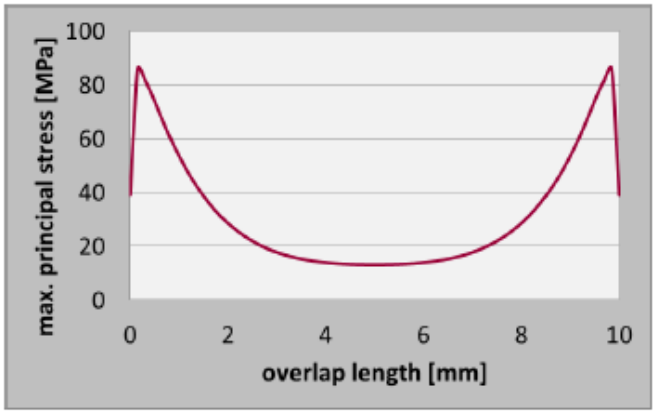

Figure 4.33 Distribution of maximum principal stress in the middle of the adhesive layer of the lap shear sample shown in the previous Figure 4.32.

Assessed on this basis of stress maxima presented in the previous tables (Table 4.9 and 4.10), load cases LC3 for HS and LC1 for Urban are critical for both types of joints A and B. Nevertheless the stress maxima are not as high to conclude that adhesive bonding of lateral panels is not possible. Stress maxima could be reduced by constructive techniques.

Comparison between the different joining properties

For the different general joining properties, a summary table (Table 4.11) with the particular advantages and disadvantages can be presented as:

Table 4.11 Comparative table between technologies

Joining properties	Welding	Mechanicals assemblies (bolting, riveting, screwing)	Bonding
Joining of different materials	Identical metals but difficult for certain materials (Al, Ti).	Different materials (metal/metal, plastic metal/, plastic/wood…).	All materials
Shapes and sizes of the parts	Large and small surfaces (by different types of welding joint).	Parts of all shapes but with a dimensioning and an adequate design of the parts to be assembled.	Parts of all shapes and all dimensions, but the joint must only work in shearing.
Impossibilities	Certain metals or alloys cannot be welded (cast iron, copper, bronze, zinc).	Difficulty with small parts and materials not being able to be machined bored. Risk without flat and parallel surfaces.	No impossibility.
Assembly, disassembly, repair	Permanent assembly. Reparable for MIG, not for laser, and with conventional process for FSW	Assembly easily. dismountable and repaired	Permanent assembly.
Stress distribution (see figure below)	Irregular	Concentrated stresses towards holes, screw, rivets and bolts.	Excellent distribution of shear stresses on all surface, but bad in the case of the cleavage or of peeling.
Mechanical strength	Can be very high.	Can be very high.	High in shearing. Weak in cleavage or peeling.
Fatigue and vibration strength	Good but must be studied.	The assemblies can lose tightening when they are subjected to the vibrations.	Very good fatigue strength
Heat strength	Very high strength (the same with assembled metals).	Very high strength (the same with assembled metals).	Limited (maximum temperature of 120°C for the epoxy adhesives and of 300°C for the thermostable adhesives).
Water resistance, and corrosion	Excellent. Very little risk of corrosion.	Good. Possibility of corrosion with different metals	Risk of corrosion for the assemblies with tension.
Labour and Implementation	Must be qualified	Little qualified	Must be qualified. Careful in the preparation.
Manufacturing process controls	Non-destructive tests (NDT): visual inspection, radiography, tightness test (with X-rays in particular), ultrasounds, etc.	Visual inspection (presence of the screws, bolts, rivets), checking of the tightening of the screws and bolts.	Different methods: - following test-tubes: - traction; - NDT: visual inspection, tightness test, radiography (with X-rays in particular), ultrasounds, etc.
Process constraints	MIG: Heat introduction, deformation, shrinkage (thermomechanical treated materials).	Screwing/bolting: Weight, holes in the structure, cost, accessibility, added weight.	Depending on temperature and humidity, Low fire resistance, Weathering, Process time (additional surface treatment and

	Loss in mechanical properties, especially Al-alloy.	Riveting: holes in the structure, expensive automated installation, weakness of the holes (FRP), to pass to a higher diameter of rivet for a damaged rivet, added weight	preparation is necessary), time of curing process...
	Laser: high quality of body edges and tight tolerances are necessary, High surface finish of parts…		
	FSW: Exit keyhole left when tool is withdrawn, Large down forces, higher tolerance accuracy of joints…		
Standard	Standard process, joint geometries, certification and qualification workers…	Standards exist	Only German Standard
Design calculation	Can be calculated with existing guidelines	Can be calculated with existing guidelines	Can be calculated with condition hypothesis and bonding strength qualification
Ageing	No impact	No impact	Ageing of adhesive joints is not well known, lack of experience for long term behaviour of structural adhesives
Environmental	For classic welding : safety risk due to the weld pool, toxic fumes, arc or the spatter of molten material	Drilling boreholes in FRPs cause strong wear of the drill bits	Needs dedicated area for manufacturing, maintenance and storage

In the same way, the stress distribution for the different types of joining can be presented as shown in Figure 4.34:

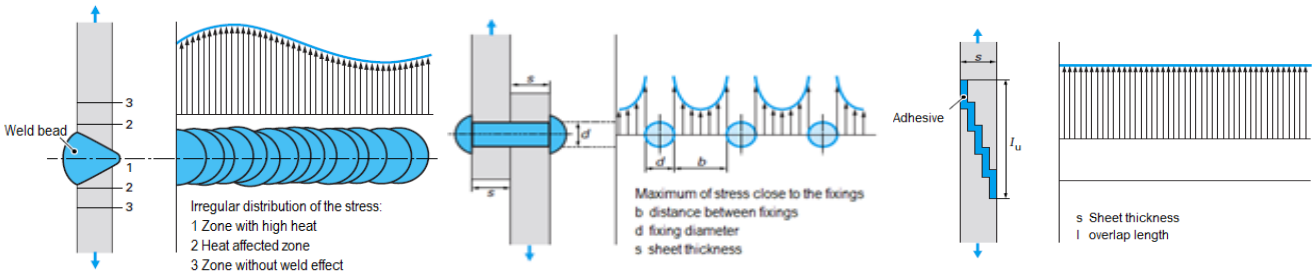

Welding **Riveting/bolting/screwing** **Step bonding**

Figure 4.34. Stress distribution in different types of assembly.

4.3 JOINTS TASK FINDINGS

The main joining technologies evaluation is presented in Table 4.11, taking into account different design parameters, being one of the more critical the assembly and disassembly of the joint. All

technologies seem structurally feasible, being only necessary to adapt the current constructive techniques designed to welding to the others technologies like bonding.

In line with bonding German standard, it is necessary to continue developing a European standard for bonding (with specification and validation method).

5. CALCULATION OF COMPOSITE ROOF WITH RIVET JOINT

5.1 INTRODUCTION

The aim of this chapter is to do a calculation putting into practice some of the concepts covered in the deliverables D3.1, D3.2, D3.3 regarding loads and boundary conditions, material assessment and joining technologies. For this purpose, the current FE model of the steel welded roof of a LRV is redesigned to a riveted composite structure.

After the analysis it have been checked the structural integrity of the composite and the rivet joints, as well as the modal response to ensure good vibration behaviour. The design has been optimized after some iterations based on the results obtained.

5.2 PREVIOUS MODEL

The previous model of the LRV roof is made of welded steel sheets. The central sheet is attached to the roof frame by means of discontinuous weld, as can be seen in Figure 5.1:

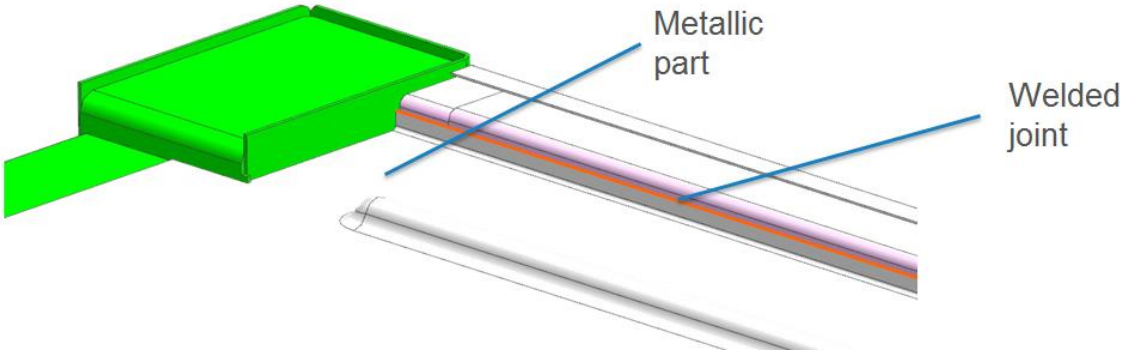

Figure 5.1 Previous model

The Finite Element model of the original structure is shown in Figure 5.2:

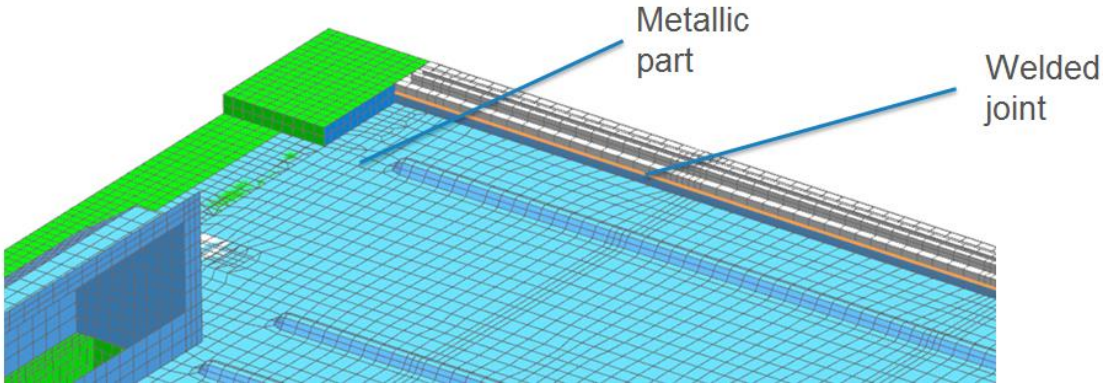

Figure 5.2 Previous FE model

The roof equipment is modelled as mass elements attached to the lateral long beams by means of RBE3 elements. The main roof equipment modelled its approximated weight are:

- HVAC: 450kg
- Pantograph: 300kg
- Transformer: 3000kg

- Batteries: 150kg

5.3 COMPOSITE MODEL

The redesign of the model consists on changing the metallic sheet by a composite one, and change the surrounding metallic frame to be at the same level for an easier joint between parts. The composite used for the analysis is the Carbon Fibre/Epoxi Biaxial described in Table 3.1 to Table 3.3. During the different iterations, the number of plies has been considered as a variable.

The selected joining technology is riveting (described at Deliverable D3.3 joining technologies). The rivets have been modelled by means 1D beam elements, taking into account its diameter. The diameter and the number of rivets have been also considered as a variable during the iterative process to reach an optimized result.

The Finite Element model of the proposed structure is shown in Figure 5.3:

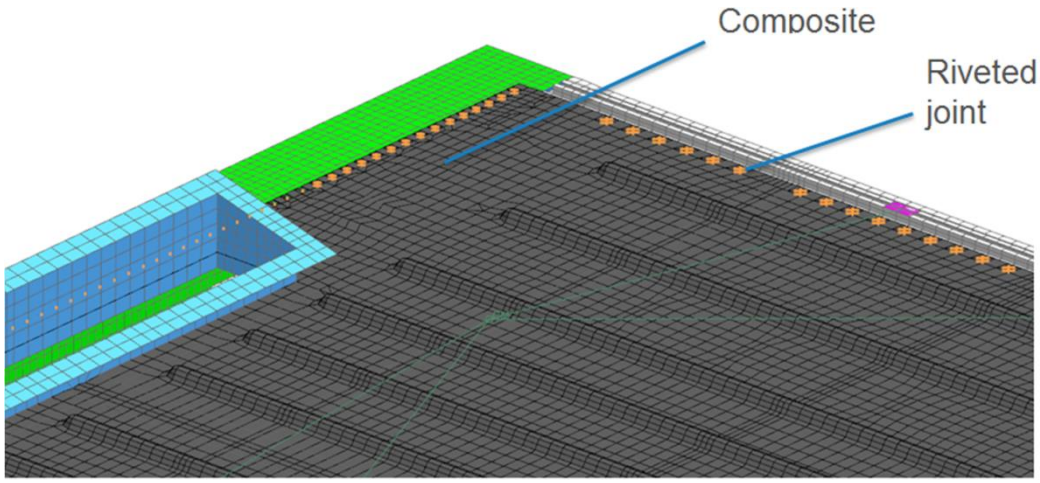

Figure 5.3 Composite FE model

5.4 LOAD CASES

Taking into account the loads described at deliverable D3.1 Carbodyshell specification Part 2 Section 7, the most critical loads for the roof are:

- Exceptional load cases:

Equipment attachments	$3g_x$ $1g_y$ $(1\pm c)g^*$ *c=2 at the vehicle end, falling linearly to 0.5 at the vehicle center

- Fatigue load cases:

- $\pm 0.15g_x$ or traction accel. - $\pm 0.15g_y$ - $(1\pm 0.15)g_z$	10^7 cycles

Finally, also a modal analysis has been carried out.

5.5 FAILURE CRITERIA

Different failure criteria are taken into account depending on the part analysed:

- For the composite part, for the static strength, Tsai-Wu criterion has been followed according to point 5.5 of the deliverable D3.2 Material Assessment. (The fatigue assessment has not been carried out due to the lack of S/N curves of the material).
- For the rivets, internal failure criteria are followed for static and fatigue.
- For the modal analysis, in order to give an adequate response, all the frequencies have to be bigger than 10Hz.

5.6 ASSESSMENT

5.6.1 Composite model V1

Introduction

The first version of the composite model has the settings described in Table 5.1:

Table 5.1 Composite model V1 settings

Composite model	V1
Total number of rivets	504
Distance between rivets (mm)	50
Rivet diameter (mm)	6.4
Composite's number of layers	16

The composite is made of 16 layers of Carbon/epoxy biaxial with different orientations. The composite layup is summarized in the Table 5.2.

Table 5.2 Composite model V1 Composite Layers

Ply Id	Material Name	Thickness (mm)	Angle (deg)
1	Carbon/epoxy biaxial	0.2875	90
2	Carbon/epoxy biaxial	0.2875	45
3	Carbon/epoxy biaxial	0.2875	90
4	Carbon/epoxy biaxial	0.2875	45
5	Carbon/epoxy biaxial	0.2875	90
6	Carbon/epoxy biaxial	0.2875	45
7	Carbon/epoxy biaxial	0.2875	90
8	Carbon/epoxy biaxial	0.2875	45
…16	Symmetric		

Composite Analysis

The results of the static resistance analysis for the composite part are shown in the Figure 5.4.

Most critical Load Case $3g_z$
Maximum Failure Index 0.05

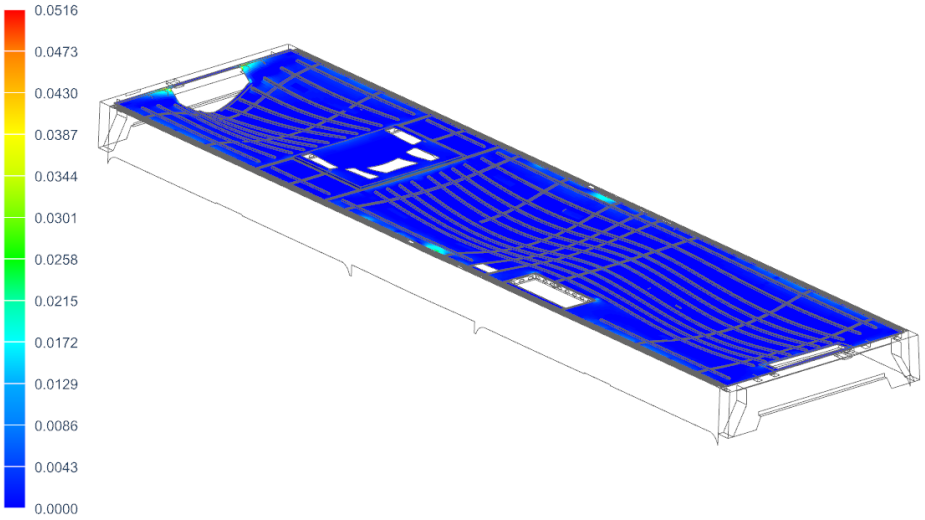

Figure 5.4 Composite model V1 Tsai-Wu failure index, $3g_z$

Riveting Analysis

The results of the worst rivet's Safety Factor for exceptional and fatigue are shown in the Table 5.3.

Table 5.3 Composite model V1 Rivet Safety Factor

Load Case	Safety Factor
Exceptional	3.63
Fatigue	2.23

Modal Analysis

A representation of the first modal frequency is represented below in the Figure 5.5.

1st mode frequency 11.89 Hz

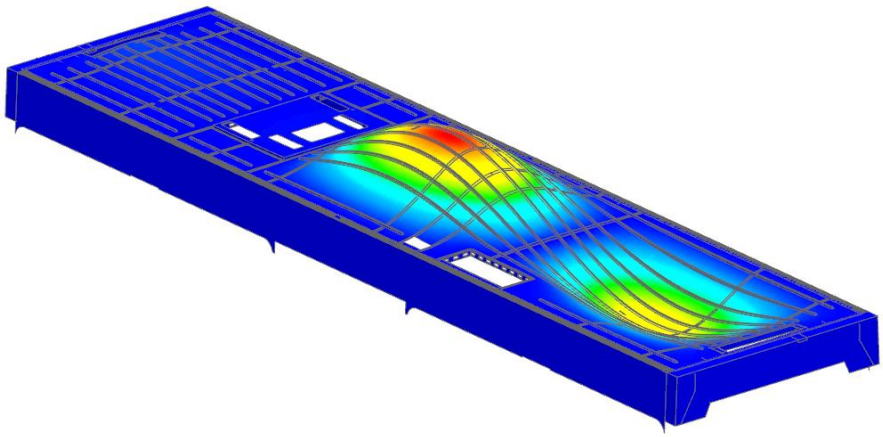

Figure 5.5 Composite model V1 Mode 1 (11.89Hz)

Discussion

According to the results obtained, there is a wide safety margin in the model, so for the next iteration the number of rivets has been reduced roughly the half (from 504 to 256). Consequently, the distance between rivets has been doubled.

5.6.2 Composite model V2

Introduction

The second version of the composite model has the settings described in the Table 5.4.

Table 5.4 Composite model V2 settings

Composite model	V2
Total number of rivets	**256**
Distance between rivets (mm)	**100**
Rivet diameter (mm)	6.4
Composite's number of layers	16

The composite is made of 16 layers of Carbon/epoxy biaxial with different orientations. The composite layup is summarized in the Table 5.5.

Table 5.5 Composite model V2 Composite Layers

Ply Id	Material Name	Thickness (mm)	Angle (deg)
1	Carbon/epoxy biaxial	0.2875	90
2	Carbon/epoxy biaxial	0.2875	45
3	Carbon/epoxy biaxial	0.2875	90
4	Carbon/epoxy biaxial	0.2875	45
5	Carbon/epoxy biaxial	0.2875	90
6	Carbon/epoxy biaxial	0.2875	45
7	Carbon/epoxy biaxial	0.2875	90
8	Carbon/epoxy biaxial	0.2875	45
…16	Symmetric		

Composite Analysis

The results of the static resistance analysis for the composite part are shown in the Figure 5.6.

Most critical Load Case	$3g_z$
Maximum Failure Index	0.07

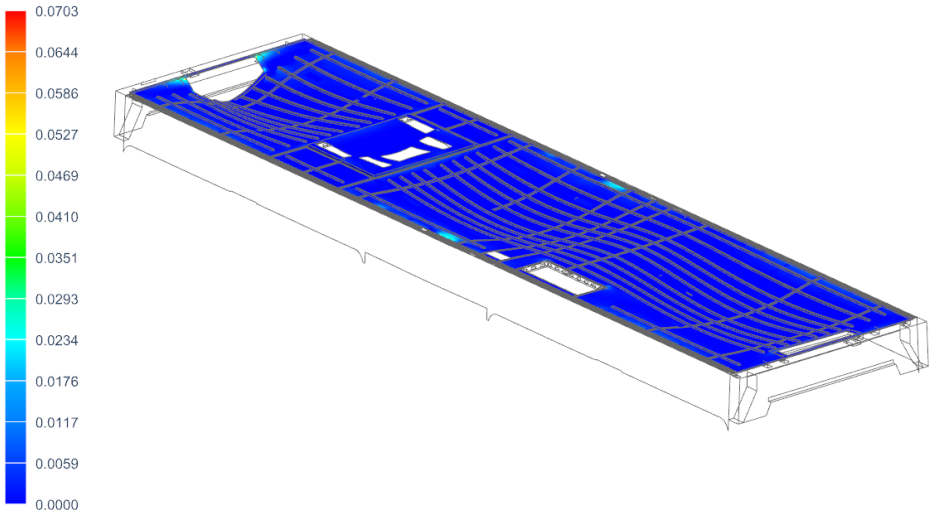

Figure 5.6 Composite model V2 Tsai-Wu failure index, $3g_z$

Riveting Analysis

The results of the worst rivet's Safety Factor for exceptional and fatigue are shown in the Table 5.6.

Table 5.6 Composite model V2 Rivet Safety Factor

Load Case	Safety Factor
Exceptional	5.01
Fatigue	1.55

Modal Analysis

A representation of the first modal frequency is represented in the Figure 5.7.

1st mode frequency 11.84 Hz

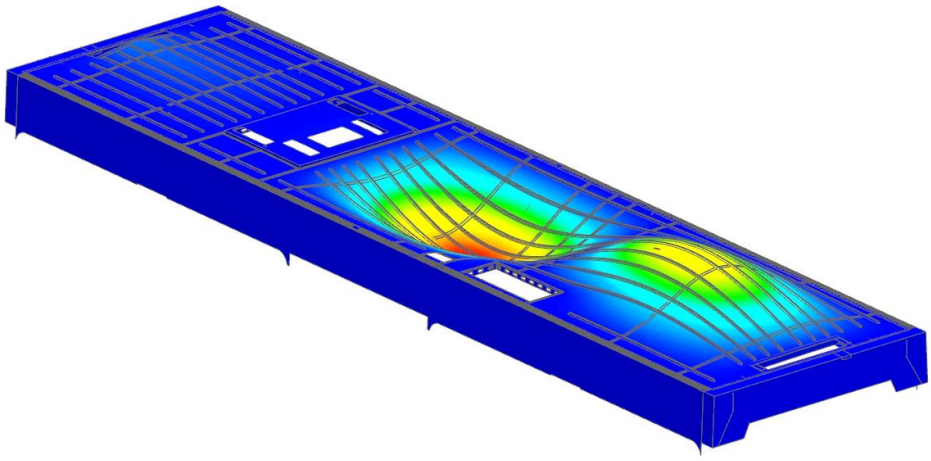

Figure 5.7 Composite model V2 Mode 1 (11.84Hz)

Discussion

According to the results obtained, there is still a wide safety margin in the model, so for the next iteration the rivet's diameter has been reduced, but the number has been 504 again, and the distance between them too.

5.6.3 Composite model v3

Introduction

The third version of the composite model has the settings described in the Table 5.7:

Table 5.7 Composite model V3 settings

Composite model	V3
Total number of rivets	**504**
Distance between rivets (mm)	**50**
Rivet diameter (mm)	**4.8**
Composite's number of layers	16

The composite is made of 16 layers of Carbon/epoxy biaxial with different orientations. The composite layup is summarized in the Table 5.8.

Table 5.8 Composite model V3 Composite Layers

Ply Id	Material Name	Thickness (mm)	Angle (deg)
1	Carbon/epoxy biaxial	0.2875	90
2	Carbon/epoxy biaxial	0.2875	45
3	Carbon/epoxy biaxial	0.2875	90
4	Carbon/epoxy biaxial	0.2875	45
5	Carbon/epoxy biaxial	0.2875	90
6	Carbon/epoxy biaxial	0.2875	45
7	Carbon/epoxy biaxial	0.2875	90
8	Carbon/epoxy biaxial	0.2875	45
…16	Symmetric		

Composite Analysis

The results of the static resistance analysis for the composite part are shown in the Figure 5.8.

Most critical Load Case	$3g_z$
Maximum Failure Index	0.06

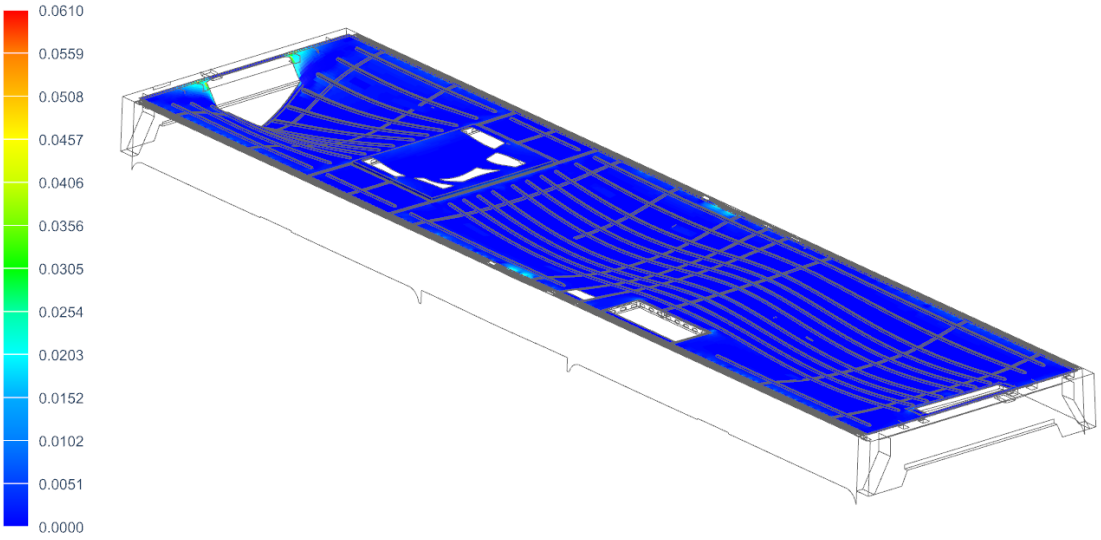

Figure 5.8 Composite model V3 Tsai-Wu failure index, $3g_z$

Riveting Analysis

The results of the worst rivet's Safety Factor for exceptional and fatigue are shown in the Table 5.9.

Table 5.9 Composite model V3 Rivet Safety Factor

Load Case	Safety Factor
Exceptional	3.49
Fatigue	1.65

Modal Analysis

A representation of the first modal frequency is represented in the Figure 5.9.

1st mode frequency 11.88 Hz

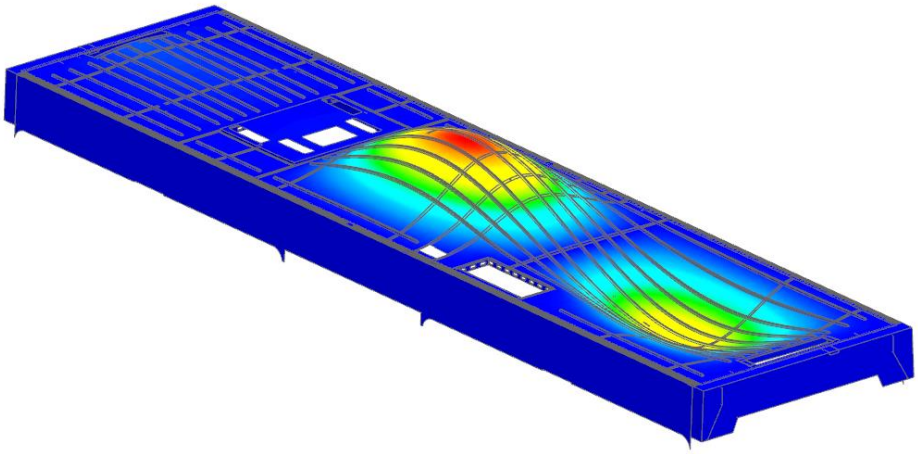

Figure 5.9 Composite model V3 Mode 1 (11.88Hz)

Discussion

According to the results obtained, there is a wide safety margin in the model. For the next iteration the number of rivets has been reduced to 268 (half approximately), so the distance between rivets is 100mm.

5.6.4 Composite model V4

Introduction

The fourth version of the composite model has the settings described in Table 5.10:

Table 5.10 Composite model V4 settings

Composite model	V4
Total number of rivets	**268**
Distance between rivets (mm)	**100**
Rivet diameter (mm)	4.8
Composite's number of layers	16

The composite is made of 16 layers of Carbon/epoxy biaxial with different orientations. The composite layup is summarized in the Table 5.11:

Table 5.11 Composite model V4 Composite Layers

Ply Id	Material Name	Thickness (mm)	Angle (deg)
1	Carbon/epoxy biaxial	0.2875	90
2	Carbon/epoxy biaxial	0.2875	45
3	Carbon/epoxy biaxial	0.2875	90
4	Carbon/epoxy biaxial	0.2875	45
5	Carbon/epoxy biaxial	0.2875	90
6	Carbon/epoxy biaxial	0.2875	45
7	Carbon/epoxy biaxial	0.2875	90
8	Carbon/epoxy biaxial	0.2875	45
…16	Symmetric		

Composite Analysis

The results of the static resistance analysis for the composite part are shown in the Figure 5.10.

Most critical Load Case	$3g_z$
Maximum Failure Index	0.08

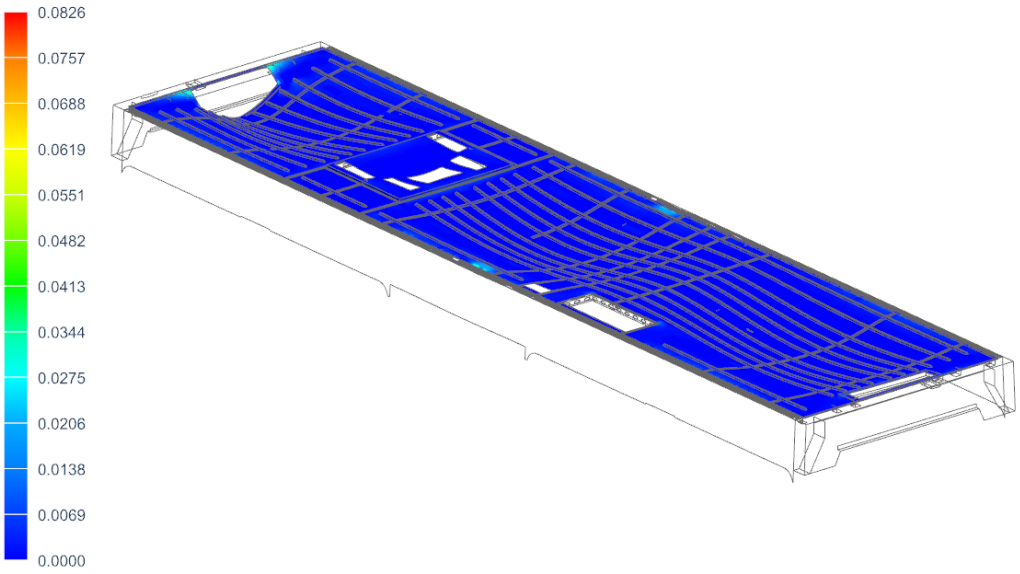

Figure 5.10 Composite model V4 Tsai-Wu failure index, $3g_z$

Riveting Analysis

The results of the worst rivet's Safety Factor for exceptional and fatigue are shown in the Table 5.12.

Table 5.12 Composite model V4 Rivet Safety Factor

Load Case	Safety Factor
Exceptional	3.16
Fatigue	1.22

Modal Analysis

A representation of the first modal frequency is represented in Figure 5.11.

1st mode frequency 11.84 Hz

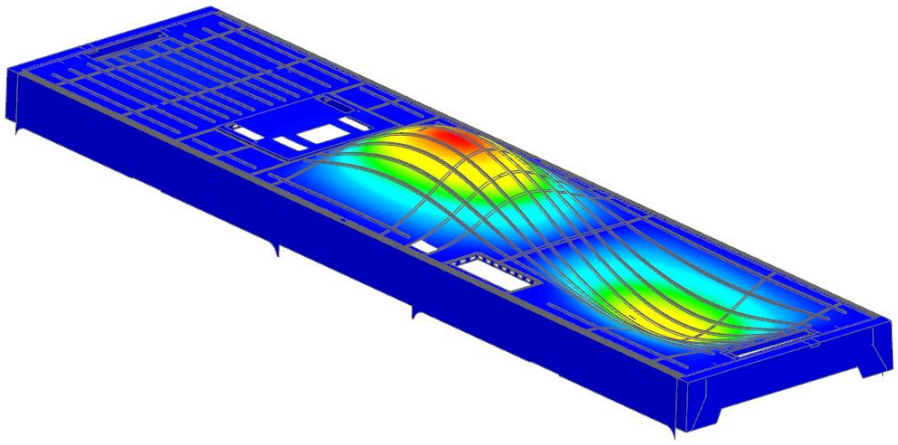

Figure 5.11 Composite model V4 Mode 1 (11.84Hz)

Discussion

According to the results obtained, there is a wide safety margin in the model, so for the next iteration the number of layers in the composite has been reduced from 16 to 12.

5.6.5 Composite model V5

Introduction

The fifth version of the composite model has the settings described in Table 5.13.

Table 5.13 Composite model V5 settings

Composite model	V5
Total number of rivets	268
Distance between rivets (mm)	100
Rivet diameter (mm)	4.8
Composite's number of layers	**12**

The composite is made of 12 layers of Carbon/epoxy biaxial with different orientations. The composite layup is summarized in Table 5.14.

Table 5.14 Composite model V5 Composite Layers

Ply Id	Material Name	Thickness (mm)	Angle (deg)
1	Carbon/epoxy biaxial	0.2875	90
2	Carbon/epoxy biaxial	0.2875	45
3	Carbon/epoxy biaxial	0.2875	90
4	Carbon/epoxy biaxial	0.2875	90
5	Carbon/epoxy biaxial	0.2875	45
6	Carbon/epoxy biaxial	0.2875	90
…12	Symmetric		

Composite Analysis

The results of the static resistance analysis for the composite part are shown in the Figure 5.12.

Most critical Load Case	$3g_z$
Maximum Failure Index	0.11

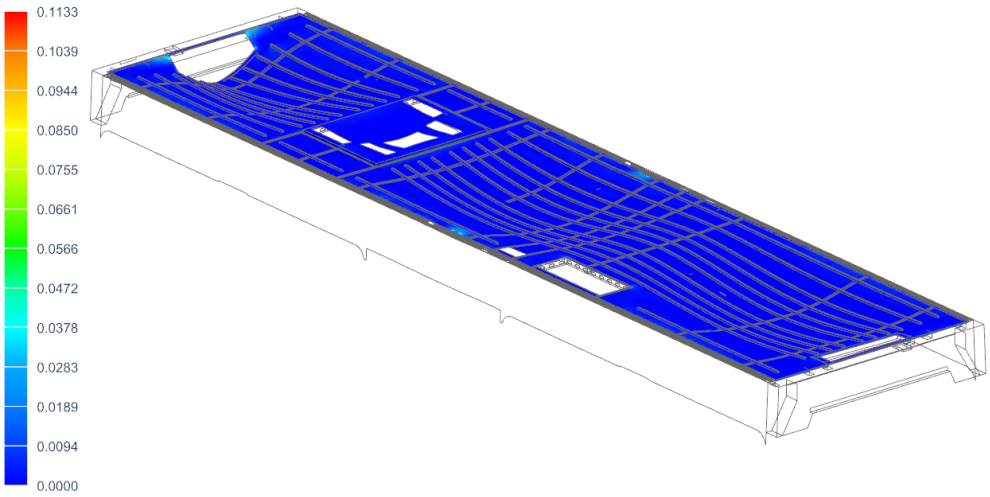

Figure 5.12 Composite model V5 Tsai-Wu failure index, $3g_z$

Riveting Analysis

The results of the worst rivet's Safety Factor for exceptional and fatigue is shown in Table 5.15.

Table 5.15 Composite model V5 Rivet Safety Factor

Load Case	Safety Factor
Exceptional	3.45
Fatigue	1.05

Modal Analysis

A representation of the first modal frequency is represented in Figure 5.13.

1st mode frequency 10.3 Hz

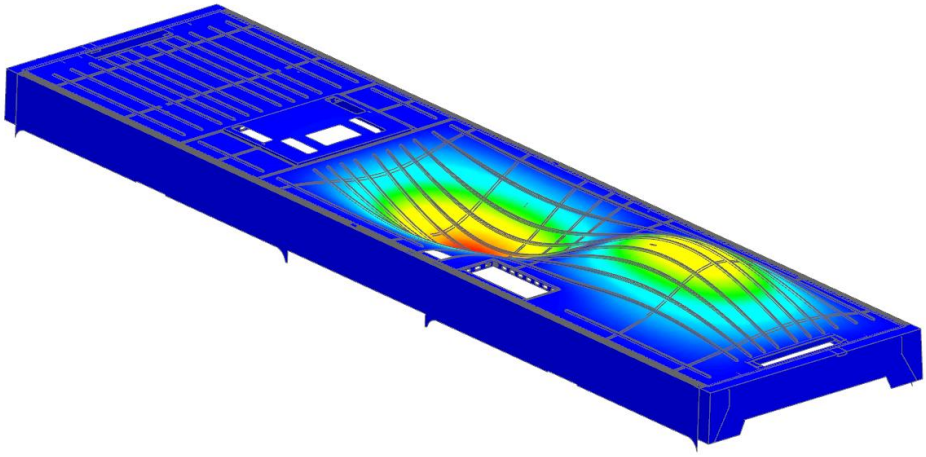

Figure 5.13 Composite model V5 Mode 1 (10.3Hz)

5.7 CONCLUSIONS

After the analysis carried out, it can be concluded that the proposed solution that takes into account the loads defined in D3.1, one of the materials and its properties from D3.2, and one of the joining technologies from D3.3; can be feasible, fulfilling the structural failure criteria for static cases.

Taking into account the different factors studied, the frequency is controlled mainly by two parameters: the number of rivets and the lay-up of the roof. The diameter of the rivets is a secondary element in the eigenfrequency due to the slight variation in the frequency when small rivet is considered (0.01Hz), see Table 5.16.

Table 5.16 Influence factors for eigenfrequency

	Diameter of rivets	No. of rivets	No. layers	Frequency
Model V1	6.4mm	504	16	11,89Hz
Model V2	6.4mm	256	16	11,84Hz
Model V3	4.8mm	504	16	11,88Hz
Model V4	4.8mm	268	16	11,84Hz
Model V5	4.8mm	268	12	10,3Hz

Furthermore, in terms of weight saving, the proposed solution is also attractive. Most of the savings are due to the reduction of the metallic structure needed to withstand the roof (see Figure 5.14).

Figure 5.14 Top: Original substructure; Bottom: New substructure

The initial model has a total weight of 304kg and the final composite solution weights 210 kg, which means a 31% of weight saved for a similar final result in terms of modal response and Safety against failure.

The influence of the fatigue on the composite part has to be investigated to complement this analysis. As stated previously the fatigue assessment has not been carried out due to the lack of S/N curves of the material

6. MAIN CONCLUSIONS AND LINKS WITH SHIFT2RAIL

The aim of the WP3 of Roll2Rail is aligned with the general objectives of Shift2Rail: cutting the life-cycle cost of railway transport and increase railway capacity.

All the results of this WP of Roll2Rail are the first step of the IP1 TD1.3 Carbodyshell of Shift2Rail.

Also, all the results of the WP3 of Roll2Rail are aligned with the expected achievements of the TD1.3 Carbodyshell of Shift2Rail:

- Weight reduction between 15 and 30%.
- Energy savings in operation, resulting from the weight reduction.
- Improvement of maintainability, coming from new concepts.

The results of the Task T3.1 Technical Specification are the first inputs for the T1.3.1 General Specification of Shift2Rail, laying the foundation for the main requirements to be met for the different demonstrator to be developed.

In addition, the definition of the High Speed and Urban carbodies made in Roll2Rail are the baseline for future collaborative developments in Shift2Rail.

With the different feasibility and structural studies the objective related with weight reduction seems possible, but need to be objectified in a complete design proposal and should be checked the compliance with EMC and fire requirements.

The optimization methodology has been shown as a powerful tool for the design phase to have a general overview of the impact of the interfaces locations, best orientations of the fibres or the proper location of reinforcements.

The results of Tasks T3.2 and T3.3 are the basic input for T1.3.2 Carbody Study of Shift2Rail, the selection of the material and manufacturing process to be used, based on a global study of available composite materials carbody and manufacturing process. Regarding materials and joints, it is identified the necessity to characterize properly and according to the railway environment the new materials and joining methods (fatigue, crash behaviour, aging…).

Considering the different steps done until now and in line with the characterization necessity, the principal obstacle to face in subsequent developments is the one related with the regulatory framework and the certification process. Discussions regarding standardisation & regulation with external experts in the field have been established through an Advisory Group. It has been concluded that the WP3 and S2R members should develop a common methodology (alternative to current framework standard) to validate the future hybrid structures which will constitute the next generation of the carbodies.

Technical specification

[A1] D3.1 Carbody shell Specification.

[A2] EN 12663-1 Railway applications. Structural requirements of railway vehicle bodies. Locomotives and passenger rolling stock.

[A3] D3.3 Joining Technologies.

[A4] EN 15663; Railway applications. Definition of vehicle reference masses.

[A5] TSI INF Technical Specification of Interoperability. Infrastructure.

[A6] D3.2 Material Assessment.

[A7] EN 15273; Railway applications. Gauges.

Material Assessment

[B1] D3.2 Material Assessment

[B2] EN 12663-1 Railway applications. Structural requirements of railway vehicle bodies. Locomotives and passenger rolling stock.

[B3] D3.1 Carbody shell Specification.

Joining Technologies

[C1] EN 12663 Railway applications. Structural requirements of railway vehicle bodies. Locomotives and passenger rolling stock.

[C2] EN 15085 Railway applications - Welding of railway vehicles and components.

[C3] ERRI-B12-RP17 Tests programme for railway steel structure vehicles.

[C4] D3.3 Joining Technologies.

[C5] DVS 1608 Design and strength assessment of welded structures from aluminium alloys in railway applications.

[C6] DIN 25201-1..7 Design guide for railway vehicles and their components. Bolted joints.

[C7] VDI 2230-1..2 Systematic calculation of highly stressed bolted joints.

[C8] NF E 25030-1..2 Éléments de fixation, assemblages vissés, conception, calcul et conditions de montage.

[C9] DIN 6701-1..4 Use of adhesive bonding in the manufacture of rail vehicles and parts of rail vehicles.

[C10] EWF 515-01 European Adhesive Bonder.

[C11] EWF 516-01 European Adhesive Specialist.

[C12] EWF 517-01 European Adhesive Engineer.